

# **Elucidating the pathomechanism behind the neurocristopathy CHARGE syndrome**

## **Doctoral Thesis**

In partial fulfillment of the requirements for the degree

“Doctor rerum naturalium (Dr. rer. nat.)“

in the Molecular Medicine Study Program  
at the Georg-August University Göttingen

submitted by

Luisa Freese

born in

Halberstadt, Germany

Göttingen, 2017

## **Members of the Thesis Committee**

### Supervisor

**PD Dr. Silke Pauli**

Institute of Human Genetics

University Medical Center Göttingen

### Second member of the Thesis Committee

**Prof. Steven A. Johnsen, PhD**

Department of General, Visceral and Pediatric Surgery

University Medical Center Göttingen

### Third member of the Thesis Committee

**Prof. Dr. Ahmed Mansouri**

Department of Molecular Cell Biology/Molecular Cell Differentiation

Max Planck Institute for Biophysical Chemistry, Göttingen

Date of Disputation:

## **AFFIDAVIT**

Herewith I declare that my doctoral thesis entitled: "Elucidating the pathomechanism behind the neurocristopathy CHARGE syndrome" has been written independently with no other sources and aids than quoted.

Göttingen, May 2017

---

Luisa Freese

## List of Publications

- Schulz Y, **Freese L**, Manz J, Zoll B, Volter C, Brockmann K, Bogershausen N, Becker J, Wollnik B, Pauli S (2014). CHARGE and Kabuki syndromes: a phenotypic and molecular link. *Human molecular genetics* 23(16): 4396–4405.
  - A manuscript is in preparation that will contain parts of this doctoral thesis.
- 

Parts of this doctoral thesis were presented at the following meetings:

- 25th Annual Meeting of the German Society of Human Genetics together with the Austrian Society of Human Genetics and the Swiss Society of Medical Genetics  
March 19–21, 2014, Essen, Germany  
“CHARGE and Kabuki syndrome. Two related syndromes?” (poster presentation)
- 26th Annual Meeting of the German Society of Human Genetics together with the Austrian Society of Human Genetics and the Swiss Society of Medical Genetics  
April 15–17, 2015, Graz, Austria  
“Chd7, the protein affected in CHARGE syndrome, regulates the neural crest cell guidance molecule Sema3a.” (poster presentation)

# Table of contents

	<b>Table of contents</b> .....	<b>I</b>
	<b>List of figures</b> .....	<b>VI</b>
	<b>List of tables</b> .....	<b>VIII</b>
	<b>Abbreviations</b> .....	<b>IX</b>
<b>1</b>	<b>Introduction</b> .....	<b>1</b>
<b>1.1</b>	<b>CHARGE Syndrome</b> .....	<b>1</b>
1.1.1	Chromodomain helicase DNA-binding protein 7 .....	1
1.1.2	Mutations in <i>CHD7</i> lead to CHARGE syndrome .....	2
<b>1.2</b>	<b>Neurocristopathies</b> .....	<b>2</b>
<b>1.3</b>	<b>Neural crest cells – the fourth germ layer</b> .....	<b>3</b>
1.3.1	Migration of NCCs .....	4
<b>1.4</b>	<b>Semaphorins</b> .....	<b>6</b>
1.4.1	Class 3 semaphorins .....	8
1.4.2	SEMA3A mutations contribute to the phenotype of Kallmann syndrome .....	8
<b>1.5</b>	<b>Aim of the present study</b> .....	<b>9</b>
<b>2</b>	<b>Materials and Methods</b> .....	<b>10</b>
<b>2.1</b>	<b>Materials</b> .....	<b>10</b>
2.1.1	Technical equipment.....	10
2.1.2	Consumable materials .....	12
2.1.3	Chemicals, biochemicals and reagents.....	13
2.1.4	Ready-to-use reaction systems .....	16
2.1.5	Sterilization .....	16
2.1.6	Buffers and solutions .....	16
2.1.7	Plasmids and vectors.....	20
2.1.8	Bacterial strains .....	21
2.1.8.1	Media and agar plates for bacterial culture .....	21

2.1.9	Eukaryotic cell lines .....	21
2.1.9.1	Media for eukaryotic cell culture.....	22
2.1.9.2	Freezing media.....	22
2.1.10	Yeast strains.....	22
2.1.10.1	Media and agar plates for yeast culture .....	23
2.1.11	Antibodies.....	24
2.1.11.1	Primary antibodies .....	24
2.1.11.2	Secondary antibodies .....	25
2.1.12	Synthetic oligonucleotides .....	25
2.1.12.1	Synthetic oligonucleotides for genotyping PCR experiments .....	25
2.1.12.2	Synthetic oligonucleotides for In-Fusion® experiments.....	25
2.1.12.3	Synthetic oligonucleotides for mutagenesis experiments .....	26
2.1.12.4	Synthetic oligonucleotides for mycoplasma contamination.....	26
2.1.12.5	Synthetic oligonucleotides for patient screening .....	26
2.1.12.6	Synthetic oligonucleotides for RT-PCR experiments.....	27
2.1.12.7	Synthetic oligonucleotides for sequencing .....	29
2.1.12.8	Synthetic oligonucleotides for qRT-PCR experiments.....	29
2.1.13	Molecular weight standards .....	30
2.1.14	Animals/ethic statement.....	30
2.1.15	Patient samples .....	31
2.1.16	Databases / Online tools / Programs .....	31
2.1.17	Statistical analysis .....	32
<b>2.2</b>	<b>Methods.....</b>	<b>33</b>
2.2.1	Molecular biology methods .....	33
2.2.1.1	Isolation of nucleic acids.....	33
2.2.1.1.1	Isolation of genomic DNA for mouse genotyping .....	33
2.2.1.1.2	Minipreparation of plasmid DNA .....	33
2.2.1.1.3	Endotoxin-free midipreparation of plasmid DNA .....	34
2.2.1.1.4	Isolation of total RNA from cultured cells .....	34
2.2.1.1.5	Isolation of RNA from mouse tissues .....	35
2.2.1.1.6	Determination of nucleic acid concentration.....	35
2.2.1.2	Polymerase Chain Reactions.....	35
2.2.1.2.1	Amplification of DNA.....	35
2.2.1.2.1.1	Standard PCR .....	36

2.2.1.2.1.2	Touchdown PCR .....	37
2.2.1.2.1.3	Genotyping PCR.....	38
2.2.1.2.1.4	Mutagenesis PCR.....	39
2.2.1.2.1.5	Mycoplasma contamination PCR.....	41
2.2.1.2.2	Reverse transcription.....	42
2.2.1.2.3	Quantitative Real-Time PCR.....	42
2.2.1.2.4	Sequencing analysis.....	43
2.2.1.3	Agarose gel electrophoresis of DNA .....	44
2.2.1.3.1	Purification of DNA fragments from agarose gels .....	45
2.2.1.4	Cloning techniques .....	45
2.2.1.4.1	Restriction digestion of plasmid DNA.....	45
2.2.1.4.2	Cloning of DNA fragments using In-Fusion® HD Cloning Kit .....	46
2.2.1.4.3	Transformation of competent cells .....	46
2.2.1.4.4	Mutagenesis .....	47
2.2.1.5	Yeast two-hybrid assay.....	47
2.2.2	Protein manipulation methods .....	48
2.2.2.1	Protein isolation from eukaryotic cells .....	48
2.2.2.2	Protein isolation from yeast cells.....	48
2.2.2.3	Protein concentration from cell culture medium .....	49
2.2.2.4	Determination of protein concentration .....	49
2.2.2.5	Co-immunoprecipitation.....	49
2.2.2.6	SDS polyacrylamide gel electrophoresis.....	50
2.2.2.7	Transfer of proteins from a polyacrylamide gel to a membrane.....	51
2.2.2.8	Protein detection on membranes using antibodies.....	51
2.2.3	Histological methods.....	52
2.2.3.1	Dissection of mouse tissues and embryos .....	52
2.2.3.2	Fixation of cells on slides .....	53
2.2.3.3	Immunofluorescence staining .....	53
2.2.4	Cell culture methods.....	53
2.2.4.1	Coating of cell culture vessels .....	53
2.2.4.1.1	Preparation of fibronectin coated cell culture vessels.....	53
2.2.4.1.2	Preparation of matrigel coated cell culture vessels .....	54
2.2.4.2	Culture of eukaryotic cells.....	54
2.2.4.2.1	Culture and passaging of murine JoMa1 and JoMa1.3 cells .....	54
2.2.4.2.2	Culture and passaging of murine O9-1 cells .....	55

2.2.4.2.3	Culture and passaging of human HEK293 cells .....	55
2.2.4.2.4	Cryopreservation and thawing of eukaryotic cells .....	56
2.2.4.3	Transfection of eukaryotic cells.....	56
2.2.4.3.1	Transfection of plasmids into eukaryotic cells .....	56
2.2.4.3.2	Transfection of short interfering RNAs .....	57
<b>3</b>	<b>Results .....</b>	<b>59</b>
<b>3.1</b>	<b>Characterization of murine NCC lines.....</b>	<b>59</b>
3.1.1	Molecular marker expression in murine JoMa cells.....	59
3.1.2	Molecular marker expression in murine O9-1 cells .....	61
3.1.3	<i>Chd7</i> expression in murine JoMa cells and O9-1 cells.....	63
<b>3.2</b>	<b>O9-1 cells express semaphorin receptors and class 3 semaphorins .....</b>	<b>66</b>
<b>3.3</b>	<b>Sema3a is expressed, processed and secreted by O9-1 cells and exists in monomeric and dimeric isoforms .....</b>	<b>69</b>
<b>3.4</b>	<b>Downregulation of <i>Chd7</i> has influence on the expression level of <i>Sema3a</i> in O9-1 cells.....</b>	<b>73</b>
<b>3.5</b>	<b><i>Chd7</i> co-immunoprecipitates with Sema3a in O9-1 cells .....</b>	<b>74</b>
<b>3.6</b>	<b>Detection of the non-synonymous <i>SEMA3A</i> variant c.2002A&gt;G (p.I668V) in a <i>CHD7</i>-positive CHARGE syndrome patient.....</b>	<b>76</b>
<b>3.7</b>	<b>Generation of <i>SEMA3A</i> plasmids .....</b>	<b>77</b>
<b>3.8</b>	<b><i>SEMA3A</i> variants have no effect on the expression, processing and secretion as well as dimerization of <i>SEMA3A</i>.....</b>	<b>78</b>
<b>3.9</b>	<b><i>CHD7</i> co-immunoprecipitates with <i>SEMA3A</i> WT and <i>SEMA3A</i> variants .....</b>	<b>83</b>
<b>3.10</b>	<b><i>CHD7</i> shows no direct interaction with <i>SEMA3A</i> WT or <i>SEMA3A</i> variants .....</b>	<b>85</b>
<b>4</b>	<b>Discussion .....</b>	<b>89</b>
<b>4.1</b>	<b>Summary of the results .....</b>	<b>89</b>



4.2	NCCs – which <i>in vitro</i> model to choose?.....	90
4.3	NCCs express class 3 semaphorins and secrete Sema3a.....	92
4.4	<i>Chd7</i> regulates <i>Sema3a</i> expression and is associated with Sema3a in NCCs .....	94
4.5	<i>SEMA3A</i> might act as modifier in CHARGE syndrome.....	95
4.6	Future perspectives.....	97
5	Summary .....	99
6	References .....	101
7	Acknowledgements .....	113
8	Curriculum vitae .....	114

## List of figures

Figure 1:	Schematic representation of the CHD7 structure.....	1
Figure 2:	Delamination and differentiation of NCCs .....	4
Figure 3:	Schematic representation of the protein structure of semaphorins and their main receptors.....	7
Figure 4:	Expression analysis of NCC, neuronal, glia, smooth muscle, melanocyte and chondrocyte marker genes in JoMa1 cells and JoMa1.3 cells .....	61
Figure 5:	Expression analysis of NCC, neuronal, glia, smooth muscle, melanocyte and chondrocyte marker genes in O9-1 cells.....	63
Figure 6:	RT-PCR analysis of <i>Chd7</i> expression in JoMa cells and O9-1 cells .....	64
Figure 7:	Western blot analysis of <i>Chd7</i> expression in JoMa cells and O9-1 cells .....	64
Figure 8:	<i>Chd7</i> immunocytochemical staining of O9-1 cells.....	66
Figure 9:	Expression analysis of semaphorin receptors in O9-1 cells .....	67
Figure 10:	Expression analysis of class 3 semaphorins in O9-1 cells .....	67
Figure 11:	Sema3a immunocytochemical staining of O9-1 cells.....	68
Figure 12:	Schematic representation of full-length Sema3a protein.....	69
Figure 13:	Isoforms of Sema3a resulting from proteolytic processing and dimerization .....	71
Figure 14:	Schematic representation of proteolytic processed and dimerized Sema3a isoforms identified in concentrated medium as well as cytoplasmic and nuclear protein extracts of O9-1 cells .....	72
Figure 15:	Analysis of the <i>Chd7</i> expression in O9-1 cells after <i>Chd7</i> downregulation...	73
Figure 16:	Analysis of the <i>Sema3a</i> expression in O9-1 cells after <i>Chd7</i> downregulation.....	74
Figure 17:	Co-immunoprecipitation of <i>Chd7</i> with Sema3a in O9-1 cells .....	75
Figure 18:	<i>SEMA3A</i> mutation found in a <i>CHD7</i> -positive CHARGE syndrome patient...	77
Figure 19:	Schematic representation of full length <i>SEMA3A</i> protein with identified mutation .....	77
Figure 20:	Expression and proteolytic processing of transient overexpressed <i>SEMA3A</i> WT and <i>SEMA3A</i> variants in HEK293 cells.....	80
Figure 21:	Secretion and dimerization of transient overexpressed <i>SEMA3A</i> WT and <i>SEMA3A</i> variants in HEK293 cells .....	82

---

Figure 22: Co-immunoprecipitation of CHD7 with SEMA3A WT and SEMA3A variants in HEK293 cells .....	84
Figure 23: Expression of the full-length SEMA3A isoform in yeast cells .....	86
Figure 24: Schematic overview of the used CHD7 yeast two-hybrid assay plasmids .....	87
Figure 25: Yeast two-hybrid assay .....	88

List of tables

Table 1:      Sema3a isoforms detected in concentrated medium as well as  
                 cytoplasmic and nuclear protein extracts of O9-1 cells .....72

## Abbreviations

---

3'	3' terminus of DNA
5'	5' terminus of DNA
4-OHT	4-hydroxytamoxifen
%	percent
$\alpha$	alpha
$\Delta$	delta
+	plus
-	minus
$\pm$	plus/minus
>	greater than <u>or</u> replacement to
<	less than
$\leq$	less than or equal to
~	tilde (approximately)
$\infty$	infinity
®	registered trademark
™	unregistered trademark

## A

---

A	adenine <u>or</u> alanine
aa	amino acids
Ab	antibody
Actg2	actin, gamma 2, smooth muscle enteric
ADA2	adaptor 2
ADAM	<u>a</u> <u>d</u> isintegrin <u>and</u> a <u>m</u> etalloprotease domain
ADAMTS1	ADAM with <u>t</u> hrombos <u>p</u> ondin motif <u>1</u>
Ade	adenine
ATCC	American Type Culture Collection
ATP	adenosine triphosphate
ATPase	adenosine triphosphatase

**B**

---

Baf47	Brahma-associated factor 47
bp	base pairs
BRG1	Brahma-related gene 1
BRK	brahma and kismet
BSA	bovine serum albumin

**C**

---

°C	centigrade
C	carboxyl-terminus <u>or</u> cytoplasmic protein extract <u>or</u> cytosine
c.	cDNA reference sequence
CaCl <sub>2</sub>	calcium chloride
cDNA	complementary deoxyribonucleic acid
CEE	chicken embryo extract
CHD	chromodomain helicase DNA-binding
CHD7 / Chd7	chromodomain helicase DNA-binding protein 7
ChIP	chromatin immunoprecipitation
Chromo	chromodomain
CIL	contact inhibition of locomotion
cM	concentrated cell culture medium
CMV	pCMV vector
Cnn1	calponin 1
CO <sub>2</sub>	carbon dioxide
Co-IP	co-immunoprecipitation
Col2a1	collagen, type II, alpha 1
CR1, 2, 3	conserved region 1, 2, 3
Cre	<u>c</u> auses <u>r</u> ecombination
Ct	threshold cycle
CUB	complement C1r/C1s-Uegf-Bmp1
Cy3	cyanine 3

**D**

---

d	day
---	-----

DAPI	4',6-diamidino-2-phenylindole
dATP	deoxyadenosine triphosphate
dCTP	deoxycytidine triphosphate
ddH <sub>2</sub> O	bi-distilled water
DEPC	diethyl pyrocarbonate
dGTP	deoxyguanosine triphosphate
DMEM	Dulbecco's Modified Eagle Medium
DMSO	dimethyl sulfoxide
DNA	deoxyribonucleic acid
DNase I	deoxyribonuclease I
dNTP	deoxynucleotide triphosphates
DO	dropout
DPBS	Dulbecco's Phosphate-Buffered Saline
DPBST	Dulbecco's Phosphate-Buffered Saline with Tween 20
<i>DpnI</i>	<i>Diplococcus pneumonia</i> I
DTT	1,4-dithiothreitol
dTTP	desoxythymidin triphosphate

---

**E**

E	<i>EcoRI</i> or embryonic day
<i>EcoRI</i>	<i>Escherichia coli</i> , strain R I
EDTA	ethylenediaminetetraacetic acid disodium salt dihydrate
EGF	epidermal growth factor
EMT	epithelial-to-mesenchymal transition
Epha3	Ephrin receptor A3
Epha5	Ephrin receptor A5
Epha7	Ephrin receptor A7
ESC	embryonic stem cell
ET	endothelin
<i>et al.</i>	<i>et alii</i> (and others)

---

**F**

FB	fibroblast
----	------------

FBS	fetal bovine serum
FGF-2	fibroblast growth factor-2
FV/VIII	coagulation factor V/VIII homology-like

---

**G**

---

G	guanine
g	gram
<i>g</i>	gravitational acceleration (9.81 m/s <sup>2</sup> )
GAD	pGADT7 vector
GAP	guanosine triphosphatase (GTPase) activating protein
gDNA	genomic deoxyribonucleic acid
GDNF	glial cell line-derived neurotrophic factor
Gfap	glial fibrillary acidic protein
GFP	green fluorescent protein
GPI	glycosylphosphatidylinositol

---

**H**

---

h	hour <u>or</u> human
H <sub>2</sub> O	water
HA	hemagglutinin
HCl	hydrochloric acid
HEK	human embryonic kidney
HeLa	Henrietta Lacks
His	histidine
Hprt	hypoxanthine-guanine phosphoribosyltransferase
HRP	horseradish peroxidase

---

**I**

---

I	isoleucine
ICC	immunocytochemistry
Ig	immunoglobulin
IPT	Ig-like-plexin-transcription factors
ISH	<i>in situ</i> hybridization



---

**K**

---

kb	kilo base
KCl	potassium chloride
kDa	kilo Dalton
KH <sub>2</sub> PO <sub>4</sub>	potassium dihydrogen phosphate

---

**L**

---

l	liter
LB	lysogeny broth
LDS	lithium dodecyl sulfate
Leu	leucine
LiAc	lithium acetate
LIF	leukemia inhibitory factor
-LT	without leucine, tryptophan
-LTHA	without leucine, tryptophan, histidine, adenine

---

**M**

---

μ	micro (10 <sup>-6</sup> )
μg	microgram
μl	microliter
μM	micromolar
μm	micrometer
M	molar
m	milli (10 <sup>-3</sup> ) <u>or</u> mouse
MAM	meprin-like
MEM	minimum essential medium
MES	2-(N-morpholino)ethanesulfonic acid
mg	milligram
MgCl <sub>2</sub>	magnesium chloride
MIM	Mendelian Inheritance in Man
min	minute
ml	milliliter
mM	millimolar

mol	mole
MWCO	molecular weight cut-off
Myco	mycoplasma

---

**N**

---

N	nuclear protein extract <u>or</u> amino-terminus
n	nano ( $10^{-9}$ )
NaCl	sodium chloride
Na <sub>2</sub> HPO <sub>4</sub>	disodium hydrogen phosphate
NaOH	sodium hydroxide
NC	negative control
NCC	neural crest cell
N-CoR	nuclear receptor co-repressor
NEAA	non-essential amino acids
Nefh	neurofilament, heavy polypeptide
ng	nanogramm
Ngfr	nerve growth factor receptor (previously named P75)
NM	NCBI accession number
nM	nanomolar
NP	NCBI reference sequence for proteins
Nrp1	neuropilin 1
Nrp2	neuropilin 2
n.s.	not significant

---

**O**

---

OD	optical density
----	-----------------

---

**P**

---

p	protein
p.	protein reference sequence
P75	nerve growth factor receptor
Pa	Pascal, unit of pressure
Pax3	paired box 3

PBAF	polybromo- and BRG1-associated factor containing complex
PBS	phosphate buffered saline
PC	positive control
pCMV	plasmid cytomegalovirus
PCR	polymerase chain reaction
PDGF	platelet derived growth factor
Pdgfc	platelet-derived growth factor C
PEG	polyethylene glycol
PFA	paraformaldehyde
pH	potential of hydrogen
PLA	proximity ligation assay
Plxna1	Plexin A1
PNS	peripheral nervous system
PSI	plexin-semaphorin-integrin
PVDF	polyvinylidene fluoride

---

**Q**

q	long arm of the chromosome
qRT	quantitative real-time PCR
qRT-PCR	quantitative real-time PCR

---

**R**

R	arginine
RbBP5	retinoblastoma-binding protein 5
RNA	ribonucleic acid
RT	room temperature
RT-PCR	real-time PCR

---

**S**

S	<i>Sfi</i> I
s	second
SANT	<u>s</u> witching-defective protein 3 (SWI3), <u>a</u> daptor 2 (ADA2), <u>n</u> uclear receptor co-repressor (N-CoR), <u>t</u> ranscription factor (TF) IIIB

SDF1	stromal cell-derived factor 1
SDS	sodium dodecyl sulfate
SDS-PAGE	sodium dodecyl sulfate polyacrylamide gel electrophoresis
SEMA / Sema	Semaphorin
SEMA3A / Sema3a	sema domain, immunoglobulin domain (Ig), short basic domain, secreted, (semaphorin) 3a
SEMA3C / Sema3c	sema domain, immunoglobulin domain (Ig), short basic domain, secreted, (semaphorin) 3c
SEMA3D / Sema3d	sema domain, immunoglobulin domain (Ig), short basic domain, secreted, (semaphorin) 3d
SEMA3E / Sema3e	sema domain, immunoglobulin domain (Ig), short basic domain, secreted, (semaphorin) 3e
seq	sequencing
<i>Sfil</i>	<i>Streptomyces fimbriatus</i> I
siRNA	short interfering RNA
Snai1	snail family zinc finger 1
Snai2	snail family zinc finger 2
SNF2	sucrose non-fermentable 2
S.O.C.	super optimal broth with catabolite repression
Sox9	sex determining region Y (SRY)-box 9
Sox10	sex determining region Y (SRY)-box 10
SRY	sex determining region of chromosome Y
SWI2	switch 2
SWI3	switching-defective protein 3

## T

---

T	threonine <u>or</u> thymine
<i>Taq</i>	<i>Thermus aquaticus</i>
TBE	tris-borate-EDTA
TBP	TATA box binding protein
TBS	Tris-buffered saline
TBST	tris-buffered saline with tween 20
TE	Tris-EDTA
TF IIIB	transcription factor IIIB

TK	tyrosine kinase
Tris	tris(hydroxymethyl)aminomethane
Trp	tryptophan
Twist1	twist basic helix-loop-helix transcription factor 1
Tyr	tyrosinase

---

**U**

U	Unit (enzyme activity)
UV	ultraviolet light

---

**V**

V	valine <u>or</u> Volt
VEGF	vascular endothelial growth factor
Vegfc	vascular endothelial growth factor C

---

**W**

W	tryptophan
WB	western blot
Whi	Whirligig
Wnt1	Wnt family member 1
WT	wild type
w/v	weight/volume

---

**X**

x <i>g</i>	multiple of gravitational acceleration
------------	--

---

**Y**

Y2H	yeast two-hybrid
YNB	yeast nitrogen base

# 1 Introduction

## 1.1 CHARGE Syndrome

### 1.1.1 Chromodomain helicase DNA-binding protein 7

Chromodomain helicase DNA-binding (CHD) proteins play a role in transcription activation and repression by ATP (adenosine triphosphate)-dependent chromatin remodeling (Kim *et al.*, 2008). For this function, all members of the CHD protein family share at the N-terminus two tandem chromodomains (chromatin organization modifier domains), followed by a SWI2/SNF2 (switch 2/sucrose non-fermentable 2)-like ATPase/helicase domain (Woodage *et al.*, 1997; Flaus *et al.*, 2006; Flanagan *et al.*, 2007). In humans, the CHD protein family consists of nine members who are divided into three subgroups according to their amino acid sequence and additional functional protein domains. CHD7 is one of the nine CHD family members and belongs to subgroup III. Characteristics of this subgroup are three conserved regions (CR1–CR3), a SANT (switching-defective protein 3 (SWI3), adaptor 2 (ADA2), nuclear receptor co-repressor (N-CoR), transcription factor (TF) IIIB) domain and two tandem BRK (brahma and kismet) domains (Hall and Georgel, 2007; Marfella and Imbalzano, 2007) (Figure 1). The human *CHD7* gene (MIM 608892) is located on chromosome 8 (8q12.2) and encodes 38 exons. It is highly conserved across species and orthologs have been identified in mouse, chicken, zebrafish, *Xenopus laevis* and others (Bosman *et al.*, 2005; Aramaki *et al.*, 2007; Bajpai *et al.*, 2010).

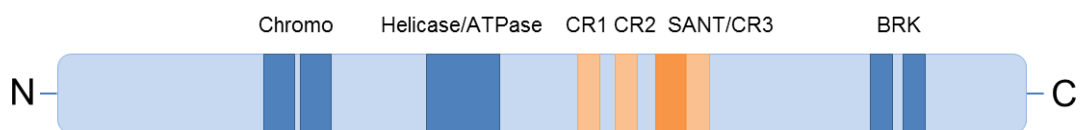


**Figure 1: Schematic representation of the CHD7 structure.** CHD7 is one of nine members of the CHD family that plays a role in controlling gene expression by ATP-dependent chromatin remodeling. CHD7 consists of two N-terminal chromodomains, a SWI2/SNF2-like ATPase/helicase domain, three conserved regions namely CR1, CR2 and CR3, a SANT domain and two BRK domains. Modified from Schulz *et al.* (2014a).

### 1.1.2 Mutations in *CHD7* lead to CHARGE syndrome

CHARGE syndrome (MIM 214800) is an autosomal dominant congenital malformation disorder known for its clinical variability. Reports of patients who were later found to have CHARGE were firstly published in 1979 independent by Hall (1979) and Hittner *et al.* (1979). Two years later, in 1981, Pagon *et al.* suggested for this disorder the acronym CHARGE. The acronym describes the main features seen in patients namely coloboma, heart defects, atresia of the choanae, retarded growth and development, genital hypoplasia and ear anomalies/deafness (Pagon *et al.*, 1981). The phrase 'CHARGE association' was renamed 2004 into 'CHARGE syndrome' after identification of *CHD7* mutations as the major disease cause (Vissers *et al.*, 2004; Aramaki *et al.*, 2006; Jongmans *et al.*, 2006; Lalani *et al.*, 2006; Sanlaville *et al.*, 2006; Wincent *et al.*, 2008). Blake *et al.* (1998) defined clinical criteria for the diagnosis of CHARGE syndrome. They were updated by Verloes (2005) defining coloboma, atresia of the choanae and hypoplastic semicircular canals as major signs and rhombencephalic dysfunction, hypothalamo-hypophyseal dysfunction, abnormal middle or external ear, malformations of mediastinal organs and mental retardation as minor signs. The incidence varies from 1:8500 to 1:10,000 (Blake *et al.*, 1998; Issekutz *et al.*, 2005). In the majority of patients with the suspected diagnosis CHARGE syndrome heterozygous mutations in the *CHD7* gene are found. Most of them are nonsense or frameshift mutations (due to small deletions or insertions), but also missense mutations can occur (Janssen *et al.*, 2012). To date, over 500 different pathogenic mutations have been identified which are distributed throughout the coding sequence as well as in some intronic sequences (Aramaki *et al.*, 2006; Jongmans *et al.*, 2006; Lalani *et al.*, 2006; Sanlaville *et al.*, 2006; Sanlaville and Verloes, 2007; Vuorela *et al.*, 2007; Janssen *et al.*, 2012; Martin, 2015). Most of them are *de novo* mutations, but also somatic and germline mosaicism in a parent were reported in families with more than one affected child (Jongmans *et al.*, 2006; Delahaye *et al.*, 2007; Jongmans *et al.*, 2008; Pauli *et al.*, 2009).

## 1.2 Neurocristopathies

Alterations in the complex succession of events required for induction, proliferation, migration and final differentiation of neural crest cells resulting in a large group of birth defects, which were firstly termed by Bolande (1974) neurocristopathies. The classification

of syndromes as a neurocristopathy evolved over the years now including numerous congenital malformation syndromes such as CHARGE, Kallmann, DiGeorge, Treacher-Collins, Waardenburg or Hirschsprung's disease (Siebert *et al.*, 1985; Etchevers *et al.*, 2006, 2007; Jones *et al.*, 2008; Passos-Bueno *et al.*, 2009; Keyte and Hutson, 2012). Interestingly, already in 1985, Siebert *et al.* postulated the belonging of CHARGE syndrome to the neurocristopathies (Siebert *et al.*, 1985) because of the affected structures. The most common clinical features seen in neurocristopathies include craniofacial defects, hearing loss, pigmentation and cardiac defects as well as missing of enteric ganglia (Mayor and Theveneau, 2013).

### **1.3 Neural crest cells – the fourth germ layer**

Neural crest cells (NCCs) are a population of multipotent and migratory progenitors found in all vertebrate embryos (Knecht and Bronner-Fraser, 2002; Milet and Monsoro-Burq, 2012). During embryogenesis they arise from the neural plate border which is induced by signaling between the neural and the non-neural ectoderm and from the underlying paraxial mesoderm (Gammill and Bronner-Fraser, 2003). The neural plate borders elevate during neurulation and cause the neural plate to fold over itself to form the neural tube (Gammill and Bronner-Fraser, 2003). In the neural plate border as well as in neighboring structures neural plate border specifier genes are upregulated (Bronner and LeDouarin, 2012). A further refinement of the border region results from the activation of neural crest specifiers, genes allowing NCCs the delamination from the neural folds or neural tube, the migration and differentiation into various derivatives (Bronner and LeDouarin, 2012) (Figure 2). NCCs migrate from the closing neural folds or from the dorsal neural tube through the embryo, following specific pathways to contribute to the formation of different organs and tissues like skin, heart or peripheral nervous system (PNS) (Gammill and Bronner-Fraser, 2003; Kuriyama and Mayor, 2008). Because of their ability to differentiate into various cell types like melanocytes, craniofacial cartilage and bone, smooth muscle, peripheral and enteric neurons and glia (Kuriyama and Mayor, 2008; Dupin and Sommer, 2012; Prasad *et al.*, 2012) (Figure 2), they were termed the 'fourth germ layer' (Hall, 2000). NCCs are divided into the cranial (cephalic), cardiac, trunk and enteric NCCs. The cranial NCCs contribute to craniofacial structures like bones and cartilages of the face and neck as well as tendons, muscles and connective tissue of the ear, eye, teeth and blood vessels (Mayor and Theveneau, 2013). In addition, they form most of the cranial PNS and



modulate brain growth and patterning (Mayor and Theveneau, 2013). The cardiac NCCs are a subpopulation of the cranial NCCs and essential for the septation of the heart outflow tract (Mayor and Theveneau, 2013). The trunk NCCs form pigment cells, the dorsal root and sympathetic ganglia of the PNS and endocrine cells of the adrenal gland, whereas the enteric NCCs form the enteric PNS of the gut, which controls the digestive track (Mayor and Theveneau, 2013).

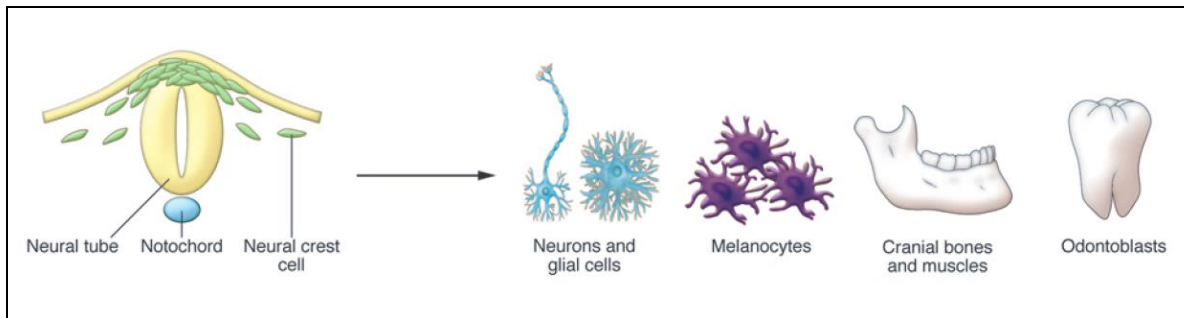


**Figure 2: Delamination and differentiation of NCCs.** NCCs delaminate from the closing neural folds or from the dorsal neural tube and differentiate into neurons of the peripheral nervous system, glial cells, melanocytes, cranial bones and muscles, odontoblasts or other cell types. Modified from Acloque *et al.* (2009).

### 1.3.1 Migration of NCCs

The migration of NCCs is a complex and multi-step process. Interestingly, Bajpai *et al.* (2010) demonstrated in humans and in the animal model *Xenopus laevis* an essential role for CHD7 in the formation and migration of NCCs by activating neural crest specifier genes as the transcription factors *SNAI2* (snail family zinc finger 2, previously named *Slug*), *TWIST* (twist basic helix-loop-helix transcription factor) and *SOX9* (SRY(sex determining region Y)-box containing gene 9). NCCs originate at the border between the neural and the non-neural ectoderm along the anteroposterior length of the developing embryo (Gong, 2014). Before NCCs are able to delaminate from the closing neural folds or from the dorsal neural tube, they undergo a process called epithelial-to-mesenchymal transition (EMT) in which the NCCs lose their cell-cell contacts, reorganize their cytoskeleton and acquire a motile phenotype (Kirby and Hutson, 2014). Premigratory NCCs form an epithelium with a typical apical-basal polarity which is surrounded by an underlying basement membrane (Kerosuo and Bronner-Fraser, 2012). During EMT, the polarity gets lost due to a progressive replacement of tight junctions by gap junctions

(Kuriyama and Mayor, 2008). Furthermore, a shift from type I to type II cadherins, a group of transmembrane proteins, results in a lower adhesiveness of the cells which allows them to increase their motility (Mayanil, 2013). Kerosuo and Bronner-Fraser (2012) point out that extracellular matrix proteins, such as ADAM proteins (proteins containing a disintegrin and a metalloprotease domain) and matrix metalloproteinases induce a breakdown of the basement membrane to allow migration. After undergoing EMT, the NCCs initially delaminate as a continuous wave which quickly splits into discrete streams ventrally down the embryo displaying a range of migratory behaviors (Shellard and Mayor, 2016). Some NCCs exhibit an individual migratory behavior. But although the NCCs undergo EMT, most of them migrate together, either as chains, groups or even single sheets (Kulesa *et al.*, 2010; Theveneau and Mayor, 2012; Shellard and Mayor, 2016). A process called contact inhibition of locomotion (CIL) prevent the NCCs during migration from overlapping with each other (Mayor and Carmona-Fontaine, 2010). After contact with one another, the migrating NCCs momentarily stop and favors dispersion in the opposite direction (Mayor and Carmona-Fontaine, 2010). Nevertheless, the chemoattractant mediated phenomenon of co-attraction allows collective migration of the NCCs in spite of reduced cell-cell adhesion due to EMT and dispersion of the cells induced by CIL (Carmona-Fontaine *et al.*, 2011). The split of NCCs into distinct streams and their precise targeting to their destinations are controlled by a plethora of positive and negative regulators including signaling molecules and mediated via binding of external ligands to receptors on the NCC surface (Theveneau and Mayor, 2012). Negative guidance cues are located at the borders of the migration pathways whereas the locations of positive guidance cues are along the pathways or within the NCC target regions (Theveneau and Mayor, 2012). Some of the main signals regulating NCC migration are semaphorins, ephrins/Ephs, slits, ETs (endothelins), SDF1 (stromal cell-derived factor 1), VEGFs and PDGFs (vascular endothelial and platelet-derived growth factors), FGFs (fibroblast growth factors) and GDNF (glial cell line-derived neurotrophic factor) (Theveneau and Mayor, 2012). Schulz *et al.* (2014b) performed a genome-wide microarray expression analysis on whole wildtype and Chd7 deficient (Chd7<sup>Whi/+</sup> and Chd7<sup>Whi/Whi</sup>) mouse embryos of the *Whirligig* mouse line at E9.5, a point in time of NCC migration. They identified a misregulation of genes involved in the migration and guidance of NCCs such as the semaphorins *Sema3a*, *3c* and *3d*, the ephrin receptors *Epha3*, *Epha5* and *Epha7* and the growth factors *Vegfc* and *Pdgfc* (vascular endothelial and platelet-derived growth factor C) that further underlines the important role of CHD7 in NCC development (Schulz *et al.*, 2014b).

## 1.4 Semaphorins

Semaphorins are a large family of phylogenetically conserved guidance cues and were originally identified as molecules that control axon pathfinding during the development of the nervous system (Kolodkin *et al.*, 1993). They are involved in many biological processes, including the regulation of immune responses (Suzuki *et al.*, 2008; Takamatsu and Kumanogoh, 2012), cardiogenesis (Toyofuku *et al.*, 2007; Toyofuku *et al.*, 2008), angiogenesis (Serini *et al.*, 2003) and vasculogenesis (Gu *et al.*, 2005) as well as oncogenesis (Sekido *et al.*, 1996). Furthermore, Semaphorins act as guidance cues for a range of migrating cells like the NCCs (Eickholt *et al.*, 1999). In these processes semaphorins can function either as positive or as negative guidance cues (Tamagnone and Comoglio, 2004). To date, more than 20 semaphorin types, secreted or membrane-associated proteins, have been discovered. All semaphorins are characterized by the presence of a conserved extracellular amino-terminal Sema (Semaphorin) domain, important for dimerization and binding specificity with receptors, followed by a PSI (plexin-semaphorin-integrin) domain and a C-terminus domain, which confers class specific features, such as basic, Ig (immunoglobulin)-like and thrombospondin domains (Janssen *et al.*, 2010; Liu *et al.*, 2010; Nogi *et al.*, 2010). Semaphorins are grouped into eight subfamily classes on the basis of structural and amino acid sequence similarity, containing invertebrate (classes 1 and 2), vertebrate (classes 3–7) and viral semaphorins (class V) (Jongbloets and Pasterkamp, 2014) (Figure 3). Semaphorins of the classes 2, 3 and V are secreted proteins while the other semaphorins are transmembrane proteins (classes 1, 4, 5 and 6) or GPI (glycosylphosphatidylinositol)-linked proteins (class 7) (Jongbloets and Pasterkamp, 2014). Nevertheless, membrane-associated semaphorins of the classes 4 and 7 can be further processed into soluble proteins by proteolytic degradation (Neufeld *et al.*, 2012). Although additional receptors as TK (tyrosine kinase) receptors or integrins have been described, the main semaphorin receptors are plexins and neuropilins (Winberg *et al.*, 1998; Takahashi *et al.*, 1999; Tamagnone *et al.*, 1999) (Figure 3). The nine vertebrate plexins are grouped into four subfamilies (A–D) and serve for the most semaphorins as direct binding receptors (Jongbloets and Pasterkamp, 2014). However, some secreted semaphorins, like most of class 3 semaphorins, require the presence of one of the two in vertebrates identified neuropilins (Nrp1 or Nrp2) as ligand-binding co-receptor (Jongbloets and Pasterkamp, 2014).

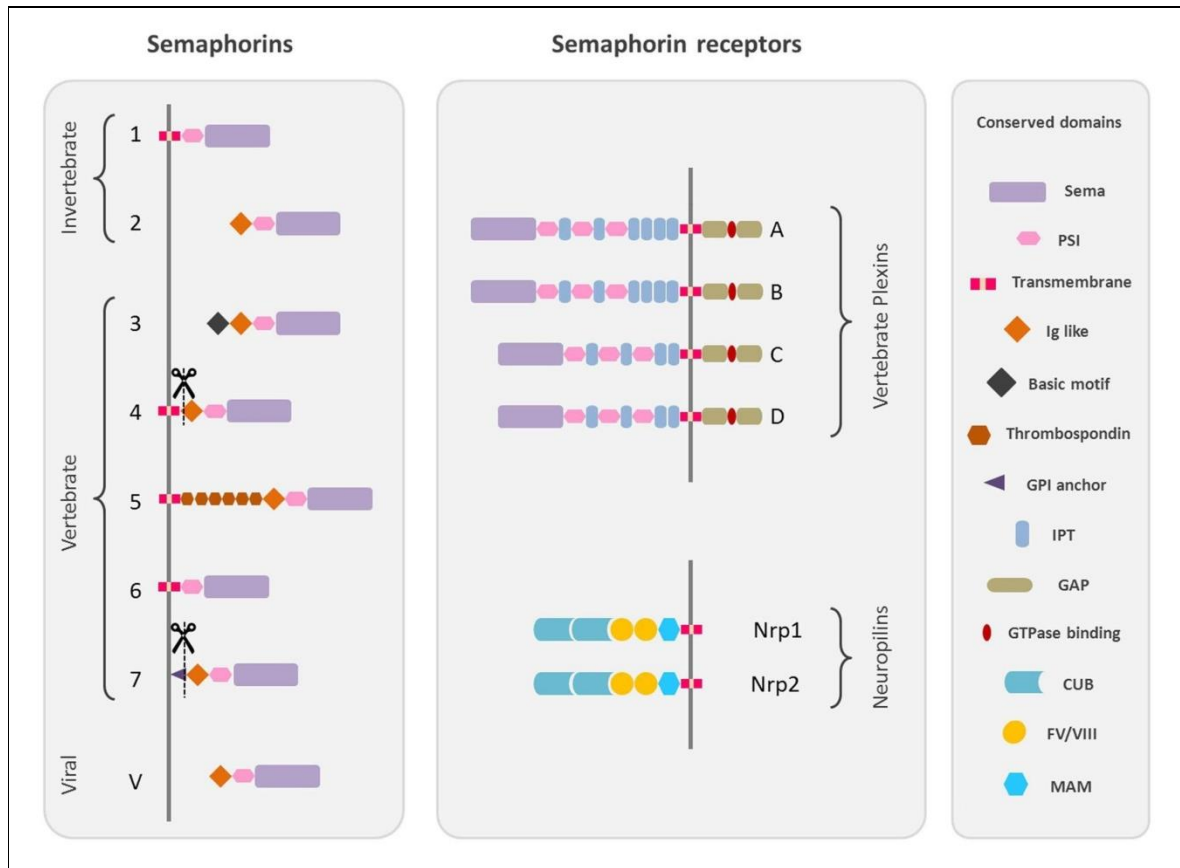


**Figure 3: Schematic representation of the protein structure of semaphorins and their main receptors.** Left column: Semaphorins are grouped into eight subfamily classes on the basis of structural and amino acid sequence similarity. The classes 1 and 2 contain invertebrate semaphorins, the classes 3–7 vertebrate semaphorins and the class V viral semaphorins. Semaphorins of the classes 2 and 3 are secreted proteins, the semaphorin classes 1, 4, 5 and 6 contain transmembrane proteins and the class 7 semaphorins are GPI-linked proteins. The membrane-associated semaphorins of the classes 4 and 7 can be processed into soluble proteins by proteolytic degradation indicated with scissors. All semaphorins are characterized by a Sema domain, a PSI domain and a specific C-terminus domain. Middle column: The main receptors for semaphorins are the plexins and neuropilins. The four subfamilies (A–D) of the nine vertebrate plexins, the two vertebrate neuropilins (Nrp 1 and Nrp 2) and their structures are shown. Right column: The structural conserved domains are drawn in different shapes and colors as indicated in the figure. Domains abbreviations: sema, semaphorin; PSI, plexin-semaphorin-integrin; Ig-like, immunoglobulin-like; GPI, glycosylphosphatidylinositol; IPT, Ig-like-plexin-transcription factors; GAP, guanosine triphosphatase (GTPase) activating protein; CUB, complement C1r/C1s-Uegf-Bmp1; FV/VIII, coagulation factor V/VIII homology-like; MAM, meprin-like. Modified from Messina and Giacobini (2013).

### 1.4.1 Class 3 semaphorins

The class 3 semaphorins are produced as secreted proteins and consist of seven subgroups (3A-3G). Adams *et al.* (1997) verified that the initially synthesized pro-form undergoes proteolytic processing by furin or furin-like endoproteases generating functionally different isoforms. They pointed out that the consensus sequences for furin-dependent processing are highly conserved in all class 3 semaphorin proteins indicating a similar mechanism of regulation for all secreted semaphorins (Adams *et al.*, 1997). For semaphorin 3C (SEMA3C), the proteolytic processing also induced by the matrix metalloprotease ADAMTS1 (ADAM with thrombospondin motif 1), resulting in a promoted cell migration in contrast to other class 3 semaphorins, was proved by Esselens *et al.* (2010). Adams *et al.* (1997) assumed that the activity of all secreted class 3 semaphorins depends on the extent of their proteolytic processing. Furthermore, dimerization of class 3 semaphorins were identified (Klostermann *et al.*, 1998; Koppel and Raper, 1998). The existence of monomeric, dimeric and processed isoforms were proved for semaphorin 3E (SEMA3E) (Christensen *et al.*, 2005).

### 1.4.2 SEMA3A mutations contribute to the phenotype of Kallmann syndrome

The involvement of semaphorin 3A (SEMA3A) in the navigation of primary olfactory axons during embryogenesis contributes to the phenotype of Kallmann syndrome (MIM 147950) (Hanchate *et al.*, 2012; Young *et al.*, 2012). This genetically heterogeneous congenital disorder is characterized by hypogonadotropic hypogonadism and an impaired sense of smell (Dodé and Hardelin, 2009). SEMA3A mutations were identified in Kallmann syndrome patients (Hanchate *et al.*, 2012). Nevertheless, it was suggested that one heterozygous SEMA3A mutation alone cannot cause the symptoms, while a combination of a SEMA3A mutation with other gene mutations (digenic inheritance) can lead to the disease phenotype (Hanchate *et al.*, 2012). Mutations in the *Chd7* gene can be found in a minority of Kallmann syndrome patients (Kim *et al.*, 2008; Bergman *et al.*, 2011) and for this reason it was assumed that Kallmann syndrome represents the mild end of the phenotypic spectrum of CHARGE syndrome (Jongmans *et al.*, 2009). Interestingly, Schulz *et al.* (2014b) confirmed an regulatory loop between *Chd7* and *Sema3a* in mouse and *Xenopus laevis*.

## 1.5 Aim of the present study

It was shown that *CHD7*, the gene mutated in CHARGE syndrome, regulates genes which are involved in NCC formation and guidance as well as in interactions between NCCs and other tissues (Schulz *et al.*, 2014b). Furthermore, it was assumed that *SEMA3A* mutations contribute to the pathogenesis of CHARGE syndrome (Schulz *et al.*, 2014b).

The aim of the present study was to elucidate the pathomechanism behind the neurocristopathy CHARGE syndrome and especially the role of *SEMA3A* in the pathogenesis of this complex malformation disorder.

### Establishment of an NCC model

- To provide a suitable cell culture model for the analysis of NCCs *in vitro*, two different mouse NCC lines (a truncal and a cranial) should be tested for different marker genes using RT-PCR analysis in order to confirm the status of the NCCs.
- In both the truncal and the cranial NCC line the expression of *Chd7* should be analyzed by RT-PCR and western blot analysis.
- The expression of the main class 3 semaphorin receptors, namely plexins and neuropilins, should be verified in NCCs using RT-PCR analysis.

### Role of *SEMA3A* in the pathogenesis of CHARGE syndrome

- CHARGE syndrome patients with a pathogenic *CHD7* mutation should be screened for additional mutations in the *SEMA3A* gene by sequencing analysis.
- The effect of the identified *SEMA3A* mutations should be investigated *in vitro*. Therefore, plasmids with the wildtype *SEMA3A* and the identified *SEMA3A* mutations should be generated. By western blot analysis, the wildtype and the variants of *SEMA3A* should be analyzed using a human cell culture system. Interactions between *CHD7* and the wildtype *SEMA3A* as well as the *SEMA3A* variants should be identified with co-immunoprecipitation experiments and should be further examined using yeast two-hybrid assay.

## 2 Materials and Methods

### 2.1 Materials

#### 2.1.1 Technical equipment

Technical equipment	Manufacturer
6-Tube Magnetic Separation Rack	New England Biolabs, Frankfurt/M
2720 Thermal Cycler	Applied Biosystems, Darmstadt
3500xL Genetic Analyzer	Applied Biosystems, Darmstadt
7900HT Fast Real-Time PCR System	Applied Biosystems, Darmstadt
Accu-jet®	Brand, Wertheim
Arium® 611	Sartorius, Göttingen
Autoclaves	
DX-150	Systec, Linden
FVS/2	Fedegari, Bedano (Suisse)
VX-95	Systec, Linden
Balance CP3202S	Sartorius, Göttingen
Camera (gel electrophoresis documentation)	Vilbert Lourmat, Eberhardzell
Centrifuges	
4K15	Sigma, Osterode
Heraeus Biofuge™ Primo	Thermo Electron LED, Osterode
Heraeus Fresco™ 21	Thermo Electron LED, Osterode
Micro Centrifuge IR	Carl Roth, Karlsruhe
Microfuge 1-15	Sigma, Osterode
Heraeus Multifuge X3R	Thermo Electron LED, Osterode
Dry cabinet	Memmert, Schwabach
Electrophoresis chamber	Central workshop, University of Göttingen
FluorChem® Q	Alpha Innotech, Logan (USA)
Freezers	
–20°C	Liebherr, Ochsenhausen
–80°C	Sanyo, Moriguchi (Japan)
Herasafe™ (biological safety cabinet)	Thermo Electron LED, Langenselbold
Incubators	
for bacteria (37°C)	Memmert, Schwabach
for cell culture (37°C)	Sanyo, Munich
for yeast (30°C)	Memmert, Schwabach
Innova® 40 (incubation shaker)	New Brunswick Scientific, Nürtingen
Laboport®-Membrane-Vacuumpump N86KN.18	KNF Neuberger, Freiburg

Magnetic stirrer	IKA Labortechnik, Staufen
Microscopes	
confocal laser scanning microscope IX81	Olympus, Hamburg
inverted routine microscope Primovert	Zeiss, Göttingen
stereo microscope Stemi SV 11	Zeiss, Göttingen
Microwave OMW 310-S	ok. / Venalisia Import, Ingolstadt
Mini Protean® II Cell	Bio-Rad, Munich
NanoDrop 2000c	Peqlab, Erlangen
Novex® Mini-Cell Electrophoresis System	Invitrogen, Karlsruhe
pH-Meter PB-11	Sartorius, Göttingen
Pipettes	
Multipette® M4	Eppendorf, Hamburg
Pipetman	Gilson, Limburg-Offheim
Research	Eppendorf, Hamburg
Transferpette®-8	Brand, Wertheim
Power supplies	
Apelex PS 304 minipac II	Biostep, Jahnsdorf
Power PAC 3000	Bio-Rad, Munich
Printer system (gel electrophoresis documentation)	
Doc print™ VX2	Peqlab, Erlangen
P95	Mitsubishi Electric, Tokyo (Japan)
Refrigerators	Liebherr, Ochsenhausen
	Bosch, Stuttgart
	Karl Hecht, Sondheim
Roll shaker RM5 Assistent 348	
Scissors	
HSB 006-10	Hammacher, Solingen
HSB 530-08	Hammacher, Solingen
Semi-Automatic Sheet Heat Sealer	4titude, Berlin
Shaker	IKA Labortechnik, Staufen
Steel bead, stainless (ø 5 mm)	Qiagen, Hilden
Sterilizer	Memmert, Schwabach
Stuart® SB2 rotator	Bibby Scientific, Staffordshire (UK)
Synergy™ Mx plate reader	BioTek, Friedrichshall
Thermomixer 5436 / compact	Eppendorf, Hamburg
TissueLyser LT	Qiagen, Hilden
Tweezer HWC 110-10	Hammacher, Solingen
UVsolo TS Imaging System	Biometra, Göttingen
UV table ECX-F20.M	PeqLab, Erlangen
Vortex-Genie® 2	Scientific Industries, New York (USA)
Water bath	GFL, Großburgwedel



### 2.1.2 Consumable materials

Product name	Manufacturer
Blotting Paper Sheets	Sartorius, Göttingen
Cell culture flasks	
25 cm <sup>2</sup> , 75 cm <sup>2</sup> with filter	Sarstedt, Nümbrecht
75 cm <sup>2</sup> without filter	Greiner Bio-One, Frickenhausen
300 cm <sup>2</sup> with filter	TPP, Trasadingen (Switzerland)
Cell culture plates	
96-well	Nuclon A/S, Roskilde (Danmark)
24-well	Th. Geyer, Renningen
12-well	Greiner Bio-One, Frickenhausen
6-well	Greiner Bio-One, Frickenhausen
10 cm ø	Nuclon A/S, Roskilde (Danmark)
Glas bottles	Schott, Mainz / Biochrom, Berlin
Combitips (advanced)	Eppendorf, Hamburg
Counting chamber, bright-lined (Neubauer)	Sarstedt, Nümbrecht
Cover glasses (24 x 60 mm)	Menzel Gläser, Braunschweig
Cryovials	Greiner Bio-One, Frickenhausen
Culture slides (8-well)	BD Biosciences, Heidelberg
Cuvettes, 10 mm	Sarstedt, Nümbrecht
Disposable syringes	BD Biosciences, Heidelberg
Filter (ø 0.20 µm, ø 0.45 µm)	Th. Geyer, Renningen
Gas cartouche (propane/butane)	Th. Geyer, Renningen
Glass pipettes	Schütt, Göttingen
Gloves	Lab Logistic Group, Meckenheim
Amersham <sup>TM</sup> Protran <sup>TM</sup> Supported 0.45 µm NC	GE Healthcare, Freiburg
Amersham <sup>TM</sup> Hybond <sup>TM</sup> -P PVDF Transfer Membrane	GE Healthcare, Freiburg
0.45 µm	
Mr. Frosty <sup>TM</sup> Freezing Container	Kisker, Steinfurt
MultiScreen <sup>®</sup> PCR96 Filter Plates	Merck Millipore, Darmstadt
NuPAGE <sup>®</sup> 3–8% Tris-Acetate Gels, 1.0 mm, 10-well	Invitrogen, Karlsruhe
NuPAGE <sup>®</sup> 4–12% Bis-Tris Gels, 1.0 mm, 10-well	Invitrogen, Karlsruhe
NuPAGE <sup>®</sup> 4–12% Bis-Tris Midi Gels, 1.0 mm, 20-well	Invitrogen, Karlsruhe
Pasteur pipettes	Th. Geyer, Renningen
PCR cups (0.2 ml)	Sarstedt, Nümbrecht
Petri dishes	Sarstedt, Nümbrecht
Pipette tips (without filter)	Glasgerätebau Ochs, Bovenden
Pipette tips (with filter)	Kisker, Steinfurt
qRT-PCR plates (384-well)	4titude, Berlin

qRT-PCR Adhesive Clear Seals	4titude, Berlin
Reaction tubes (1.5 ml, 2 ml)	Glasgerätebau Ochs, Bovenden
Scalpel	Pfm medical, Cologne
Serological pipettes	
2 ml, 5 ml, 10 ml	Sarstedt, Nümbrecht
25 ml	Greiner Bio-One, Frickenhausen
Transfection tubes	Sarstedt, Nümbrecht
Transfer pipettes (3.5 ml)	Sarstedt, Nümbrecht
Tubes	
13 ml	Sarstedt, Nümbrecht
15 ml, 50 ml	Greiner Bio-One, Frickenhausen
Vivaspin® Turbo 15 (30 kDa MWCO)	Sartorius, Göttingen

### 2.1.3 Chemicals, biochemicals and reagents

Chemical / Biochemical / Reagent	Manufacturer
1-Thioglycerol	Sigma-Aldrich, Deisenhofen
1,4-Dithiothreitol (DTT)	AppliChem, Darmstadt
4-Hydroxytamoxifen (4-OHT)	Sigma-Aldrich, Deisenhofen
Acetic acid	Merck, Darmstadt
Adenine hemisulfate salt	Sigma-Aldrich, Deisenhofen
Agar-Agar, Kobe I	Carl Roth, Karlsruhe
Agarose	Peqlab, Erlangen
Ammonium sulfate	Carl Roth, Karlsruhe
Ampicillin sodium salt	Carl Roth, Karlsruhe
Ampuwa®	Fresenius, Bad Homburg
B-27® Supplement (50x)	Gibco, Eggenstein
Barricidal®	Interchem Hygiene, Zürich (Switzerland)
Boric acid	ICN Biomedicals, Eschwege
Bovine serum albumin (BSA) Fraction V	PAA Laboratories, Linz (Austria)
Bovine Serum Albumin Standard Ampules (2 mg/ml)	Thermo Scientific, Rockford (USA)
Bromphenolblue	Carl Roth, Karlsruhe
Calcium chloride (CaCl <sub>2</sub> )	Carl Roth, Karlsruhe
Chloroform	J.T. Baker, Griesheim
Chicken embryo extract (CEE)	Dr. Sven Lindner, Ruhr-University Bochum
Complete ES Cell Medium with 15% FBS and LIF	Merck Millipore, Darmstadt
cOmplete™ Protease Inhibitor Cocktail Tablets	Roche, Penzberg
Cryo-SFM	PromoCell, Heidelberg

D(+)-Glucose	Carl Roth, Karlsruhe
Deoxynucleotide triphosphates (dNTPs)	Bio-Budget Technologies, Krefeld
Diethyl pyrocarbonate (DEPC)	Carl Roth, Karlsruhe
Dimethyl sulfoxide (DMSO)	Carl Roth, Karlsruhe
DirectPCR <sup>®</sup> Lysis Reagent Tail	Peqlab, Erlangen
Disodium hydrogen phosphate (Na <sub>2</sub> HPO <sub>4</sub> )	Carl Roth, Karlsruhe
DO Supplement (–Ade/–His/–Leu/–Trp)	Clontech, Heidelberg
Dulbecco's Modified Eagle Medium (DMEM)	PAN-Biotech, Aidenbach
Dulbecco's Modified Eagle Medium/Nutrient Mixture F-12 (DMEM/F-12)	Gibco, Eggenstein
Dulbecco's Phosphate-Buffered Saline (DPBS)	PAN-Biotech, Aidenbach
Epidermal growth factor, human (EGF)	Sigma-Aldrich, Deisenhofen
Ethanol	J.T. Baker, Griesheim
Ethidium bromide	Inno-Train Diagnostik, Kronberg/Ts.
Ethylenediaminetetraacetic acid disodium salt dihydrate (EDTA)	MP Biomedicals, Eschwege
Fetal bovine serum, SeraPlus (FBS)	PAN-Biotech, Aidenbach
Fibroblast growth factor 2, human (FGF-2)	Merck Millipore, Darmstadt PeproTech, Hamburg
Fibronectin, human (FC010)	Merck Millipore, Darmstadt
Fluoroshield <sup>™</sup> with Dapi	Sigma-Aldrich, Deisenhofen
Glycerol	Carl Roth, Karlsruhe
Glycine	Carl Roth, Karlsruhe
Halt <sup>™</sup> Protease Inhibitor Single Use Cocktail, EDTA-free (100x)	Thermo Scientific, Rockford (USA)
Hydrochloric acid (HCl)	J.T. Baker, Griesheim
Immersol <sup>™</sup> 518F	Zeiss, Oberkochen
Isopropanol	J.T. Baker, Griesheim
Kanamycin sulfate	Carl Roth, Karlsruhe
L-Histidine monohydrochloride monohydrate	Sigma-Aldrich, Deisenhofen
Lipofectamine <sup>®</sup> 2000 Transfection Reagent	Invitrogen, Karlsruhe
Lithium acetate (LiAc)	Carl Roth, Karlsruhe
Matrigel <sup>®</sup> Basement Membrane Matrix	Corning, Wiesbaden
Methanol	J.T. Baker, Griesheim
Milk powder	Carl Roth, Karlsruhe
MEM Non-Essential Amino Acids (NEAA)	Gibco, Eggenstein
N-2 Supplement (100x)	Gibco, Eggenstein
NuPAGE <sup>®</sup> LDS Sample Buffer (4x)	Invitrogen, Karlsruhe
NuPAGE <sup>®</sup> MES SDS Running Buffer (20x)	Invitrogen, Karlsruhe
NuPAGE <sup>®</sup> Tris-Acetate SDS Running Buffer (20x)	Invitrogen, Karlsruhe

Opti-MEM® I Reduced Serum Medium	Gibco, Eggenstein
P1 / P2 / P3 Buffer	Qiagen, Hilden
Paraformaldehyde (PFA)	Carl Roth, Karlsruhe
Penicillin-Streptomycin	Gibco, Eggenstein
Peptone ex casein	Carl Roth, Karlsruhe
Polyethylene glycol 4000 (PEG4000)	Carl Roth, Karlsruhe
Potassium chloride (KCl)	Carl Roth, Karlsruhe
Potassium dihydrogen phosphate (KH <sub>2</sub> PO <sub>4</sub> )	Carl Roth, Karlsruhe
Proteinase K	Carl Roth, Karlsruhe
Protein G Magnetic Beads	New England Biolabs, Frankfurt/M
Random Hexamers (50 µM)	Invitrogen, Karlsruhe
Restriction endonucleases	Invitrogen, Karlsruhe
	New England Biolabs, Frankfurt/M
Roti®-Nanoquant	Carl Roth, Karlsruhe
Roti®-Safe	Carl Roth, Karlsruhe
S.O.C. medium	Invitrogen, Karlsruhe
Sodium acetate	Carl Roth, Karlsruhe
Sodium chloride (NaCl)	AppliChem, Darmstadt
Sodium hydroxide (NaOH)	J.T. Baker, Griesheim
Streptomycin sulfate salt	Sigma-Aldrich, Deisenhofen
TE buffer	Invitrogen, Karlsruhe
Thimerosal	Sigma-Aldrich, Deisenhofen
Tris(hydroxymethyl)aminomethane (Tris)	AppliChem, Darmstadt
Triton X-100	Serva, Heidelberg
Trizol Reagent	Invitrogen, Karlsruhe
TrypLE™ Express	Gibco, Eggenstein
Trypsin-EDTA	PAN-Biotech, Aidenbach
Trypsin Inhibitor, from <i>Glycine max</i> (soy-bean)	Sigma-Aldrich, Deisenhofen
Tunicamycin from <i>Streptomyces</i> sp.	Sigma-Aldrich, Deisenhofen
Tween® 20	Carl Roth, Karlsruhe
Western Blocking Reagent	Sigma-Aldrich, Deisenhofen
Yeast extract	Carl Roth, Karlsruhe
Yeastmaker™ Carrier DNA	Clontech, Saint-Germain-en-Laye (France)
Yeast Nitrogen Base Without Amino Acids and Ammonium Sulfate (YNB)	Sigma-Aldrich, Deisenhofen

### 2.1.4 Ready-to-use reaction systems

Reaction system	Manufacturer
BigDye <sup>®</sup> Terminator v1.1 Cycle Sequencing Kit	Applied Biosystems, Darmstadt
DNase I Kit	Sigma-Aldrich, Deisenhofen
HiPure Plasmid Midiprep Kit	Invitrogen, Karlsruhe
HotStarTaq <sup>®</sup> Plus Master Mix Kit	Qiagen, Hilden
Immobilon <sup>™</sup> Western Chemiluminescent HRP Substrate	Merck Millipore, Darmstadt
Immolase <sup>™</sup> DNA Polymerase	Bioline, Luckenwalde
In-Fusion <sup>®</sup> HD Cloning Kit	Clontech, Saint-Germain-en-Laye (France)
MSB <sup>®</sup> Spin PCRapace Kit	Invitek, Berlin
NE-PER <sup>®</sup> Nuclear and Cytoplasmic Extraction Reagents Kit	Thermo Scientific, Rockford (USA)
<i>PfuUltra</i> <sup>®</sup> High-Fidelity DNA Polymerase	Agilent Technologies, Waldbronn
Platinum <sup>®</sup> Taq DNA Polymerase	Invitrogen, Karlsruhe
Q5 <sup>®</sup> High-Fidelity DNA Polymerase	New England Biolabs, Frankfurt/M
QIAquick <sup>®</sup> Gel Extraction Kit	Qiagen, Hilden
QuantiTect <sup>®</sup> SYBR <sup>®</sup> Green PCR Kit	Qiagen, Hilden
QuikChange II XL Site-Directed Mutagenesis Kit	Agilent Technologies, Waldbronn
Superscript <sup>™</sup> II Reverse Transcriptase Kit	Invitrogen, Karlsruhe

### 2.1.5 Sterilization

If not indicated differently, buffers and solutions were sterilized in a vapor autoclave for 20 min at 120°C and 10<sup>5</sup> Pa. Heat sensitive solutions were sterile filtrated using filtration units of 0.20–0.45 µm pore size. Laboratory equipment were either autoclaved as mentioned above or heat sterilized at 180°C overnight.

### 2.1.6 Buffers and solutions

Buffer / Solution	Composition
4-OHT solution	5.16 mM 4-OHT in Ethanol
Adenine solution	10 mg/ml Adenine in Ampuwa
Ampicillin solution	50 mg/ml Ampicillin in Ampuwa

Antibody diluent solution (Immunofluorescence staining)	1% BSA in DPBST
Antibody diluent solution I (Western blot analysis)	1% BSA or 2% milk powder in TBST
Antibody diluent solution II (Western blot analysis)	0.1% Casein solution in TBST
Blocking solution (Immunofluorescence staining)	300 mM Glycine 3% BSA 0.1% Tween 20 in PBS
Blocking solution I (Western blot analysis)	5% BSA or milk powder in TBST
Blocking solution II (Western blot analysis)	0.1% Casein solution in TBST
Casein solution (10%)	Western Blocking Reagent (with 10% Casein) 1% Thimerosal
dNTPs solution	10 mM dATP 10 mM dCTP 10 mM dGTP 10 mM dTTP in Ampuwa
DPBS with 0.1% Tween 20 (DPBST)	0.1% Tween 20 in DPBS
EGF (human) solution	0.25 mg/ml EGF in 0.1% BSA/10 mM Acetic acid
DEPC-H <sub>2</sub> O	0.1% Diethylpyrocarbonate in ddH <sub>2</sub> O Incubation for 24 h by stirring
FGF-2 (human) solution	25 µg/ml FGF-2 (Merck Millipore) in 1 mM 1-Thioglycerol / 0.01 mM Tris, pH 7.0  0.1 mg/ml FGF-2 (PeproTech) in 0.1% BSA/PBS

Fibronectin (human) solution	50 µg/ml Fibronectin in PBS
Glucose solution (40%)	40% Glucose in ddH <sub>2</sub> O autoclave for 15 min at 121°C
Glycerol solution (50%)	50% Glycerol in ddH <sub>2</sub> O
Histidine solution	10 mg/ml Histidine in Ampuwa
Kanamycin solution	50 mg/ml Kanamycin in Ampuwa
LiAc solution (10x)	100 mM LiAc in ddH <sub>2</sub> O adjust to pH 7.5 autoclave for 15 min at 121°C
Loading buffer (Agarose gel electrophoresis)	0.1 M EDTA 50% Glycerol 0.02% Xylene cyanol 0.02% Bromphenol blue 0.02% SDS in Ampuwa
Lysis buffer	300 mM NaCl 50 mM Tris-HCl, pH 7.5 5 mM EDTA 0.1% Triton X-100 Protease inhibitor cocktail tablet in ddH <sub>2</sub> O
PBS buffer (10x)	1.4 M NaCl 90 mM Na <sub>2</sub> HPO <sub>4</sub> 27 mM KCl 15 mM KH <sub>2</sub> PO <sub>4</sub> in ddH <sub>2</sub> O adjust to pH 7.4
PEG 4000 solution (50%)	50% PEG 4000 in ddH <sub>2</sub> O autoclave for 15 min at 121°C

PEG/LiAc solution	1 ml TE buffer (10x) 1 ml LiAc solution (10x) 8 ml PEG 4000 solution (50%)
PFA solution (4%)	4% PFA in PBS adjust to pH 6–7
Proteinase K solution	10 mg/ml Proteinase K in Ampuwa
TBE buffer (5x)	445 mM Tris 445 mM Boric acid 0.01 M EDTA in ddH <sub>2</sub> O
TBS buffer	154 mM NaCl 10 mM Tris-HCl, pH 7.5 in ddH <sub>2</sub> O
TBST buffer	154 mM NaCl 10 mM Tris-HCl, pH 7.5 0.1% Tween 20 in ddH <sub>2</sub> O
TE buffer (10x)	10% 1 M Tris-HCl, pH 7.5 2% 0.5 M EDTA, pH 8.0 in ddH <sub>2</sub> O autoclave for 15 min at 121°C
TE/LiAc solution	500 µl TE buffer (10x) 500 µl LiAc solution (10x) 4 ml Ampuwa
Transfer buffer (10x, without Methanol) (Western blot analysis)	1.92 M Glycine 250 mM Tris in ddH <sub>2</sub> O
Transfer buffer I (Western blot analysis)	8% Transfer buffer (10x, without Methanol) 20% Methanol in ddH <sub>2</sub> O



Transfer buffer II (Western blot analysis)	192 mM Glycine 25 mM Tris 10% Methanol 0.025% SDS in ddH <sub>2</sub> O adjust to pH 8.3
Tris/HCl buffer	1 M Tris in ddH <sub>2</sub> O adjust with HCl to pH 7.5
Triton X-100 solution (0.1%)	0.1% Triton X-100 in DPBS

### 2.1.7 Plasmids and vectors

Plasmid / Vector	Source
CHD7-2-pGBKT7	Schulz <i>et al.</i> (2014a)
CHD7-3-pGBKT7	Schulz <i>et al.</i> (2014a)
CHD7-4-pGBKT7	Schulz <i>et al.</i> (2014a)
CHD7-Cr1-3-pGBKT7	Batsukh <i>et al.</i> (2010)
CHD8-pGADT7-Rec	Batsukh <i>et al.</i> (2010)
RbBP5-pCMV-HA	Schulz <i>et al.</i> (2014a)
SEMA3A WT-pcDNA3.1/ <i>myc</i> -His B	AG Pauli, Institute of Human Genetics (Göttingen)
SEMA3A WT-pCMV-HA	generated in the present thesis (chapter 3.7)
SEMA3A c.196C>T/p.R66W-pCMV-HA	generated in the present thesis (chapter 3.7)
SEMA3A c.2002A>G/p.I668V-pCMV-HA	generated in the present thesis (chapter 3.7)
SEMA3A WT-pGADT7	generated in the present thesis (chapter 3.7)
SEMA3A c.196C>T/p.R66W-pGADT7	generated in the present thesis (chapter 3.7)
SEMA3A c.2002A>G/p.I668V-pGADT7	generated in the present thesis (chapter 3.7)
pcDNA <sup>TM</sup> 3.1/ <i>myc</i> -His B	Invitrogen, Karlsruhe
pCMV-HA	Clontech, Saint-Germain-en-Laye (France)
pGADT7	Clontech, Saint-Germain-en-Laye (France)
pGBKT7	Clontech, Saint-Germain-en-Laye (France)

### 2.1.8 Bacterial strains

Bacterial strain	Source
<i>Escherichia coli</i> DH5 $\alpha$ competent cells (Subcloning Efficiency <sup>TM</sup> DH5 $\alpha$ <sup>TM</sup> , Chemically Competent Cells)	Invitrogen, Karlsruhe

#### 2.1.8.1 Media and agar plates for bacterial culture

Medium / Plate	Composition
LB medium	1% Peptone ex casein 1% NaCl 0.5% Yeast extract in ddH <sub>2</sub> O
LB/Ampicillin	0.1% mg/ml Ampicillin in LB Medium
LB/Kanamycin	0.1% mg/ml Kanamycin in LB Medium
LB agar plates	1% Peptone ex casein 1% NaCl 0.5% Yeast extract 1.5% Agar-Agar in ddH <sub>2</sub> O

### 2.1.9 Eukaryotic cell lines

Cell line	Description	Source	Culture medium
HEK293	human embryonic kidney 293 cells	ATCC <sup>®</sup> (CRL-1573 <sup>TM</sup> ) LGC Standards (Wesel)	FB medium
JoMa1	murine trunk NCC line	Dr. Sven Lindner (Ruhr-University Bochum)	NCC medium
JoMa1.3	murine trunk NCC line (clonally derived subline from JoMa1)	Dr. Sven Lindner (Ruhr-University Bochum)	NCC medium
O9-1	murine cranial NCC line	Merck Millipore (SCC049) (Darmstadt)	ESC medium

### 2.1.9.1 Media for eukaryotic cell culture

Medium	Composition
ESC medium	Complete ES Cell Medium with FBS and LIF 25 ng/ml FGF-2 (human, PeproTech)
Fibroblast medium (FB medium)	DMEM 10% FBS 1x NEAA 100 U/ml / 0.1 mg/ml Penicillin/Streptomycin
NCC medium	DMEM/F-12 10% CEE 1x B-27 Supplement 1x N-2 Supplement 100 U/ml / 0.1 mg/ml Penicillin/Streptomycin 10 ng/ml EGF (human) 1 ng/ml FGF-2 (human, Merck Millipore) 200 nM 4-OHT

### 2.1.9.2 Freezing media

Medium	Composition
ESC freezing medium	Cryo-SFM (ready to use)
Fibroblast freezing medium (FB freezing medium)	60% DMEM 20% FBS 20% DMSO
NCC freezing medium	90% Complete ES Cell Medium with FBS and LIF 10% DMSO

### 2.1.10 Yeast strains

Yeast strain	Source
Y2HGold	Clontech, Saint-Germain-en-Laye (France)

**2.1.10.1 Media and agar plates for yeast culture**

Medium / Agar plate	Composition
SD medium	2.5 g Ammonium sulfate / 475 ml ddH <sub>2</sub> O 0.85 g YNB / 475 ml ddH <sub>2</sub> O 0.3 g DO Supplement / 475 ml ddH <sub>2</sub> O adjust to pH 5.8 autoclave for 15 min at 121°C add 25 ml Glucose (40%) add 0.5 ml Kanamycin
SD medium with Adenine and Histidine	2.5 g Ammonium sulfate / 475 ml ddH <sub>2</sub> O 0.85 g YNB / 475 ml ddH <sub>2</sub> O 0.3 g DO Supplement / 475 ml ddH <sub>2</sub> O adjust to pH 5.8 autoclave for 15 min at 121°C add 25 ml Glucose (40%) add 0.5 ml Kanamycin add 1ml Adenine add 1 ml Histidine
YPDA medium	20 g Peptone ex casein / 950 ml ddH <sub>2</sub> O 10 g Yeast extract / 950 ml ddH <sub>2</sub> O adjust to pH 6.5 autoclave for 15 min at 121°C add 50 ml Glucose (40%) add 2 ml Adenine add 1 ml Kanamycin
-LT agar plates	2.5 g Ammonium sulfate / 475 ml ddH <sub>2</sub> O 0.85 g YNB / 475 ml ddH <sub>2</sub> O 0.3 g DO Supplement / 475 ml ddH <sub>2</sub> O adjust to pH 5.8 add 10 g Agar-Agar autoclave for 15 min at 121°C add 25 ml Glucose (40%) add 0.5 ml Kanamycin add 1ml Adenine add 1 ml Histidine

-LTHA agar plates	2.5 g Ammonium sulfate / 475 ml ddH <sub>2</sub> O 0.85 g YNB / 475 ml ddH <sub>2</sub> O 0.3 g DO Supplement / 475 ml ddH <sub>2</sub> O adjust to pH 5.8 add 10 g Agar-Agar autoclave for 15 min at 121°C add 25 ml Glucose (40%) add 0.5 ml Kanamycin
YPDA agar plates	20 g Peptone ex casein / 950 ml ddH <sub>2</sub> O 10 g Yeast extract / 950 ml ddH <sub>2</sub> O adjust to pH 6.5 add 20 g Agar-Agar autoclave for 15 min at 121°C add 50 ml Glucose (40%) add 2 ml Adenine add 1 ml Kanamycin

## 2.1.11 Antibodies

### 2.1.11.1 Primary antibodies

Antigen	Company	Code	Species	Clonality	Dilution
α-Tubulin	Sigma-Aldrich, Deisenhofen	T5168	mouse	monoclonal	ICC 1:10,000 WB 1:4000
Baf47	Abcam, Cambridge (UK)	ab126734	rabbit	monoclonal	WB 1:1000
Chd7	Cell Signaling, Danvers (USA)	6505	rabbit	monoclonal	ICC 1:20
	Abcam, Cambridge, (UK)	ab31824	rabbit	polyclonal	WB 1:1000
HA	Sigma-Aldrich, Deisenhofen	11867431001	rat	monoclonal, 3F10	WB 1:1000
Sema3a	Abcam, Cambridge (UK)	ab23393	rabbit	polyclonal	ICC 1:20 WB 1:1000

### 2.1.11.2 Secondary antibodies

Antibody	Company	Code	Dilution
Anti-Rabbit IgG (whole molecule), F(ab') <sub>2</sub> fragment-Cy3 antibody produced in sheep	Sigma-Aldrich, Deisenhofen	C2306	ICC 1:500
F(ab') <sub>2</sub> -Goat anti-Mouse IgG (H+L) Cross-Adsorbed Secondary Antibody, Alexa Fluor <sup>®</sup> 488	Invitrogen, Karlsruhe	A11017	ICC 1:500
Goat IgG anti-Mouse IgG (H+L)-HRPO	Dianova, Hamburg	115-035-062	WB 1:10,000
Goat IgG anti-Rabbit IgG (H+L)-HRPO	Dianova, Hamburg	111-035-003	WB 1:10,000
Peroxidase AffiniPure Goat Anti-Rat IgG, F(ab') <sub>2</sub> fragment specific	Jackson ImmunoResearch, West Grove (USA)	112-035-006	WB 1:10,000

### 2.1.12 Synthetic oligonucleotides

All synthetic DNA oligonucleotides were purchased from Eurofins MWG Operon (Ebersberg). Ampuwa dissolved primer stocks with a final concentration of 100 pmol/μl were stored at -20°C. Primers were used at a concentration of 10 pmol/μl for PCR experiments.

#### 2.1.12.1 Synthetic oligonucleotides for genotyping PCR experiments

Name	Direction	Primer sequence 5' → 3'	Annealing (°C)	Cycles
Whi-Genotype	forward	CCTGCTGATGACTGGAAGAAAT	65	35
	reverse	CAAAGAAAAGTTCCCAGCAAAC		

#### 2.1.12.2 Synthetic oligonucleotides for In-Fusion<sup>®</sup> experiments

Name	Direction	Primer sequence 5' → 3'	Annealing (°C)	Cycles
hSEMA3A-CMV-S-1	forward	ACGCTCTTATGGCCATGGAGGCCATG GGCTGGTTAACTAGGATTG	60	35
hSEMA3A-CMV-E-1	reverse	TCGGTTCGACCGAATTCCTAGAGGTAAT GCAGCTCAGACACT		

hSEMA3A-GAD-S-1	forward	ACGCTCATATGGCCATGGAGGCCATG GGCTGGTTAACTAGGATTG	60	35
hSEMA3A-GAD-E-1	reverse	CACCCGGGTGGAATTCCTAGAGGTAA TGCAGCTCAGACACT		

### 2.1.12.3 Synthetic oligonucleotides for mutagenesis experiments

Name	Direction	Primer sequence 5' → 3'	Annealing (°C)	Cycles
SEMA3A_c196t	forward	CTTCCTTTTGGATGAGGAATGGAGTAG GCTGTATGTT	60	20
	reverse	AACATACAGCCTACTCCATTCCTCATC CAAAAGGAAG		
SEMA3A_a2002g	forward	AGGTAACCCTGGAAGTCGTTGACACA GAGCATTTG	60	20
	reverse	CAAATGCTCTGTGTCAACGACTTCCAG GGTTACCT		

### 2.1.12.4 Synthetic oligonucleotides for mycoplasma contamination

Name	Direction	Primer sequence 5' → 3'	Annealing (°C)	Cycles
Myco1	forward	ACACCATGGGAGCTGGTAAT	55	35
	reverse	CTTCWTCGACTTYCAGACCCAAGGCAT		

### 2.1.12.5 Synthetic oligonucleotides for patient screening

Name	Direction	Primer sequence 5' → 3'	Annealing (°C)	Cycles
SEMA3A 1	forward	TCACCTGTTACCTCCAGTTTCC	65 – 1	5
	reverse	GGTTTGATGATTTGGGGTTG	60	35
SEMA3A 2	forward	TCAGGTTACCATGTACCAACAGTC	65 – 1	5
	reverse	TGCATCCATTGATTCACTACTGTC	60	35
SEMA3A 3	forward	ACTTCAGTTGCCCAATGT	65 – 1	5
	reverse	CACATGACCCACAAGTGGAA	60	35
SEMA3A 4	forward	CAGTCATGCTGATTGCTGAAA	65 – 1	5
	reverse	TGAACCACAAGCAAAATAAACTG	60	35

SEMA3A 5	forward	TCTCTGATTAAGTATGTGTTGAAA	65 – 1	5
	reverse	TTATTTTCATAATGGAAAATCTTGGT	60	35
SEMA3A 6	forward	CATGGTCATAACATGAAACTTGC	65 – 1	5
	reverse	CCATCATGAAGTCACCACCA	60	35
SEMA3A 7	forward	TGGACTGTTCAGAATGGTATTATTT	65 – 1	5
	reverse	CCTGTACCTGTATATTTGACTGCG	60	35
SEMA3A 8/9	forward	GGAACGATTTCGACCACAAAT	65 – 1	5
	reverse	TGCAAAATATGAGTACTTGGATAGC	60	35
SEMA3A 10	forward	GCCATTTTTCACCTATGCCTT	65 – 1	5
	reverse	TCTGTCTGTAGCTGCATTGTTTT	60	35
SEMA3A 11	forward	GAACCATTGAGGCCATGTGT	65 – 1	5
	reverse	CCAACCCCTGAGATGTTCAA	60	35
SEMA3A 12	forward	AAAAGGAAGACCGATATCAAAGG	65 – 1	5
	reverse	TGAGAAAACAAAATATGAGCCAAA	60	35
SEMA3A 13	forward	AGCAATAACCCCAACTTGGTC	65 – 1	5
	reverse	ATCAAAAACATGAGGGCAATG	60	35
SEMA3A 14	forward	AGAAGGCCTTTAAAGAAATTAGCA	65 – 1	5
	reverse	TTGATGCACTTATTTGAAGAAAGC	60	35
SEMA3A 15	forward	TCTGGTAGTGAAAAAGCCATGA	65 – 1	5
	reverse	TCTCTTCGGCTGCATTTCTT	60	35
SEMA3A 16	forward	TGGCAATAACTTGTCTCCTGAA	65 – 1	5
	reverse	TGAATGAGCGATTGATTGGT	60	35
SEMA3A 17	forward	ACAGACACGGAGTTTCAGAGC	65 – 1 60	5
	reverse	AGATTGGGGTGGTTGATGAG		35
	reverse	CCCACCATTGTAAACATCCA		

### 2.1.12.6 Synthetic oligonucleotides for RT-PCR experiments

Name	Direction	Primer sequence 5' → 3'	Annealing (°C)	Cycles
Actg2	forward	GGCTTTGCAGGAGATGATGC	64 – 1	5
	reverse	GGCAGTGCATAGCCCTCATA	59	25
mChd7_qRT-5	forward	GCAGTCAGAGCAGCAGGAAT	65 – 1	5
	reverse	GCTCTGGCCCTGTTTTGACT	60	30
Cnn1	forward	TGGCCCAGAAATACGACCAT	64 – 1	5
	reverse	CCTTTTGTCTTGGCCATGCT	59	25
Col2a1	forward	GAAGAGCGGAGACTACTGGATT	64 – 1	5
	reverse	AGGTAGGCGATGCTGTTCTT	59	25



Gfap	forward	GCCTCGGTCCTAGTCGAC	64 – 1	5
	reverse	TCCTGTCTATACGCAGCCAG	59	25
Nefh	forward	GCAGCCAAAGTGAACACAGA	64 – 1	5
	reverse	TGTAAGCGGCAATCTCAATGT	59	25
mNrp1RT	forward	CCACAGAGAAGCCAACCATT	65 – 1	5
	reverse	TGAAGTTGCCATCTCCTGTATG	60	30
mNrp2RT	forward	GGGGAAAAGTGCAGCTTTGA	65 – 1	5
	reverse	GGCCATCACTCTGCAGTTTC	60	30
P75	forward	CTCAGATGAAGCCAACCACG	63 – 1	5
	reverse	GGAGCAATAGACAGGAATGAGG	58	30
Pax3_Seaberg	forward	GGAGGCGGATCTAGAAAGGAAGGA	64 – 1	5
	reverse	CCCCCGGAATGAGATGGTTGAA	59	25
PlxnA1RT	forward	TTGGAATGTGCCTGACCTCT	65 – 1	5
	reverse	TGAGGTAGAGCTTCACCACC	60	30
mSema3a_RT_3	forward	TGCAGTCCGAAGTCACAGAG	65 – 1	5
	reverse	TTGCATGAATCCGTGTTCCAC	60	30
mSema3c_RT_3	forward	GGATCGGCAGTGTGTGTGTA	65 – 1	5
	reverse	ACAACGTCATCTGGGAAGTCC	60	30
mSema3d_RT_2	forward	AAGGCTCTGCTGTCTGTGTG	68 – 1	5
	reverse	CTGGAAAGTCTCGGGTGGAC	63	30
mSema3e_RT_4	forward	GCATGGGGAAGTTAGGCCAT	68 – 1	5
	reverse	CTCGGGTGTAGATCGTGTGG	63	30
Slug	forward	TGCCATCGAAGCTGAGAAGT	64 – 1	5
	reverse	GCAGAAAGCGACATTCTGGAG	59	25
Snail_Seaberg	forward	AAGCCCAACTATAGCGAGCTG	64 – 1	5
	reverse	AGTTGAAGATCTTCCGCGACT	59	25
Sox10	forward	CCCTTCATTGAGGAGGCTGA	63 – 1	5
	reverse	TTGGTCCAGCTCAGTCACAT	58	30
Twist_26.01.15	forward	GCCAGGTACATCGACTTCCTG	64 – 1	5
	reverse	CCACGCCCTGATTCTTGTGA	59	25
Tyr	forward	AGCATGCACAATGCCTTACA	65 – 1	5
	reverse	GAGCGGTATGAAAGGAACCA	60	30

### 2.1.12.7 Synthetic oligonucleotides for sequencing

Name	Direction	Primer sequence 5' → 3'	Annealing (°C)	Cycles
seq_hSEMA3A-1	forward	ATGGGCTGGTTAACTAGGATTG	60	30
	reverse	CACATTGTTCTTCCCATTCTGA		
seq_hSEMA3A-2	forward	AATGGACAACATTCTCA	60	30
	reverse	GGAATACATCCTGCAGTTCATC		
seq_hSEMA3A-3n	forward	AGACGCACAAGACGACAAGATA	60	30
	reverse	ATTCTCTCTTCAGGGCTGTGG		
seq_hSEMA3A-4	forward	GGAACAGTAACAAATGGAAGC	60	30
seq_hSEMA3A-5	forward	GACAGAGCAGCATGATTCCA	60	30
	reverse	ATGGCTGGATGACTTCTTGC		
seq_hSEMA3A-6	forward	AGAGGTTCTGCTGGAAGAAATG	60	30
	reverse	ATTGCCTGAATCCTTCTGTTGT		
seq_mSema3A-1	forward	CACTGGGATTGCCTGTCTTT	60	30
	reverse	GGCCAAGCCATTAAAAGTGA		
seq_mSema3A-2	forward	CGGGACTTCGCTATCTTCAG	60	30
	reverse	GATGAGATGGGCACTGATGA		
seq_mSema3A-3	forward	ACATTTGGCGGATTTGACTC	60	30
	reverse	CTGCATCCACTCGGTCTACA		
seq_mSema3A-4	forward	GCGCACAAGACGACAAGATA	60	30
	reverse	TCTGTGACTTCGGACTGCAT		
seq_mSema3A-5	forward	GTGGAAGCACATGCAAGAGA	60	30
	reverse	AACTCGTGGGTCTCTCTGT		
pCMV	forward	CTCAGTGGATGTTGCCTTTACTTCT	60	30
	reverse	AAGCAATAGCATCACAAATTTTACA		
T7cDNA3	forward	TAATACGACTCACTATAGG	60	30

### 2.1.12.8 Synthetic oligonucleotides for qRT-PCR experiments

Name	Direction	Primer sequence 5' → 3'	Annealing (°C)	Cycles
mChd7_qRT-3	forward	AGAAGAGAAGCTGGAGGACGA	60	40
	reverse	TGATTTCCAGGGCCTTGTC		
qRT_mHprt	forward	AGCCCCAAAATGGTTAAGGTTGC	60	40
	reverse	TTGCAGATTCAACTTGCGCTCAT		
mSema3a_RT-1	forward	CGGGACTTCGCTATCTTCAGAACACT	60	40
	reverse	TCATCTTCAGGGTTGTCACTCTCTGG		

qRT_mTbp	forward	CCCACAACTCTTCCATTCTCAAAC	60	40
	reverse	TCAAGTTTACAGCCAAGATTACAG		

### 2.1.13 Molecular weight standards

Application	Standard and Manufacturer
DNA molecular weight standards	100 bp DNA Ladder (Invitrogen, Karlsruhe)
	1 kb DNA Ladder (Invitrogen, Karlsruhe)
	1 kb Plus DNA Ladder (Invitrogen, Karlsruhe)
	DNA molecular weight standards were diluted with loading buffer according to manufacturer's instructions.
Protein molecular weight standards	SeeBlue® Plus2 Pre-Stained Protein Standard (Invitrogen, Karlsruhe)
	HiMark™ Pre-Stained High Molecular Weight Protein Standard (Invitrogen, Karlsruhe)

### 2.1.14 Animals/ethic statement

The used mouse line *Whirligig* (Bosman *et al.*, 2005) was kindly provided from K. P. Steel (Sanger Centre, Cambridge, United Kingdom) and the Helmholtz Zentrum (Munich). The mice were housed in the animal facility of the Institute of Human Genetics (Göttingen) under conventional conditions (12 h light/dark cycle, 22°C, 55 ± 5% relative humidity and free access to food and water). Animal food was purchased from ssniff Spezialdiäten (Soest). All experiments were approved by the Institutional Animal Care and Use Committee of the University of Göttingen and conducted according to the European and German protection of animal act. The number of sacrificed animals and the stress and pain the mice were suffering was kept to a minimum. Euthanasia of mice was performed by CO<sub>2</sub>-asphyxiation or cervical dislocation.

### 2.1.15 Patient samples

Genomic DNA of patient samples was provided by the genetic diagnostics laboratory of the Institute of Human Genetics (University Medical Center Göttingen) and by collaboration with Conny van Ravenswaaij-Arts of the Department of Genetics (University Medical Center Groningen, The Netherlands). The ethical approval was obtained from the Ethics Committee of the University Göttingen.

### 2.1.16 Databases / Online tools / Programs

Analysis of / Designing of / Usage for	Database / Online tool / Program
Gene domains	SMART <a href="http://smart.embl-heidelberg.de">http://smart.embl-heidelberg.de</a>
	UniProtKB <a href="http://www.uniprot.org/">http://www.uniprot.org/</a>
Genome variants	Exome Aggregation Consortium (ExAC) Browser <a href="http://exac.broadinstitute.org/">http://exac.broadinstitute.org/</a>
Information about human genes and genetic disorders	Online Mendelian Inheritance in Man (OMIM) <a href="https://www.omim.org/">https://www.omim.org/</a>
In-Fusion® PCR Cloning System	<a href="http://bioinfo.clontech.com/infusion/">http://bioinfo.clontech.com/infusion/</a>
Mice administration	Tierbase Client 4D v15.1
Nucleotide exchanges	MutationTaster <a href="http://www.mutationtaster.org/">http://www.mutationtaster.org/</a>
	PolyPhen-2 <a href="http://genetics.bwh.harvard.edu/pph2/">http://genetics.bwh.harvard.edu/pph2/</a>
	SIFT <a href="http://sift.jcvi.org/">http://sift.jcvi.org/</a>
Nucleotide sequences	Ensembl genome browser 87 <a href="http://www.ensembl.org/">http://www.ensembl.org/</a>
	National Center for Biotechnology Information (NCBI) <a href="https://www.ncbi.nlm.nih.gov/">https://www.ncbi.nlm.nih.gov/</a>

Plasmid maps	Savvy Version 0.1 <a href="http://www.bioinformatics.org/savvy/">http://www.bioinformatics.org/savvy/</a>
Primers	Primer3 <a href="http://bioinfo.ut.ee/primer3-0.4.0/">http://bioinfo.ut.ee/primer3-0.4.0/</a>
Protein molecular weights	ExPASy <a href="http://web.expasy.org/compute_pi/">http://web.expasy.org/compute_pi/</a>
Repetitive gene sequences	RepeatMasker <a href="http://www.repeatmasker.org/">http://www.repeatmasker.org/</a>
Restriction sites	NEBcutter V2.0 <a href="http://nc2.neb.com/NEBcutter2/">http://nc2.neb.com/NEBcutter2/</a>
Searching for publications	PubMed <a href="https://www.ncbi.nlm.nih.gov/pubmed/">https://www.ncbi.nlm.nih.gov/pubmed/</a>
Sequences	Chromas Lite 2.01 (Technelysium Pty Ltd.)  Sequence Pilot 4.3.1 (JSI medical systems)
Sequence alignments	Basic Local Alignment Search Tool (BLAST) provided by NCBI <a href="https://blast.ncbi.nlm.nih.gov/Blast.cgi">https://blast.ncbi.nlm.nih.gov/Blast.cgi</a>

### 2.1.17 Statistical analysis

An unpaired student's *t* test was performed to test for statistical significance. The calculated *p*-value indicates the probability that the results are not different from each other. A *p*-value smaller than \*  $p \leq 0.05$  means statistically significant, \*\*  $p \leq 0.01$  means very significant, \*\*\*  $p \leq 0.001$  means extremely significant.

## **2.2 Methods**

### **2.2.1 Molecular biology methods**

#### **2.2.1.1 Isolation of nucleic acids**

##### **2.2.1.1.1 Isolation of genomic DNA for mouse genotyping**

For mouse genotyping, genomic DNA (gDNA) was isolated from tail biopsy taken at the age of four weeks. The tail biopsy was mixed with 200 µl of DirectPCR<sup>®</sup> Lysis Reagent Tail (Peqlab) and 8 µl of proteinase K (10 mg/ml) and incubated at 55°C by shaking at 950 rpm overnight. The tail biopsy from a mouse embryo was mixed with 100 µl of DirectPCR Lysis Reagent Tail and 4 µl of proteinase K (10 mg/ml) and incubated as previously described. The following day, proteinase K was inactivated by incubation for 45 min at 85°C. The samples were short centrifuged, transferred on ice and used for genotyping PCR (chapter 2.2.1.2.1.3). Isolated gDNA was finally stored at 4°C.

##### **2.2.1.1.2 Minipreparation of plasmid DNA**

Small amounts of plasmid DNA from bacteria were isolated with the ready-to-use buffers (P1/P2/P3) for minipreparation (Qiagen). 3 ml of LB medium containing the appropriate antibiotic was inoculated with a single bacterial colony or a small amount of a glycerol stock and incubated at 37°C by shaking at 160 rpm overnight. For preparation of a glycerol stock the following day, 500 µl of the bacterial culture was mixed with 320 µl of 50% sterile glycerol and stored at -80°C. The extant overnight culture was centrifuged at 4000 x *g* for 10 min at 4°C. The bacterial cell pellet was resuspended in 200 µl of P1 buffer, transferred into a 1.5 ml reaction tube and 200 µl of P2 buffer (modified alkaline lysis) was added. The solution was mixed by inverting and incubated for 5 min at RT. After addition of 200 µl P3 buffer (neutralization) and repeated mixing by inverting, the solution was centrifuged at 16,000 x *g* for 10 min at RT. The received supernatant was transferred into a new 1.5 ml reaction tube. DNA was precipitated with 800 µl of 100% isopropanol (chilled at -20°C) and repeated mixed by inverting before centrifuged at 16,000 x *g* for 30 min at 4°C. The DNA pellet was washed with 300 µl of 70% ethanol (chilled at -20°C) and centrifuged at 16,000 x *g* for 5 min at 4°C. After discarding the supernatant, the plasmid DNA pellet was dried at 56°C and resolved in an appropriate volume of Ampuwa

by gently shaking for 10 min at 56°C. Afterwards, isolated plasmid DNA was stored at -20°C.

#### **2.2.1.1.3 Endotoxin-free midipreparation of plasmid DNA**

Large amounts of plasmid DNA from bacteria were isolated with ready-to-use reaction system HiPure Plasmid Midiprep Kit (Invitrogen, Karlsruhe). 50 ml of LB medium, containing the appropriate antibiotic, was inoculated with either 50 µl of bacterial overnight culture (taken before minipreparation and stored at 4°C) or a small amount of a glycerol stock and incubated at 37°C by shaking at 160 rpm overnight. The overnight culture was centrifuged at 4000 x *g* for 10 min at RT. The bacterial cell pellet was resuspended in 4 ml of R3 buffer, further mixed with 4 ml of L7 buffer (modified alkaline lysis), inverted five times and incubated for 5 min at RT. After addition of 4 ml N3 buffer (neutralization) the suspension was mixed by inverting until the suspension was homogenous and centrifuged at 12,000 x *g* for 10 min at RT. The supernatant was loaded onto a with EQ1 buffer equilibrated column. The column was washed twice with 10 ml of W8 buffer. The DNA was eluted with 5 ml of E4 buffer and further precipitated by addition of 2.5 ml 100% isopropanol (chilled at -20°C). The suspension was mixed by repeated inverting and centrifuged at 16,000 x *g* for 30 min at 4°C. The DNA pellet was washed with 2.5 ml of 70% ethanol (chilled at -20°C). After centrifugation at 16,000 x *g* for 5 min at 4°C, the supernatant was discarded and the DNA pellet was dried at 56°C. The plasmid DNA pellet was resolved in an appropriate volume of Ampuwa by shaking for 10 min at 56°C and finally stored at -20°C.

#### **2.2.1.1.4 Isolation of total RNA from cultured cells**

For total RNA isolation from cultured cells either fresh or at -80°C stored cell pellets were used. Pellet was thoroughly mixed with 1 ml of Trizol Reagent (Invitrogen), incubated for 5 min at RT and 200 µl of chloroform was added. The suspension was vigorously mixed for 15 s, incubated for 15 min at RT and centrifuged at 18,600 x *g* for 15 min at 4°C. After centrifugation, the upper aqueous phase containing the RNA was transferred into a new reaction tube. For precipitation of the RNA 500 µl of 100% isopropanol (chilled at -20°C) was added, the suspension was mixed by inverting, incubated for 10 min before

centrifuged at  $18,600 \times g$  for 8 min at  $4^{\circ}\text{C}$ . The RNA pellet was washed with 1 ml of 75% ethanol/DEPC- $\text{H}_2\text{O}$  and centrifuged at  $18,600 \times g$  for 5 min at  $4^{\circ}\text{C}$ . The supernatant was discarded and the RNA pellet was dried at  $60^{\circ}\text{C}$ . For resolving the pellet, an appropriate volume of DEPC- $\text{H}_2\text{O}$  was used by shaking for 10 min at  $60^{\circ}\text{C}$ . The isolated RNA was stored at  $-80^{\circ}\text{C}$ .

#### **2.2.1.1.5 Isolation of RNA from mouse tissues**

The mouse tissue was initially homogenized using the TissueLyser LT (Qiagen). Together with a stainless steel bead ( $\varnothing$  5 mm, Qiagen) and 1 ml of Trizol Reagent (Invitrogen) a small sample of the tissue was transferred into a 2 ml reaction tube. The tissue was homogenized in the TissueLyser LT for 5 min at 50 1/s oscillation. Afterwards, the reaction tube was kept on ice for 5 min. After centrifugation at  $16,000 \times g$  for 10 min at  $4^{\circ}\text{C}$ , the lysed cells containing supernatant was transferred into a new 1.5 ml reaction tube. The RNA isolation was continued by using the total RNA isolation protocol from cultured cells (chapter 2.2.1.1.4) starting with addition of 200  $\mu\text{l}$  chloroform to the supernatant with the lysed cells.

#### **2.2.1.1.6 Determination of nucleic acid concentration**

Nucleic acid concentrations and purities were determined by measuring the absorption at 260 nm using the NanoDrop 2000c UV-Vis spectrophotometer (Pqclab) according to manufacturer's instructions. Contaminations of protein and salt were estimated with the absorbance ratios of  $A_{260/280}$  and  $A_{260/230}$ , respectively.

### **2.2.1.2 Polymerase Chain Reactions**

#### **2.2.1.2.1 Amplification of DNA**

The polymerase chain reaction (PCR) represents a standard *in vitro* method to amplify specific DNA fragments (Mullis *et al.*, 1986). The double stranded template DNA is denatured at high temperatures (denaturation). This allows short oligonucleotides (primers) to bind to the now single stranded DNA (annealing). Bound oligonucleotides are



extended by a polymerase (elongation). Periodic repetition of denaturation, annealing and elongation results in an exponential increase of specific DNA fragments. The result of the PCR can be visualized by agarose gel electrophoresis (chapter 2.2.1.3).

#### 2.2.1.2.1.1 Standard PCR

The standard PCR was used to control the efficiency of cDNA synthesis from RNA (chapter 2.2.1.2.2). Specific primers for the housekeeping gene mouse *Hprt* (hypoxanthine-guanine phosphoribosyltransferase) (chapter 2.1.12.8) and the Q5<sup>®</sup> High-Fidelity DNA Polymerase (New England Biolabs) with the supplied reagents were used.

The following reagents for 25 µl of reaction mixture were pipetted into a PCR reaction tube:

Component	Volume
cDNA	1.0 µl
Q5 Reaction Buffer (5x)	5.0 µl
Q5 High GC Enhancer (5x)	5.0 µl
Primer forward (10 pmol/µl)	1.25 µl
Primer reverse (10 pmol/µl)	1.25 µl
dNTP mix (10 mM)	0.5 µl
Q5 High-Fidelity DNA Polymerase (2 U/µl)	0.25 µl
Ampuwa	10.75 µl

The reaction mixture was incubated in a thermocycler using the following standard PCR program:

Step	Temperature	Time	Repeats
Initial denaturation	98°C	30 s	1
Denaturation	98°C	10 s	25
Annealing	60°C	30 s	
Elongation	72°C	20 s	
Final elongation	72°C	2 min	1
Storage	4°C	∞	1

After completion of the thermocycler program, loading buffer was added to 5 µl of the reaction mixture and loaded on a 1.5% agarose gel together with 100 bp DNA Ladder (Invitrogen).

#### 2.2.1.2.1.2 Touchdown PCR

Generally, the components of the reaction mixture were the same as for standard PCR (chapter 2.2.1.2.1.1) with the exception of the touchdown PCR using patients DNA. To increase specificity, sensitivity and yield of PCR, a touchdown PCR program was applied.

The reaction mixture was incubated in a thermocycler using the following touchdown PCR program:

Step	Temperature	Time	Repeats
Initial denaturation	98°C	30 s	1
Denaturation	98°C	10 s	5
Annealing	(2.1.12.6) – 1°C	30 s	
Elongation	72°C	20 s	
Denaturation	98°C	10 s	(2.1.12.6)
Annealing	(2.1.12.6)	30 s	
Elongation	72°C	20 s	
Final elongation	72°C	2 min	1
Storage	4°C	∞	1

After completion of the thermocycler program, loading buffer was added to 3–5 µl of the reaction mixture and loaded on a 1.5% agarose gel together with 100 bp DNA Ladder (Invitrogen).

#### Touchdown PCR with patients DNA samples for mutational analysis

For touchdown PCR with patient DNA samples the HotStarTaq® Plus Master Mix Kit (Qiagen) and specific primers (chapter 2.1.12.5) were used.

The following reagents for 25.5 µl of reaction mixture were pipetted into a 96-well plate:

Component	Volume
gDNA	1.0 µl
Primer forward (10 pmol/µl)	1.0 µl
Primer reverse (10 pmol/µl)	1.0 µl
HotStarTaq Plus Master Mix	12.5 µl
Ampuwa	10.0 µl

The reaction mixture was incubated in a thermocycler using the following touchdown PCR program:

Step	Temperature	Time	Repeats
Initial denaturation	95°C	7 min	1
Denaturation	95°C	30 s	5
Annealing	(2.1.12.5) – 1°C	1 min	
Elongation	72°C	1 min	
Denaturation	95°C	30 s	(2.1.12.5)
Annealing	(2.1.12.5)	1 min	
Elongation	72°C	1 min	
Final elongation	72°C	5 min	1
Storage	4°C	∞	1

After completion of the thermocycler program, loading buffer was added to 3 µl of the reaction mixture and loaded on a 1.0% agarose gel together with 1 kb Plus DNA Ladder (Invitrogen).

#### 2.2.1.2.1.3 Genotyping PCR

The genotyping PCR was used for mouse genotyping using gDNA isolated from tail biopsy (chapter 2.2.1.1.1). Specific primers for the DNA region which contains the nonsense mutation c.2918G>A (p.W973X) in case of the heterozygous or homozygous genotype (chapter 2.1.12.1) and the Immolase<sup>TM</sup> DNA Polymerase (Bioline) with the supplied reagents were used.

The following reagents for 50  $\mu$ l of reaction mixture were pipetted into a PCR reaction tube:

Component	Volume
gDNA	2.0 $\mu$ l
ImmoBuffer (10x)	5.0 $\mu$ l
MgCl <sub>2</sub> Solution (50mM)	1.5 $\mu$ l
Primer forward (10 pmol/ $\mu$ l)	1.0 $\mu$ l
Primer reverse (10 pmol/ $\mu$ l)	1.0 $\mu$ l
dNTP mix (10 mM)	1.0 $\mu$ l
Immolase DNA Polymerase (5 U/ $\mu$ l)	0.4 $\mu$ l
Ampuwa	38.1 $\mu$ l

The reaction mixture was incubated in a thermocycler using the following standard PCR program:

Step	Temperature	Time	Repeats
Initial denaturation	94°C	5 min	1
Denaturation	94°C	30 s	35
Annealing	65°C	45 s	
Elongation	72°C	1 min	
Final elongation	72°C	7 min	1
Storage	4°C	$\infty$	1

After completion of the thermocycler program, loading buffer was added to 3  $\mu$ l of the reaction mixture and loaded on a 1.5% agarose gel together with 100 bp DNA Ladder (Invitrogen). The purified PCR product was further used for sequencing analysis (chapter 2.2.1.2.4) to distinguish between the wildtype, heterozygous and homozygous state of *Whirligig* mice.

#### 2.2.1.2.1.4 Mutagenesis PCR

The mutagenesis PCR was used to create specific, targeted changes in double stranded plasmid DNA with the QuikChange II XL Site-Directed Mutagenesis Kit according to

manufacturer's instructions (chapter 2.2.1.4.4). Specific primers for mutagenesis (chapter 2.1.12.3) and the *PfuUltra*<sup>®</sup> High-Fidelity DNA Polymerase (Agilent Technologies) with the supplied reagents were used.

The following reagents for 50 µl of reaction mixture were pipetted into a PCR reaction tube:

Component	Volume
Double stranded plasmid DNA	(75 ng) x µl
Reaction buffer (10x)	5.0 µl
QuikSolution	3.0 µl
Primer forward (125 ng/µl)	1.0 µl
Primer reverse (125 ng/µl)	1.0 µl
dNTP mix	2.0 µl
<i>PfuUltra</i> High-Fidelity DNA Polymerase (2.5 U/µl)	1.0 µl
Ampuwa	x µl

The reaction mixture was incubated in a thermocycler using the following PCR program:

Step	Temperature	Time	Repeats
Initial denaturation	95°C	1 min	1
Denaturation	95°C	50 s	20
Annealing	60°C	1 min	
Elongation	68°C	6 min*	
Final elongation	68°C	7 min	1
Storage	4°C	∞	1

\* 1 min/kb of plasmid length

After completion of the thermocycler program, the mutagenesis protocol was continued with *DpnI* digestion of the amplification products (chapter 2.2.1.4.4).

### 2.2.1.2.1.5 Mycoplasma contamination PCR

To detect a possible contamination of eukaryotic cells by mycoplasma, a PCR with mycoplasma specific primers (chapter 2.1.12.4) and the Platinum<sup>®</sup> *Taq* DNA Polymerase (Invitrogen) with the supplied reagents was performed. Therefore, 200 µl of used cell culture medium was incubated for 5 min at 95°C. After mixing and centrifugation at 1500 x *g* for 1 min the supernatant was used for reaction mixture. A mycoplasma contaminated cell culture medium was used as positive control.

The following reagents for 50 µl of reaction mixture were pipetted into a PCR reaction tube:

Component	Volume
Supernatant from cell culture	1.0 µl
PCR Buffer (10x)	5.0 µl
MgCl <sub>2</sub> (50 mM)	2.0 µl
Primer forward (10 pmol/µl)	0.5 µl
Primer reverse (10 pmol/µl)	0.5 µl
dNTP mix (10 mM)	1.0 µl
Platinum <i>Taq</i> DNA Polymerase (5 U/µl)	0.2 µl
Ampuwa	39.8 µl

The reaction mixture was incubated in a thermocycler using the following PCR program:

Step	Temperature	Time	Repeats
Initial denaturation	94°C	1 min	1
Denaturation	94°C	30 s	35
Annealing	55°C	2 min	
Elongation	72°C	1 min	
Final elongation	72°C	7 min	1
Storage	4°C	∞	1

After completion of the thermocycler program, loading buffer was added to 10 µl of the reaction mixture and loaded on a 1.5% agarose gel together with 100 bp DNA Ladder (Invitrogen).

### 2.2.1.2.2 Reverse transcription

To remove remaining DNA; a DNase digestion (Sigma-Aldrich) prior to transcription of mRNA into cDNA using the SuperScript® II Reverse Transcriptase (Invitrogen) was performed. 5 µg of RNA was diluted with DEPC-H<sub>2</sub>O in a total volume of 8 µl and further mixed with 1 µl of 10x reaction buffer and 1 µl of DNase I by pipetting. After incubation for 15 min at RT, the reaction was stopped by addition of 1 µl Stop Solution, following incubation for 10 min at 70°C and 1 min on ice. Afterwards, DNase I digested RNA was mixed with 1 µl of Random Hexamers (Invitrogen) and 1 µl of 10mM dNTPs and incubated for 5 min at 65°C. After incubation for 1 min on ice, 2 µl of 0.1 M DTT and 4 µl of 5x First-Strand Buffer was added and mixed by pipetting. After incubation for 2 min at 42°C, 1 µl of SuperScript II Reverse Transcriptase was added. The solution was mixed by pipetting and incubated for 50 min at 42°C. The reaction was stopped by enzyme inactivation at 70°C for 15 min. Amplified cDNA was cooled down for 5 min on ice and stored at -20°C.

The efficiency of cDNA synthesis was controlled by PCR analysis using specific primers for the housekeeping gene mouse *Hprt* (chapter 2.2.1.2.1.1).

### 2.2.1.2.3 Quantitative Real-Time PCR

To quantify the relative mRNA expression levels of a certain gene of interest a quantitative Real-Time PCR (qRT-PCR) analysis was performed by using fluorescent labeled dNTPs for PCR reactions. After each PCR cycle the fluorescent intensity of labeled double stranded DNA was measured using the 7900HT Fast Real-Time PCR System (Applied Biosystems). During the exponential phase a threshold value of PCR cycles was determined in a Ct value. This value defines the PCR cycle with the optimal PCR conditions and was used for quantification calculations. The generated data were evaluated with the SDS 2.2.1 software (Applied Biosystems) and transferred to MS Excel (Microsoft) for further calculations using the  $\Delta\Delta$ -Ct method. The mRNA expression of two housekeeping genes, mouse *Hprt* and mouse *Tbp* (TATA box binding protein) were used for normalization.

Prior to the qRT-PCR analysis, the used cDNA was usually diluted 1:10 with Ampuwa. The analysis was carried out in 10 µl reactions with 2.5 µl of diluted cDNA, 2.5 µl of primer solution with forward and reverse primer (1 pmol/µl each primer) and 5.0 µl of QuantiTect®

SYBR® Green PCR Kit (Qiagen). The reactions were performed in triplicate in a 384-well plate on 7900HT Fast Real-Time PCR System using the following PCR program:

Step	Temperature	Time	Repeats
	50°C	2 min	1
Initial denaturation	95°C	15 min	1
Denaturation	94°C	15 s	40
Annealing	60°C	30 s	
Elongation	72°C	1 min	
Dissociation curve	95°C	15 s	1
	60°C	15 s	1
	95°C	15 s	1

#### 2.2.1.2.4 Sequencing analysis

The sequencing analysis was performed based on the chain-terminating Sanger sequencing in order to determine the nucleotide sequence of a DNA fragment of interest (Sanger *et al.*, 1977). During the elongation step of the sequence reaction, deoxynucleotides and dideoxynucleotides, which are labeled with different fluorescent dyes, were incorporated into the DNA. The elongation of the chain was terminated selectively at A, C, G or T when dideoxynucleotides were incorporated at the 3' end of the growing chain. Further elongation of the chain was prevented, because the chain lacks a 3'-hydroxyl group once a dideoxynucleotide was incorporated. The nucleotides were determined due to the detected dye and the positions of the nucleotides within the DNA strand were determined due to the length of the fragments.

The generated PCR product or plasmid was purified before sequencing analysis using the ready to use reaction system MSB® Spin PCRapace Kit (Invitex) or the MultiScreen® PCR96 Filter Plates (Merck Millipore). The purification was done according to manufacturer's instructions.

The sequencing analysis was carried out in a 10 µl reaction using the BigDye® Terminator v1.1 Cycle Sequencing Kit (Applied Biosystems).

For sequencing of gDNA isolated from tail biopsy for mouse genotyping, 6 µl of purified gDNA, 1 µl of forward or reverse primer (10 pmol/µl), 1 µl of BigDye Terminator Ready Reaction Mix and 2 µl of BigDye Terminator 5x Sequencing Buffer were pipetted into a PCR reaction tube.



For sequencing of a generated plasmid, 0.5 µl of purified plasmid DNA, 1 µl of forward or reverse primer (10 pmol/µl), 1 µl of BigDye Terminator Ready Reaction Mix, 2 µl of BigDye Terminator 5x Sequencing Buffer and 5.5 µl of Ampuwa were pipetted into a PCR reaction tube.

For sequencing of a patient sample 5 µl of purified DNA, 1 µl of forward or reverse primer (10 pmol/µl), 2 µl of BigDye Terminator Ready Reaction Mix and 2 µl of BigDye Terminator 5x Sequencing Buffer were pipetted into a 96-well plate.

The reaction mixture was incubated in a thermocycler using the following PCR program:

Step	Temperature	Time	Repeats
Denaturation	95°C	20 s	30
Annealing	60°C	2 min	
Storage	8°C	∞	1

After completion of the thermocycler program each sample was mixed with 10 µl of Ampuwa. The final sequencing analysis was performed in house sequencing service (Institute of Human Genetics, Göttingen) using the 3500xL Genetic Analyzer (Applied Biosystems). The generated data were evaluated with the Chromas Lite 2.01 software (Technelysium Pty Ltd.) or the Sequence Pilot 4.3.1 software (JSI medical systems).

### 2.2.1.3 Agarose gel electrophoresis of DNA

The agarose gel electrophoresis is used to separate DNA fragments within an electric field according to their length.

Depending on the expected fragment size of the DNA fragments, gels with an agarose concentration of 0.8–2.0% (w/v) were prepared. The appropriate amount of agarose was dissolved in the appropriate amount of 0.5x Tris-Borate EDTA (TBE) buffer by boiling in a microwave. Either Roti®-Safe (Carl Roth) or ethidium bromide (Inno-Train Diagnostik) were added to visualize the DNA later under UV light before the mixture was poured into a horizontal gel chamber. After polymerization of the gel, it was loaded with the samples and an appropriate DNA length standard (chapter 2.1.13) in order to be able to determine the length of the DNA fragments. The separation of the DNA fragments was performed in

0.5x TBE buffer by the application of an electric field (100–120 V) and afterwards visualized using an UV transilluminator.

#### **2.2.1.3.1 Purification of DNA fragments from agarose gels**

The purification of DNA fragments from agarose gels was performed using the ready to use reaction system QIAquick® Gel Extraction Kit (Qiagen, Hilden). After separation of DNA fragments, the DNA fragment of interest was excised from the gel with a sterile scalpel on an UV transilluminator and the gel piece was transferred into a reaction tube and weighed. The 3-fold volume of QG Buffer was added according to the weight of the excised DNA fragment (1 mg is equivalent to 100 µl). The mixture was incubated for 10 min at 50°C by shaking and mixing every 2–3 min. After dissolving of the gel piece further purification was performed according to manufacturer's instructions. The DNA was eluted with an appropriate volume of Ampuwa and stored at –20°C.

#### **2.2.1.4 Cloning techniques**

##### **2.2.1.4.1 Restriction digestion of plasmid DNA**

Enzymatic cleavage of plasmid DNA was performed with restriction endonucleases derived from the companies Invitrogen and New England Biolabs. Generally, per 1 µg DNA 10 units of the enzyme were incubated in 1x appropriate buffer at the required temperature for at least 2 h, preferentially 3 h, in a total volume of 20–50 µl filled up with Ampuwa. The complete digestion of the plasmid DNA was checked by agarose gel electrophoresis (chapter 2.2.1.3).

If for the restriction digestion two different enzymes had to be used, either a buffer compatible for both enzymes was chosen or a sequential restriction digestion was performed. For sequential restriction digestion, the digested DNA had to be precipitated after the use of the first restriction enzyme. Therefore, the reaction volume was filled up with Ampuwa to a total volume of 100 µl. 10 µl of 3 M sodium acetate (pH 5.2) was added and the solution was mixed for 12 s. After addition of 300 µl 100% ethanol (chilled at –20°C), the solution was mixed by inverting and incubated either for 5 min at RT or overnight at –20°C. The precipitated DNA was centrifuged at 16,000 x g for 10 min at RT

and the received DNA pellet was washed with 1 ml of 70% ethanol (chilled at  $-20^{\circ}\text{C}$ ). After centrifugation at  $16,000 \times g$  for 5 min at RT, the pellet was dried at  $56^{\circ}\text{C}$  and resolved in an appropriate volume of Ampuwa by shaking for 10 min at  $56^{\circ}\text{C}$ . Afterwards, restriction digestion with the second restriction enzyme was performed.

#### **2.2.1.4.2 Cloning of DNA fragments using In-Fusion<sup>®</sup> HD Cloning Kit**

For cloning of DNA fragments into vectors the In-Fusion<sup>®</sup> HD Cloning Kit (Clontech) was used according to manufacturer's instructions. The gene of interest was amplified by PCR using gene-specific In-Fusion primers. For the In-Fusion cloning reaction the linearized vector, the purified PCR fragment and 2  $\mu\text{l}$  of 5x In-Fusion HD Enzyme Premix were adjusted with Ampuwa to a total reaction volume of 10  $\mu\text{l}$ . The reaction mixture was incubated for 15 min at  $37^{\circ}\text{C}$  followed by an additional incubation for 15 min at  $50^{\circ}\text{C}$ . After addition of 40  $\mu\text{l}$  TE buffer (Invitrogen), *E. coli* DH5 $\alpha$  competent cells were transformed with 2.5  $\mu\text{l}$  of the reaction mixture (chapter 2.2.1.4.3).

#### **2.2.1.4.3 Transformation of competent cells**

For transformation of competent cells with the In-Fusion reaction mixture, 50  $\mu\text{l}$  of *E. coli* DH5 $\alpha$  competent cells (Invitrogen) was thawed on ice and 2.5  $\mu\text{l}$  of the reaction mixture was added. The mixture was incubated for 30 min on ice and after a heat shock for 45 s at  $42^{\circ}\text{C}$  placed for 2 min on ice. Afterwards, 450  $\mu\text{l}$  of S.O.C. medium (Invitrogen) was added and the bacteria were incubated for 1 h at  $37^{\circ}\text{C}$  by slight shaking. 50  $\mu\text{l}$  and 100  $\mu\text{l}$  of the transformed bacteria were separately spread on LB agar plates containing an antibiotic appropriate for the cloning vector and incubated at  $37^{\circ}\text{C}$  overnight.

For transformation of competent cells with *DpnI*-treated mutagenesis reaction mixture, 100  $\mu\text{l}$  of *E. coli* DH5 $\alpha$  competent cells was thawed on ice and 5  $\mu\text{l}$  of the reaction mixture was added. After incubating the mixture for 30 min on ice, a heat shock was performed for 45 s at  $42^{\circ}\text{C}$ . The mixture was further placed for 2 min on ice and 700  $\mu\text{l}$  of S.O.C. medium was added. By slight shaking, the bacteria were incubated for 1 h at  $37^{\circ}\text{C}$ . On LB agar plates containing an antibiotic appropriate for the cloning vector, 250  $\mu\text{l}$  and 550  $\mu\text{l}$  of the transformed bacteria were spread separately. The agar plates were incubated at  $37^{\circ}\text{C}$  overnight.

#### 2.2.1.4.4 Mutagenesis

The QuikChange II XL Site-Directed Mutagenesis Kit (Agilent Technologies) was used to create specific, targeted changes in double stranded plasmid DNA. PCR reaction using *PfuUltra* High-Fidelity DNA Polymerase and specific primers were performed (chapter 2.2.1.2.1.4). The amplification products were digested by addition of 1  $\mu$ l *DpnI* restriction enzyme (10 U/ $\mu$ l) directly to each amplification reaction, following incubation for 1 h at 37°C and transformation into *E. coli* DH5 $\alpha$  competent cells (chapter 2.2.1.4.3). The next day, minipreparation of plasmid DNA (chapter 2.2.1.1.2) was performed followed by test restriction digestion of the isolated plasmid DNA (chapter 2.2.1.4.1) using appropriate restriction enzymes to identify positive clones. Plasmid DNA was purified with MSB Spin PCRapace Kit and the correct nucleotide sequences of the generated plasmids were validated by sequencing analysis (chapter 2.2.1.2.4).

#### 2.2.1.5 Yeast two-hybrid assay

The yeast two-hybrid assay represents an *in vivo* method to identify novel protein interactions, confirm putative direct interactions and define interacting domains using yeast cells. The Matchmaker<sup>®</sup> Gold Yeast two-Hybrid System (Clontech) and the yeast strain Y2HGold (Clontech) were used.

50 ml of YPDA medium was inoculated with 3–4 yeast colonies from an YPDA agar plate and incubated (16–18 h) at 30°C by shaking at 220 rpm overnight. 4–8 ml of the overnight culture ( $OD_{600} > 1.5$ ) was transferred into 300 ml of YPDA medium ( $OD_{600} \sim 0.3$ ) and incubated for 3–4 h at 30°C by shaking at 220 rpm until an  $OD_{600}$  between 0.4–0.6 was reached. The yeast cell suspension was portioned into 50 ml falcons and centrifuged at 1000 x *g* for 5 min at RT. Meanwhile, Yeastmaker<sup>™</sup> Carrier DNA (10 mg/ml) (Clontech) was denatured for 10 min at 95°C and placed for 5 min on ice. Each yeast cell pellet was resuspended in 30 ml Ampuwa and centrifuged at 1000 x *g* for 5 min at RT. Thereafter, each yeast cell pellet was resuspended in 1.5 ml of freshly prepared TE/LiAc solution. 10  $\mu$ l of denatured Carrier DNA was added to 1  $\mu$ g of each plasmid and mixed by pipetting. After addition of 100  $\mu$ l yeast cell solution and mixing, 600  $\mu$ l of freshly prepared PEG/LiAc solution was added and mixed. The reaction mixture was incubated for 30 min at 30°C by shaking at 500 rpm. Afterwards, 70  $\mu$ l of DMSO solution was added and mixed by inverting. Next, heat shock for 15 min at 42°C was performed, followed by incubation

for 2 min on ice and centrifugation at 16,000 x *g* for 1 min. Each yeast cell pellet was resuspended in 300 µl of Ampuwa and plated as drops of 10 µl each on –LT and –LTHA agar plates, respectively. The agar plates were incubated for 5–7 d at 30°C.

## **2.2.2 Protein manipulation methods**

### **2.2.2.1 Protein isolation from eukaryotic cells**

For protein isolation, eukaryotic cells were harvested from cell culture vessel using an appropriate protocol (chapter 2.2.4.2). Nuclear and cytoplasmic protein extracts were isolated using the NE-PER® Nuclear and Cytoplasmic Extraction Reagents Kit (Thermo Scientific) according to manufacturer's instructions.

### **2.2.2.2 Protein isolation from yeast cells**

For protein isolation from yeast cells, 8 ml of SD medium with addition of adenine and histidine (chapter 2.1.10.1) was inoculated with a single yeast colony from a –LT agar plate and incubated (16–18 h) at 30°C by shaking at 250 rpm overnight. The overnight culture ( $OD_{600} \sim 1.0$ ) was centrifuged at 1000 x *g* for 5 min at RT. The yeast cell pellet was resuspended in 500 µl of 2 M chilled LiAc and incubated for 5 min on ice. After centrifugation at 1000 x *g* for 5 min at RT, the cell pellet was resuspended in 100 µl of 0.4 M chilled NaOH, incubated for 5 min on ice and centrifuged at 1000 x *g* for 5 min. The cell pellet was resuspended in 100 µl of sample buffer containing 25 µl of NuPAGE® LDS Sample Buffer (4x) (Invitrogen), 10 µl of 1 M DTT and 65 µl of Ampuwa. After yeast proteins were denatured for 10 min at 70°C, the mixture was placed for 5 min on ice and was further centrifuged at 16,000 x *g* for 1 min to pellet cell debris. The protein containing supernatant was transferred into a new reaction tube and 28 µl of the supernatant was used for SDS-PAGE (chapter 2.2.2.6).

### **2.2.2.3 Protein concentration from cell culture medium**

Proteins from cell culture medium were concentrated using the Vivaspin<sup>®</sup> Turbo 15 centrifugal concentrators (30 kDa MWCO) (Sartorius) according to manufacturer's instructions.

### **2.2.2.4 Determination of protein concentration**

Protein concentration was determined according to the method of Bradford (1976). The used solution Roti<sup>®</sup>-Nanoquant (5x) (Carl Roth) consists of the Coomassie Brilliant Blue dye that has the property to bind unspecifically to proteins in acidic solution, resulting in a shift of its absorption maximum from 465 nm to 595 nm.

A Bovine Serum Albumin Standard Ampule (Thermo Scientific) was diluted to generate standard protein concentrations for a calibration curve to determine the protein concentration by extrapolating to this curve.

To determine protein concentration 5x Roti-Nanoquant was diluted with ddH<sub>2</sub>O to a final 1x concentration and further stored at 4°C up to 3 month. Protein sample was diluted 1:100 with Ampuwa and 50 µl of the sample was pipetted into a 96-well plate in triplicate. Ampuwa was used as control. Each diluted protein sample was mixed with 200 µl of 1x Roti-Nanoquant and incubated for 5 min at RT. The absorptions were measured using the Synergy<sup>™</sup> Mx plate reader (BioTek) and calculated with the provided Gen5<sup>™</sup> software.

### **2.2.2.5 Co-immunoprecipitation**

Co-immunoprecipitation (Co-IP) is a technique to identify protein-protein interactions by using a target protein antibody for the indirect capture of proteins that are bound to the target protein. These protein complexes can be further analyzed for example by western blot analysis to identify unknown complex members.

To pre-clear isolated protein extract of proteins which can bind unspecifically to the beads, 500–1000 µg of protein extract and 20 µl of Protein G Magnetic Beads (New England Biolabs) were gently mixed, filled up with lysis buffer (chapter 2.1.6) to a total volume of 500 µl and rotated on the Stuart<sup>®</sup> SB2 rotator (Bibby Scientific) for 1 h at 4°C. Afterwards, a magnetic field was applied for 1 min by placing the reaction tube into a 6-Tube Magnetic

Separation Rack (New England Biolabs) to pull the beads to the side of the tube. The supernatant was pipetted into a new reaction tube, 2 µg of appropriate antibody (chapter 2.1.11.1) was added and the mixture was incubated on the rotator at 4°C overnight. No antibody was added to the negative control. The following day, 20 µl of Protein G Magnetic Beads was added and the mixture was incubated on the rotator for 2 h at 4°C. After brief centrifugation, a magnetic field was applied for 1 min and the supernatant was removed. The beads were washed with 500 µl of lysis buffer and incubated on the rotator for 5 min at 4°C. The mixture was briefly centrifuged and the washing step was additionally repeated 4 times as previously described. For the final washing step, 500 µl of TBS buffer was used. Thereafter, a magnetic field was applied for 1 min, the supernatant was removed and the bead pellet was gently mixed with 16.3 µl of lysis buffer, 6.25 µl of LDS Sample Buffer (4x) and 2.5 µl of 1 M DTT. Proteins were denatured for 10 min at 70°C and separated from the beads meanwhile. The mixture was placed for 5 min on ice and after applying a magnetic field for 1 min, the supernatant was completely used for SDS-PAGE (chapter 2.2.2.6).

#### **2.2.2.6 SDS polyacrylamide gel electrophoresis**

SDS polyacrylamide gel electrophoresis (SDS-PAGE) was used for the separation of proteins according to their molecular weight based on the method described by (Laemmli, 1970). The method bases on the use of gels and buffers with an operating pH of 7.0. This neutral pH increases the stability of both proteins and gels and leads to a better result of electrophoresis.

In general, samples consisted of 30 µg protein, 0.25 volume LDS Sample Buffer (4x) and 10% 1 M DTT (reducing agent), filled up with Ampuwa to a total volume of 20–28 µl, depending on the maximum sample loading volume of the gel. Proteins were denatured for 10 min at 70°C and placed on ice for 5 min. After brief centrifugation, protein samples were loaded onto a gradient gel (NuPAGE® 3–8% Tris-Acetate Gel or NuPAGE® 4–12% Bis-Tris Gel, Invitrogen) placed in Novex® Mini-Cell Electrophoresis System (Invitrogen). Pre-stained molecular weight standard (10 µl of SeeBlue® Plus2 Pre-Stained Protein Standard or 20 µl of HiMark™ Pre-Stained High Molecular Weight Protein Standard, Invitrogen) was additionally loaded on the gel for determination the size of the separated proteins. Gel electrophoresis was performed for 10 min at 80 V and further at either 120 V (10-well gel) or 160 V (20-well gel) and depending on the composition of the gel, in

1x NuPAGE<sup>®</sup> Tris-Acetate SDS Running Buffer or 1x NuPAGE<sup>®</sup> MES SDS Running Buffer (Invitrogen).

#### **2.2.2.7 Transfer of proteins from a polyacrylamide gel to a membrane**

For detection of proteins by western blot analysis, separated proteins from a polyacrylamide gel were transferred to a membrane based on the method described by (Gershoni and Palade, 1983). Proteins <150 kDa were transferred on a nitrocellulose membrane (Amersham<sup>™</sup> Protran<sup>™</sup> Supported 0.45 µm NC, GE Healthcare), whereas proteins >150 kDa were transferred on a PVDF membrane (Amersham<sup>™</sup> Hybond<sup>™</sup>-P PVDF Transfer Membrane 0.45 µm, GE Healthcare).

One membrane and four Blotting Paper Sheets (Sartorius) were cut to the size of the gradient gel. The nitrocellulose membrane was activated in ddH<sub>2</sub>O and further equilibrated in chilled transfer buffer I (chapter 2.1.6), while the PVDF membrane was activated in 100% methanol for approximately 30 s and then equilibrated in chilled transfer buffer II (chapter 2.1.6) for 5 min. Blotting papers and foam pads were soaked in appropriate transfer buffer. For transfer, the tank blotting system Mini Protean<sup>®</sup> II Cell (Bio-Rad) was used and the components were placed in a provided cassette on top of each other as follows: two sheets of blotting paper, membrane, polyacrylamide gel and two sheets of blotting paper. Potential air bubbles were carefully removed. The cassette was inserted into the tank in the way that the gel was located near to the cathode of the blotting system. The tank further contained appropriate and chilled transfer buffer and a cooling unit. The transfer of proteins <150 kDa was performed at 250 mA per gel for 1 h at 4°C. The transfer of proteins >150 kDa was performed at 25 V overnight. Additionally, the buffer tank was put in an ice box and the buffer was agitated by a magnetic stirrer to avoid the formation of an ion gradient and to insure homogeneity of the buffer temperature.

#### **2.2.2.8 Protein detection on membranes using antibodies**

After protein transfer to a membrane, unspecific binding sites were blocked by incubating the membrane, depending on the used antibody, with blocking solution I or II (chapter 2.1.6) for at least 1 h at RT. Primary antibody (chapter 2.1.11.1) was diluted, depending on the antibody, in antibody diluent solution I or II (chapter 2.1.6) at 4°C overnight. The



following day, the membrane was washed with TBST buffer three times for 10 min to remove unbound antibody. The membrane was further incubated with appropriate secondary antibody (chapter 2.1.11.2) diluted, depending on the antibody, in antibody diluent solution I or II for 1.5–2 h at RT. To remove unbound antibody, the membrane was washed three times for 10 min with TBST buffer. The Immobilon™ Western Chemiluminescent HRP Substrate (Merck Millipore) was used to visualize membrane bound proteins and was prepared according to manufacturer's instructions. The membrane was covered with the prepared solution, placed between a plastic wrap and incubated for 5 min at RT. The chemiluminescent signals were digitally detected using FluorChem® Q (Alpha Innotech) and evaluated with the provided AlphaView® Q software (Alpha Innotech).

## **2.2.3 Histological methods**

### **2.2.3.1 Dissection of mouse tissues and embryos**

For dissection of mouse tissues, the mouse was killed by CO<sub>2</sub>-asphyxiation and the required tissues were dissected. For RNA isolation (chapter 2.2.1.1.5) the tissues were immediately frozen in liquid nitrogen and further stored at –80°C.

For dissection of mouse embryos, one-to-one matings of wildtype *Whirligig* (Chd7<sup>+/+</sup>) female and wildtype *Whirligig* (Chd7<sup>+/+</sup>) male mice were set up. Female *Whirligig* mice were daily checked for a vaginal plug, to determine the age of the embryos. When a vaginal plug was observed, the day was counted as embryonic stage 0.5 (E0.5). At the desired embryonic stage, the pregnant *Whirligig* mouse was killed by cervical dislocation and the uterus was removed. The embryos were dissected out of the yolk sacs, a tail biopsy was performed for gDNA isolation (chapter 2.2.1.1.1), further genotyping PCR (chapter 2.2.1.2.1.3) and sequencing analysis (chapter 2.2.1.2.4) to confirm the genotype. The embryos were immediately frozen in liquid nitrogen and further stored at –80°C for RNA isolation (chapter 2.2.1.1.5).

### **2.2.3.2 Fixation of cells on slides**

For histological analysis, O9-1 cells were grown on culture slides (BD Biosciences) providing eight chambers. Before plating the cells, slides were coated with matrigel (chapter 2.2.4.1.2).

Before further histological analysis, cells were washed two to three times with DPBS and fixed with 4% PFA for 10 min at RT.

### **2.2.3.3 Immunofluorescence staining**

Before immunofluorescence staining, O9-1 cells were fixed (chapter 2.2.3.2) and further washed two to three times with ice cold DPBS. Cells were permeabilized with 0.1% Triton X-100 solution for 10 min. After washing the cells with DPBS three times for 5 min, unspecific binding sites were blocked by incubation with blocking solution (chapter 2.1.6) for at least 1 h at RT. Cells were incubated with the appropriate primary antibody (chapter 2.1.11.1) diluted in antibody diluent solution (chapter 2.1.6) in a humidified chamber at 4°C overnight. The following day, cells were washed with DPBS three times for 10 min and incubated with the appropriate secondary antibody (chapter 2.1.11.2) diluted in antibody diluent solution (chapter 2.1.6) in a humidified chamber for 1.5–2 h at RT. Afterwards, cells were washed with DPBS three times for 10 min and shortly air-dried. Cells were mounted with Fluoroshield™ with Dapi (Sigma-Aldrich), sealed with nail polish and stored in the dark at 4°C. Immunofluorescence staining was analyzed with the confocal laser scanning microscope IX81 (Olympus) using the provided FV10-ASW1.7 software.

## **2.2.4 Cell culture methods**

### **2.2.4.1 Coating of cell culture vessels**

#### **2.2.4.1.1 Preparation of fibronectin coated cell culture vessels**

Human fibronectin (Merck Millipore) was used for the preparation of fibronectin coated cell culture vessels. The fibronectin was diluted in chilled DPBS to a concentration of 50 µg/ml. One cell culture plate (ø 10 cm) was coated with 5 ml fibronectin solution and

left on the culture vessel for at least 10 min. Then, the solution was aspirated and could be reused several times when stored at 4°C. The culture vessel was left open until it got dry (approximately 10 min) and afterwards the cells were plated on the coated culture vessel.

#### **2.2.4.1.2 Preparation of matrigel coated cell culture vessels**

For the preparation of matrigel coated cell culture vessels the Matrigel® Basement Membrane Matrix (Corning) was used. During the work with matrigel, chilled pipette tips and DPBS were used. After thawing on ice at 4°C, aliquots of 100 µl were prepared on ice and further stored at -20°C. Before use, required quantity of aliquots was thawed on ice at 4°C either at least for 1 h or overnight. One aliquot was diluted 1:50 in DPBS, respectively. To coat one cell culture plate (ø 10 cm), 5 ml of matrigel solution was used and left on the culture vessel for at least 1 h at RT before use. In advance coated culture vessels were stored up to 5–6 d at 4°C. The matrigel solution was carefully aspirated just before plating the cells.

#### **2.2.4.2 Culture of eukaryotic cells**

##### **2.2.4.2.1 Culture and passaging of murine JoMa1 and JoMa1.3 cells**

Murine JoMa1 and JoMa1.3 cells (chapter 2.1.9) were cultured for 3–4 d on fibronectin coated cell culture vessels (chapter 2.2.4.1.1) until they reached a confluence of approximately 80%. The NCC medium (chapter 2.1.9.1) was carefully aspirated and the cells were washed with DPBS. The DPBS was removed from the cells and 1–4 ml of Trypsin-EDTA (PAN-Biotech), depending on the size of the culture vessel, was applied. After incubation for 3–5 min at 37°C and 5% CO<sub>2</sub> in a humidified incubator, the detachment of the cells from the culture vessel was controlled under the light microscope. To inactivate the Trypsin-EDTA treatment, an equal volume of Trypsin Inhibitor (Sigma-Aldrich) was added and the cell suspension was centrifuged at 150 x g for 5 min. The supernatant was discarded and the cell pellet was resuspended in NCC medium. The cells were generally split 1:10 and plated on fibronectin coated culture vessels in an appropriate volume of NCC medium. The cells were cultivated at 37°C in a 5% CO<sub>2</sub>

humidified incubator. The medium was daily replaced with freshly added 4-OHT to remove not adherent cells and in order to keep the cells in their proliferating and undifferentiated state.

#### **2.2.4.2.2 Culture and passaging of murine O9-1 cells**

Until the murine O9-1 cells (chapter 2.1.9) reached a confluence of approximately 80% they were cultured for 3–4 d on matrigel coated cell culture vessels (chapter 2.2.4.1.2). After the aspiration of the ESC medium (chapter 2.1.9.1), the cells were washed with DPBS that was removed afterwards. Depending on the size of the culture vessel, the cells were treated with 1–4 ml Trypsin-EDTA (PAN-Biotech) and incubated in a 37°C and 5% CO<sub>2</sub> humidified incubator for 3–5 min. Under the light microscope the detachment of the cells was controlled. By addition of an equal volume of ESC medium, the Trypsin-EDTA treatment was stopped and the cell suspension was centrifuged at 300 x g for 3 min. After discarding the supernatant, the cell pellet was resuspended in ESC medium and the cells were typically split 1:100. The cells were plated in ESC medium on matrigel coated cell culture vessels and cultivated at 37°C in a 5% CO<sub>2</sub> humidified incubator. The next day, the medium was replaced to remove not adherent cells and changed every 2–3 d thereafter.

#### **2.2.4.2.3 Culture and passaging of human HEK293 cells**

The human HEK293 cells (chapter 2.1.9) were cultured for 3–4 d in cell culture flasks until they reached a confluence of approximately 80%. The FB medium (chapter 2.1.9.1) was aspirated and the cells were washed with DPBS. After aspiration of the DPBS, the cells were detached from the culture vessel using 1–4 ml TrypLE™ Express (Gibco), depending on the size of the culture vessel. The detachment of the cells was controlled under the light microscope after incubation in a 37°C and 5% CO<sub>2</sub> humidified incubator. To inactivate the TrypLE™ Express treatment, an equal volume of FB medium was added. The cell suspension was centrifuged at 190 x g for 5 min. The supernatant was discarded and the cell pellet resuspended in FB medium. A typically split ratio was 1:4 to 1:6. The cells were plated in culture flasks and cultivated at 37°C in a 5% CO<sub>2</sub> humidified incubator.

To remove not adherent cells, the medium was changed the next day and then replaced every 2–3 d.

#### **2.2.4.2.4 Cryopreservation and thawing of eukaryotic cells**

Cells were cryopreserved from confluent cell culture vessels. JoMa1 or JoMa1.3 cell pellet was resuspended in 1 ml chilled ready-to-use Cryo-SFM (PromoCell) medium. O9-1 cell pellet was resuspended in 1 ml NCC medium with 10% DMSO (chapter 2.1.9.2), whereas HEK293 cell pellet was resuspended in 500  $\mu$ l of FB medium (chapter 2.1.9.1) and subsequently mixed with 500  $\mu$ l of FB freezing medium (chapter 2.1.9.2). The appropriate mixture was transferred into well labeled cryovials, which were immediately placed in a Mr. Frosty<sup>TM</sup> Freezing Container (Kisker) and then frozen at  $-80^{\circ}\text{C}$ . For long term storage the cryovials were placed in liquid nitrogen.

For the procedure of thawing the cryovial was incubated in a  $37^{\circ}\text{C}$  water bath until the cells were almost completely thawed. The cells were carefully mixed with a larger volume of appropriate culture medium (chapter 2.1.9.1) and then centrifuged using appropriate conditions. After removal of the supernatant, the cells were resuspended in culture medium, seeded on appropriate cell culture vessel and cultivated at  $37^{\circ}\text{C}$  in a 5%  $\text{CO}_2$  humidified incubator. The next day, not adherent cells were removed by changing the culture medium. The further cell culture procedure was performed according to the appropriate cell line as described above.

#### **2.2.4.3 Transfection of eukaryotic cells**

##### **2.2.4.3.1 Transfection of plasmids into eukaryotic cells**

Eukaryotic cells were transfected with plasmids in order to induce a protein overexpression. Lipofectamine<sup>®</sup> 2000 Transfection Reagent (Invitrogen) was used as transfection reagent. This transfection reagent contains lipids which form vesicles with a bilayer sheet, so called liposomes, in aqueous solution. Liposomes and nucleic acids can form nucleic acid lipid complexes which eukaryotic cells can actively take up by endocytosis. The nucleic acids are able to enter the nucleus when the nuclear membrane

dissolves during mitosis. For efficient transfection, the division rate of the cells must be high as possible.

One day before transfection, cells were plated on cell culture plates or in cell culture flasks. In general,  $1.2 \times 10^6$  O9-1 cells/ml were plated on culture plates ( $\varnothing$  10 cm) and  $5.0 \times 10^6$  HEK293 cells/ml were plated in culture flasks ( $75 \text{ cm}^2$ ). The following day, 30  $\mu\text{g}$  of plasmid DNA was gently mixed with Opti-MEM<sup>®</sup> I Reduced Serum Medium (Gibco) in a total volume of 1875  $\mu\text{l}$  and incubated for 5 min at RT. Furthermore, 75  $\mu\text{l}$  of Lipofectamine 2000 was also gently mixed with 1800  $\mu\text{l}$  of Opti-MEM and incubated for 5 min at RT. Afterwards, the plasmid DNA and the Lipofectamine 2000 mixture were combined, gently mixed and incubated for 25 min at RT. Before the transfection mixture was added to the cells, the culture medium was aspirated and the cells were washed with DPBS. 9 ml of ESC medium (chapter 2.1.9.1) was used as culture medium for O9-1 cells. As culture medium for HEK293 cells, 9 ml of DMEM (PAN-Biotech) with 1x NEAA (Gibco) was used. The transfection mixture was applied dropwise to the cells, gently mixed with the culture medium and incubated for 24 h at 37°C in a 5% CO<sub>2</sub> humidified incubator. After 4–5 h, 9 ml of culture medium composed of DMEM with 20% FBS (PAN-Biotech) and 1x NEAA was added to the transfection reagent containing culture medium of HEK293 cells. After incubation time, protein was isolated from the transfected cells.

#### **2.2.4.3.2 Transfection of short interfering RNAs**

Short interfering RNAs (siRNAs) are used for silencing of a specific gene. Thereby, siRNA binds to a specific mRNA and marks it for degradation. This results in a reduced expression of the specific gene. Three different mouse siRNAs against Chd7 (s232009, s232010, s232011, *Silencer*<sup>®</sup> Select Pre-Designed & Validated siRNA, ambion<sup>®</sup>, Life Technologies, Darmstadt) were used. A siRNA with a sequence that do not target any gene product was used as control siRNA (*Silencer*<sup>®</sup> Select Negative Control No. 1 siRNA, ambion<sup>®</sup>, Life Technologies, Darmstadt). Lipofectamine 2000 was used as transfection reagent. Thereby, complexes of lipids and siRNA oligonucleotides can be formed which facilitate the uptake of the siRNA molecules into the cells.

One day before transfection, murine O9-1 cells were plated on matrigel coated 6-well cell culture plates. Per well  $0.15 \times 10^6$  cells were plated in 2.5 ml of ESC medium (chapter 2.1.9.1). The following day, 6  $\mu\text{l}$  of siRNA (stock concentration: 10  $\mu\text{M}$ ) was gently mixed with 294  $\mu\text{l}$  of Opti-MEM and incubated for 5 min at RT. Furthermore, 12  $\mu\text{l}$  of

Lipofectamine 2000 was also gently mixed with 288  $\mu$ l of Opti-MEM and incubated for 5 min at RT. Afterwards, the siRNA and the Lipofectamine 2000 mixture were combined, gently mixed and incubated for 25 min at RT. In the meantime, the cells were washed with DPBS and 2.0 ml of ESC medium was added to each well. 500  $\mu$ l of the transfection mixture was applied dropwise to the cells and gently mixed with the culture medium. Each well contained a final siRNA concentration of 20 nM. The cells were incubated for 48 h at 37°C in a 5% CO<sub>2</sub> humidified incubator. After incubation time, RNA was isolated from the transfected cells.

## 3 Results

### 3.1 Characterization of murine NCC lines

To choose a suitable cell line for *in vitro* analyses of NCCs, which are the affected cell type leading to the phenotype seen in CHARGE syndrome patients, the expression pattern of different molecular markers in the two murine cell lines JoMa and O9-1 were examined. For testing the NCC behavior of the different cell lines, the NCC marker genes *Sox10* (SRY (sex determining region Y)-box 10), *Ngfr* (nerve growth factor receptor (TNFR superfamily, member 16)), *Snai2* (snail family zinc finger 2), *Pax3* (paired box 3), *Snai1* (snail family zinc finger 1) and *Twist1* (twist basic helix-loop-helix transcription factor 1) were used. Furthermore, the expression of the neuronal marker *Nefh* (neurofilament, heavy polypeptide), the glia marker *Gfap* (glial fibrillary acidic protein) and the two smooth muscle markers *Cnn1* (calponin 1) and *Actg2* (actin, gamma 2, smooth muscle enteric) were investigated. The expression of the melanocyte marker *Tyr* (tyrosinase) and the chondrocyte marker *Col2a1* (collagen, type II, alpha 1) was also analyzed.

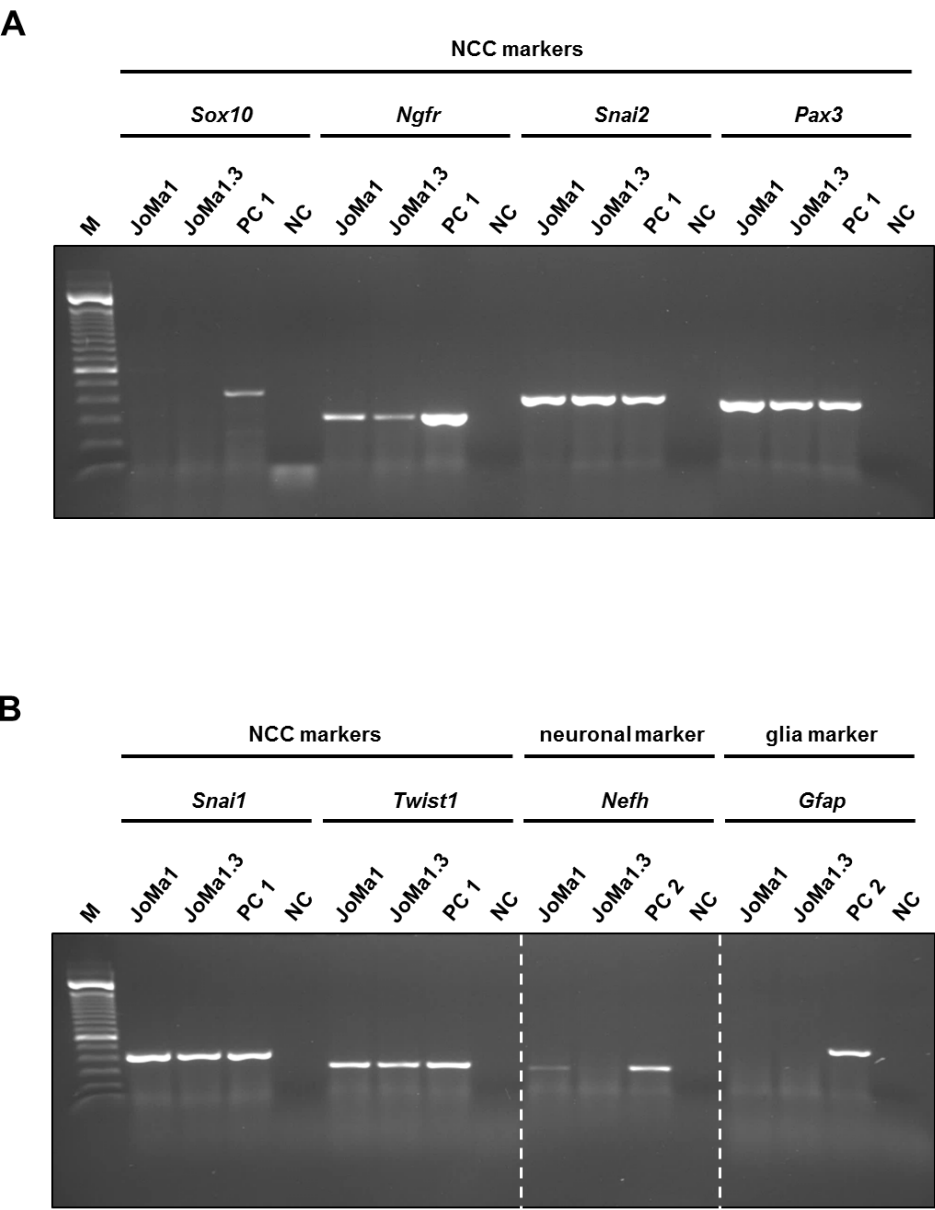
#### 3.1.1 Molecular marker expression in murine JoMa cells

The murine cell line JoMa1 and the clonally derived subline JoMa1.3 were established and described as immortalized neural crest stem cell lines by Maurer *et al.* (2007).

To monitor the initial situation both JoMa cell lines were tested for the expression pattern of different molecular marker genes by RT-PCR analysis on cDNA obtained from total RNA of JoMa1 and JoMa1.3 cells (Figure 4 A–C). Whole mouse embryo (E10.5) cDNA was used as positive control for *Sox10*, *Ngfr*, *Snai2*, *Pax3*, *Snai1*, *Twist1*, *Tyr* and *Col2a1*. Mouse brain cDNA was used as positive control for *Nefh* and *Gfap*, whereas mouse uterus cDNA was used as positive control for *Cnn1* and *Actg2*. H<sub>2</sub>O was used as negative control, respectively. All analyzed NCC markers were expressed in both JoMa cell lines in exception of *Sox10*. The neuronal marker *Nefh* could be detected with a weak signal only in JoMa1 cells, whereas the analyzed glia marker *Gfap* and the smooth muscle marker *Cnn1* were not detected in JoMa cells. The second tested smooth muscle marker gene *Actg2* were weakly expressed in both JoMa cell lines. *Tyr*, the melanocyte marker, was



detected with a weak signal only in the JoMa1 cells. An expression of the chondrocyte marker *Col2a1* was observed in JoMa1 cells as well as in JoMa1.3 cells. Earlier and later cell passages were investigated in the same way with similar results (data not shown). The data obtained by the RT-PCR analysis demonstrate based on the tested marker genes that JoMa1 and JoMa1.3 cells are undifferentiated NCCs.



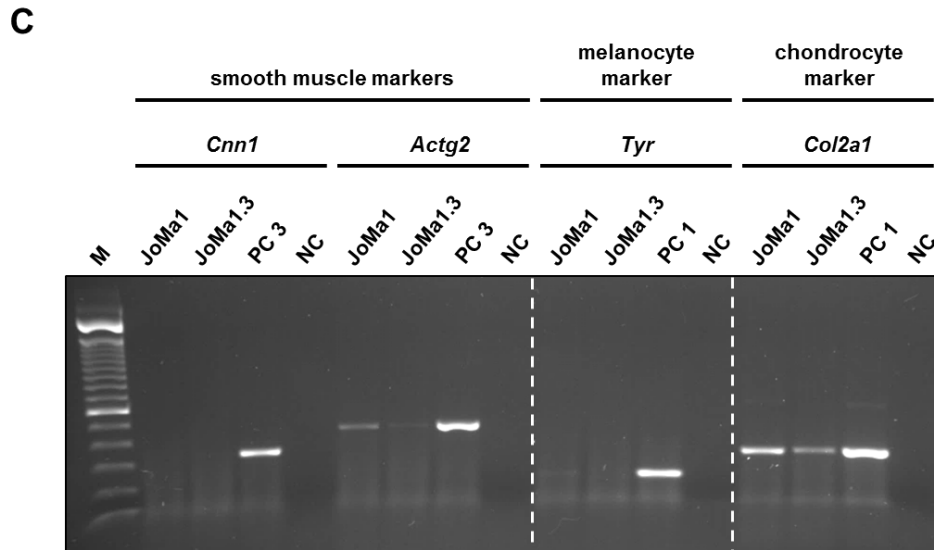


**Figure 4: Expression analysis of NCC, neuronal, glia, smooth muscle, melanocyte and chondrocyte marker genes in JoMa1 cells and JoMa1.3 cells.** RT-PCR analysis performed on cDNA obtained from total RNA of JoMa1 cells and JoMa1.3 cells. The results proved the expression of the NCC markers *Ngfr*, *Snai2*, *Pax3*, *Snai1* and *Twist1*, the neuronal marker *Nefh*, the smooth muscle marker *Actg2*, the melanocyte marker *Tyr* and the chondrocyte marker *Col2a1*. (A) Expression analysis of the NCC markers *Sox10* (444 bp), *Ngfr* (310 bp), *Snai2* (407 bp) and *Pax3* (374 bp). (B) Expression analysis of the NCC markers *Snai1* (420 bp) and *Twist1* (331 bp), the neuronal marker *Nefh* (301 bp) and the glia marker *Gfap* (454 bp). (C) Expression analysis of the smooth muscle markers *Cnn1* (340 bp) and *Actg2* (458 bp), the melanocyte marker *Tyr* (216 bp) and the chondrocyte marker *Col2a1* (321 bp). M: 100 bp DNA Ladder; PC 1: positive control 1 with whole mouse embryo (E10.5) cDNA, PC 2: positive control 2 with mouse brain cDNA, PC 3: positive control 3 with mouse uterus cDNA; NC: negative control with H<sub>2</sub>O.

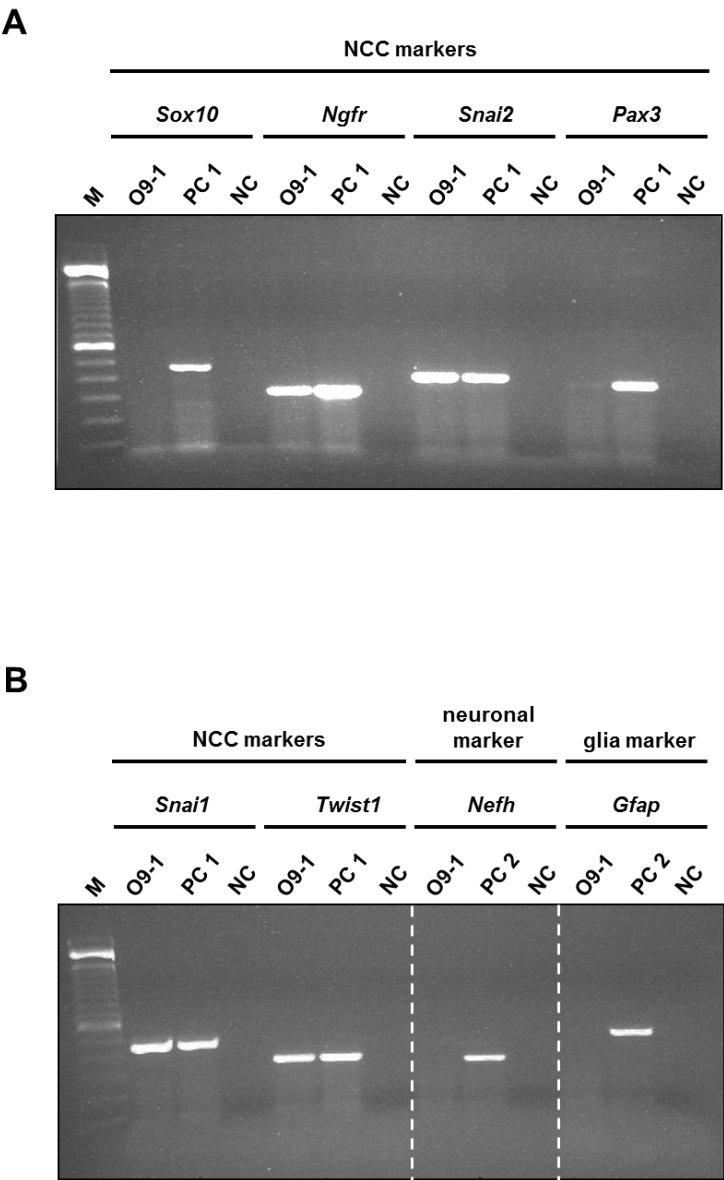
### 3.1.2 Molecular marker expression in murine O9-1 cells

The murine cell line O9-1 was established by Ishii *et al.* (2012). A whole-genome expression profiling of O9-1 cells revealed that this cell line has characteristics of both neural crest and stem cells (Ishii *et al.*, 2012).

The O9-1 cell line was characterized by RT-PCR analysis on cDNA obtained from total RNA of O9-1 cells using the same marker genes like with the JoMa1 cells and JoMa1.3 cells to monitor the initial situation also of this cell line (Figure 5 A–C). Whole mouse embryo (E10.5) cDNA was used as positive control for *Sox10*, *Ngfr*, *Snai2*, *Pax3*, *Snai1*, *Twist1*, *Tyr* and *Col2a1*. Mouse brain cDNA was used as positive control for *Nefh* and *Gfap*, whereas mouse uterus cDNA was used as positive control for *Cnn1* and *Actg2*.

H<sub>2</sub>O was used as negative control, respectively. O9-1 cells express the tested NCC markers although the expression of *Pax3* was weak. As in both JoMa cell lines no expression of *Sox10* could be detected. Furthermore, there were no expression of the neuronal marker *Nefh*, the glia marker *Gfap* and the melanocyte marker *Tyr* observed. The smooth muscle marker *Cnn1* was weak expressed, whereas the other tested smooth muscle marker *Actg2* and the chondrocyte marker *Col2a1* were strongly expressed. Earlier and later cell passages were investigated in the same way with similar results (data not shown).

The data obtained by the RT-PCR analysis demonstrate based on the tested marker genes that O9-1 cells are, like the JoMa cells, undifferentiated NCCs.



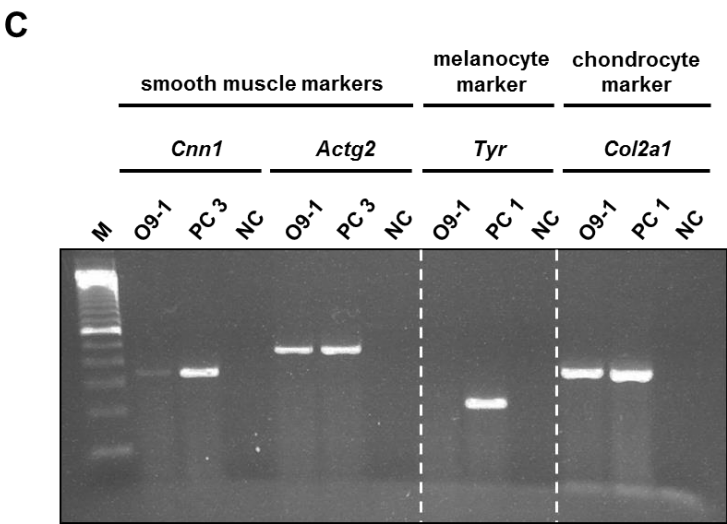


**Figure 5: Expression analysis of NCC, neuronal, glia, smooth muscle, melanocyte and chondrocyte marker genes in O9-1 cells.** RT-PCR analysis performed on cDNA obtained from total RNA of O9-1 cells. The results revealed the expression of the NCC markers *Ngfr*, *Snai2*, *Pax3*, *Snai1* and *Twist1*, the smooth muscle markers *Cnn* and *Actg2* as well as the chondrocyte marker *Col2a1*. **(A)** Expression analysis of the NCC markers *Sox10* (444 bp), *Ngfr* (310 bp), *Snai2* (407 bp) and *Pax3* (374 bp). **(B)** Expression analysis of the NCC markers *Snai1* (420 bp) and *Twist1* (331 bp), the neuronal marker *Nefh* (301 bp) and the glia marker *Gfap* (454 bp). **(C)** Expression analysis of the smooth muscle markers *Cnn1* (340 bp) and *Actg2* (458 bp), the melanocyte marker *Tyr* (216 bp) and the chondrocyte marker *Col2a1* (321 bp). M: 100 bp DNA Ladder; PC 1: positive control 1 with whole mouse embryo (E10.5) cDNA, PC 2: positive control 2 with mouse brain cDNA, PC 3: positive control 3 with mouse uterus cDNA; NC: negative control with H<sub>2</sub>O.

**3.1.3 *Chd7* expression in murine JoMa cells and O9-1 cells**

To determine whether JoMa cells and O9-1 cells also express *Chd7*, the gene mutated in most patients with CHARGE syndrome, RT-PCR analysis on cDNA obtained from total RNA of JoMa cells and O9-1 cells was performed. H<sub>2</sub>O was used as negative control, respectively. As illustrated in Figure 6 A and B, JoMa1 and JoMa1.3 cells as well as O9-1 cells showed expression of *Chd7*.

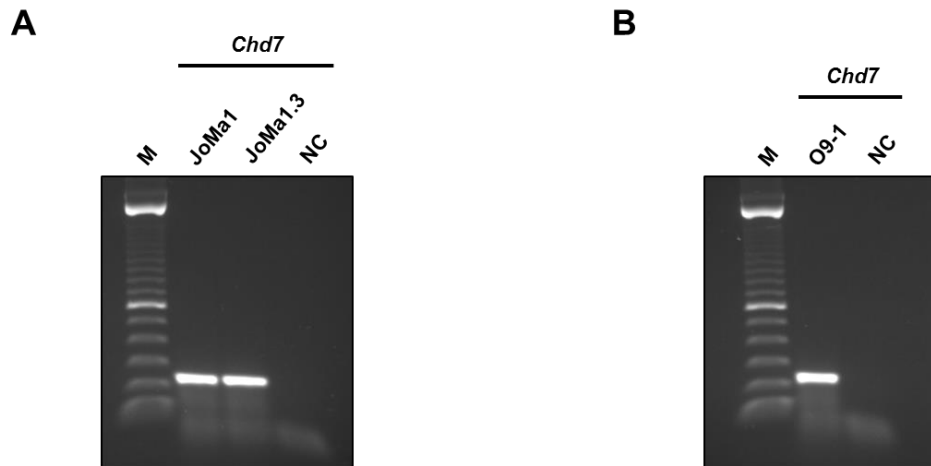


**Figure 6: RT-PCR analysis of *Chd7* expression in JoMa cells and O9-1 cells.** The RT-PCR analysis performed on cDNA obtained from total RNA of (A) JoMa1 and JoMa1.3 cells as well as (B) O9-1 cells proved the expression of *Chd7* (238 bp) in both murine NCC lines. M: 100 bp DNA Ladder; NC: negative control with H<sub>2</sub>O.

The *Chd7* expression was also investigated on protein level. Therefore, western blot analysis with an anti-*Chd7* antibody was performed to detect *Chd7* using nuclear protein extracts of JoMa cells and O9-1 cells. 30 µg of protein was applied per lane. No clear band, but rather a smear could be detected in extracts of JoMa1 and JoMa1.3 cells (Figure 7 A). In contrast, a strong ~336 kDa protein band corresponding to the estimated size of *Chd7* was received in O9-1 cell extract (Figure 7 B).

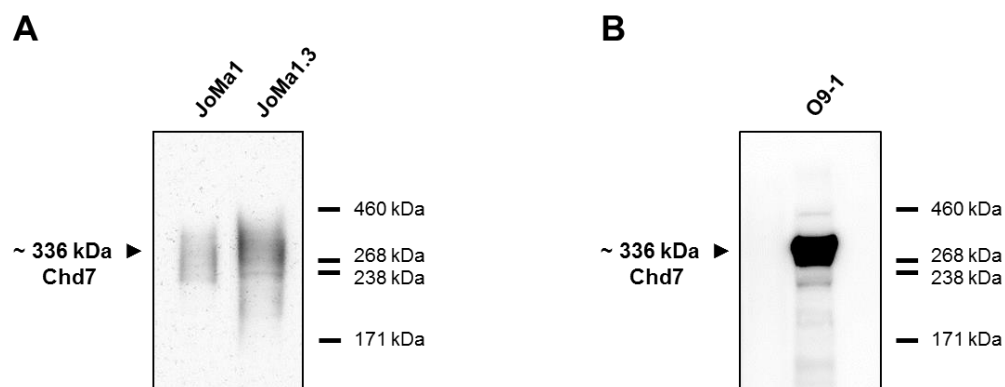


**Figure 7: Western blot analysis of *Chd7* expression in JoMa cells and O9-1 cells.** Western blot analysis using nuclear protein extracts of JoMa1 and JoMa1.3 cells as well as O9-1 cells with an anti-*Chd7* antibody to detect *Chd7*. 30 µg of protein was used per lane. (A) A noticeable protein band was received in neither JoMa1 nor JoMa1.3 cell extracts. (B) In the protein extract of O9-1 cells, a protein band corresponding to the estimated size of *Chd7* (~336 kDa) was detected. Molecular weights of proteins and marker bands are indicated in kilo Dalton (kDa).

The RT-PCR analysis results of the characterized NCC lines revealed that both JoMa cell lines in comparison with the O9-1 cell line differ not much between the tested marker genes and the expression of *Chd7*. However, the western blot analysis revealed a definite strong Chd7 expression on protein level in O9-1 cells compared to both JoMa cell lines. In addition, O9-1 cells derived from murine cranial NCCs (Ishii *et al.*, 2012), whereas the JoMa cell lines derived from murine trunk NCCs (Maurer *et al.*, 2007). Most of the symptoms seen in CHARGE syndrome patients can be explained by a defect of the induction and migration of cranial NCCs. This is consistent with the observed strong *Chd7* expression in the cranial NCC line O9-1. These facts led to the decision to choose the O9-1 cells as a suitable cell line for the investigation of NCCs *in vitro*.

To confirm the data of the RT-PCR and the western blot analysis concerning the expression of *Chd7* in the NCC line O9-1, immunocytochemical staining was performed. Representative images of O9-1 cells are shown in Figure 8. The cell nucleus was stained with DAPI, whereas the cytoskeleton was stained for  $\alpha$ -Tubulin using an anti- $\alpha$ -Tubulin antibody. To detect the target protein Chd7, an anti-Chd7 antibody was used (Figure 8 C). With secondary antibodies conjugated with either Alexa488 ( $\alpha$ -Tubulin) or Cy3 (Chd7), the localization of the proteins were visualized. Cells were incubated without first antibody as negative control. The overlay image revealed that Chd7 was localized specifically in the nucleus (Figure 8 D).

In summary, the results obtained by western blot analysis and immunocytochemical staining indicate an intense expression of *Chd7* in O9-1 cells.

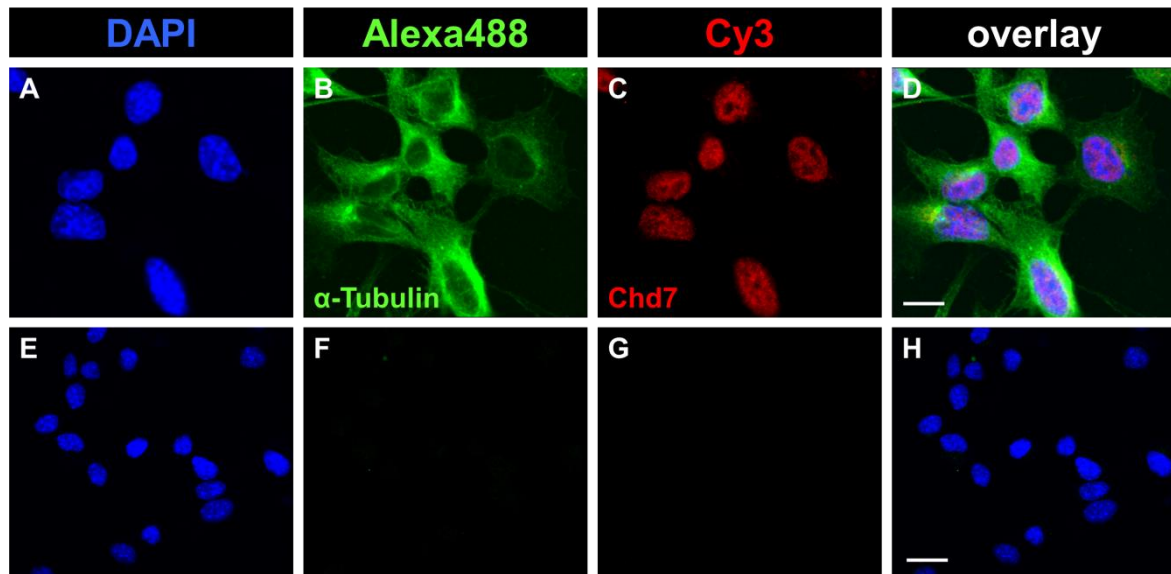


**Figure 8: Chd7 immunocytochemical staining of O9-1 cells.** Representative images of O9-1 cells identified the nuclear localization of Chd7. Cell DNA in nucleus was stained with DAPI (blue, **A** and **E**) and cytoskeleton was stained with an anti- $\alpha$ -Tubulin antibody (green, **B**). Localization of Chd7 was analyzed by an anti-Chd7 antibody (red, **C**). Incubation without first antibody was used as negative control (**F** and **G**). Overlay images are shown in the last column (**D** and **H**). Alexa488 (**B** and **F**) and Cy3 (**C** and **G**) conjugated secondary antibodies were used for visualization. Representative scale bars are indicated in the overlay images. Scale bars: **D**: 20  $\mu$ m; **H**: 10  $\mu$ m.

### 3.2 O9-1 cells express semaphorin receptors and class 3 semaphorins

NCCs are known to express semaphorin receptors namely plexins and neuropilins and they are guided by semaphorins during embryogenesis. In order to verify the expression of semaphorin receptors in the NCC line O9-1, RT-PCR analysis was performed on cDNA obtained from total RNA of O9-1 cells. H<sub>2</sub>O was used as negative control, respectively. The results proved the expression of *Plxna1* (plexin A1), *Nrp1* (neuropilin 1) and *Nrp2* (neuropilin 2) (Figure 9).

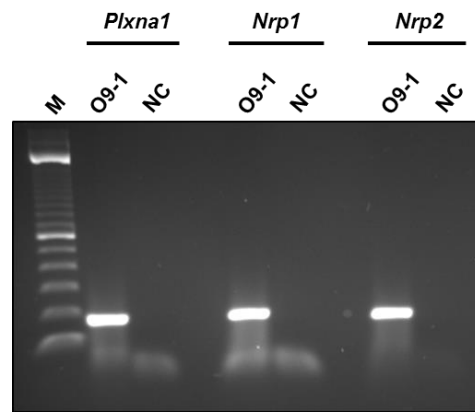


**Figure 9: Expression analysis of semaphorin receptors in O9-1 cells.** The RT-PCR analysis performed on cDNA obtained from total RNA of O9-1 cells confirmed the expression of *Plxna1* (170 bp), *Nrp1* (195 bp) and *Nrp2* (202 bp). M: 100 bp DNA Ladder; NC: negative control with H<sub>2</sub>O.

So far, it is not known that NCCs express semaphorins itself. Nevertheless, RT-PCR analysis on cDNA obtained from total RNA of O9-1 cells revealed the expression of class 3 semaphorins (*Sema3a*, *3c*, *3d* and *3e*) in NCCs for the first time (Figure 10), suggesting an additional function of these group of semaphorins. H<sub>2</sub>O was used as negative control, respectively.

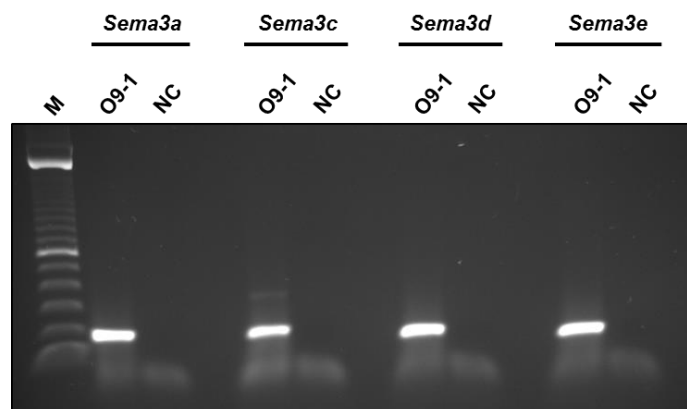


**Figure 10: Expression analysis of class 3 semaphorins in O9-1 cells.** RT-PCR analysis performed on cDNA obtained from total RNA of O9-1 cells revealed the expression of *Sema3a* (186 bp), *Sema3c* (207 bp), *Sema3d* (186 bp) and *Sema3e* (183 bp). M: 100 bp DNA Ladder; NC: negative control with H<sub>2</sub>O.



To confirm the data of the RT-PCR analysis concerning the expression of *Sema3a* in O9-1 cells, immunocytochemical staining was used. Representative images of O9-1 cells are shown in Figure 11. The cell nucleus was stained with DAPI. The cytoskeleton was stained for  $\alpha$ -Tubulin with an anti- $\alpha$ -Tubulin antibody. The target protein *Sema3a* was detected using an anti-*Sema3a* antibody (Figure 11 C). With either Alexa488 ( $\alpha$ -Tubulin) or Cy3 (*Sema3a*) conjugated secondary antibodies, the localization of the proteins were visualized. No staining was detected in negative controls using no primary antibody. The overlay image possessed that *Sema3a* was localized specifically in the nucleus as well as in the cytoplasm of O9-1 cells (Figure 11 D).

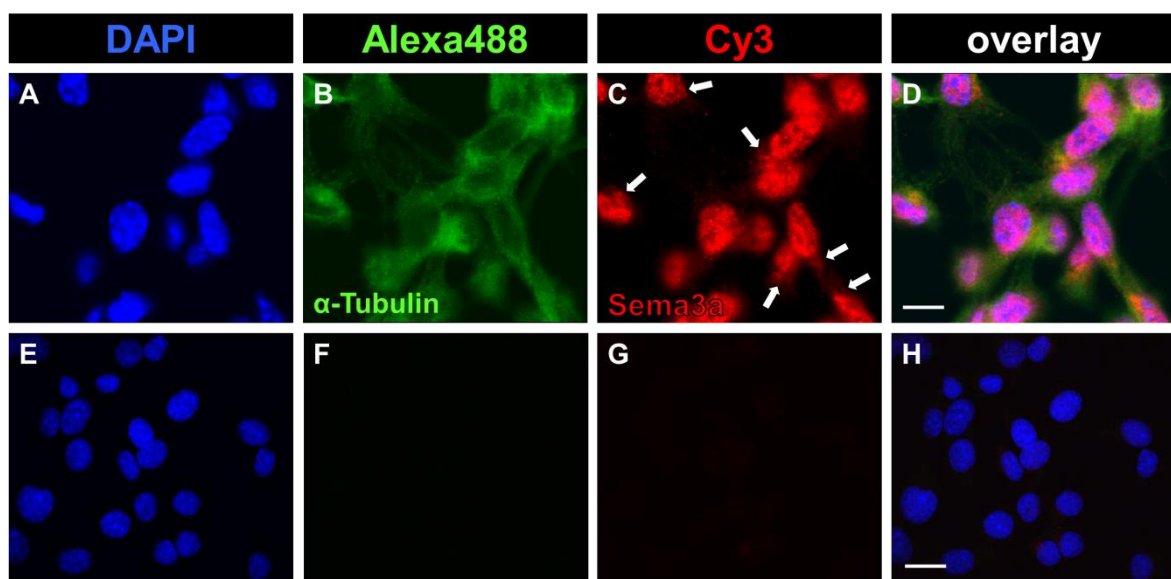


**Figure 11: Sema3a immunocytochemical staining of O9-1 cells.** Representative images of O9-1 cells revealed cytoplasmic and nuclear localization of *Sema3a*. Cell DNA in nucleus was stained with DAPI (blue, **A** and **E**) and cytoskeleton was stained with an anti- $\alpha$ -Tubulin antibody (green, **B**). Localization of *Sema3a* was analyzed by an anti-*Sema3a* antibody (red, **C**). Red arrows indicate cytoplasm areas, with high accumulation of *Sema3a*. Incubation without first antibody was used as negative control (**F** and **G**). Overlay images are shown in the last column (**D** and **H**). Alexa488 (**B** and **F**) and Cy3 (**C** and **G**) conjugated secondary antibodies were used for visualization. Representative scale bars are indicated in the overlay images. Scale bars: **D**: 20  $\mu$ m; **H**: 10  $\mu$ m.

### 3.3 Sema3a is expressed, processed and secreted by O9-1 cells and exists in monomeric and dimeric isoforms

Related class 3 semaphorins are described to exist in monomeric, dimeric and processed isoforms (Adams *et al.*, 1997; Christensen *et al.*, 2005). A schematic representation of the full-length Sema3a protein composition with the predicted processing sites and the potential isoforms, resulting from proteolytic processing, is illustrated in Figure 12.

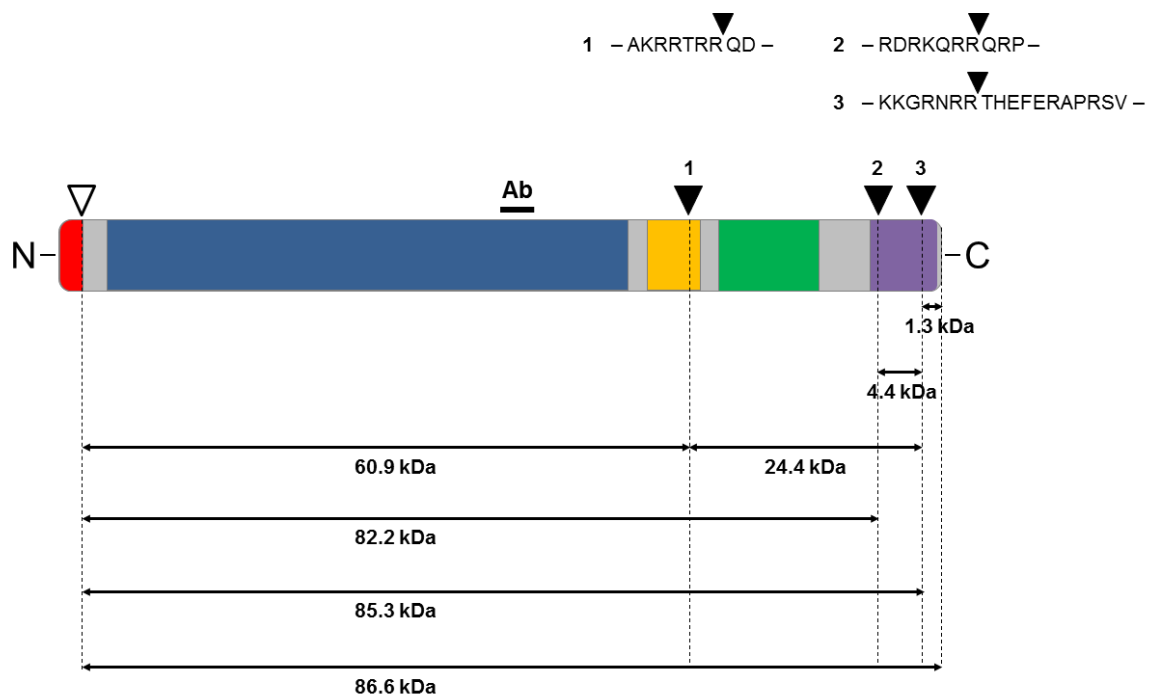


**Figure 12: Schematic representation of full-length Sema3a protein.** Positions of the signal sequence (red), the Sema (Semaphorin) domain (blue), the PSI (plexin-semaphorin-integrin) domain (yellow), the Ig (immunoglobulin)-like domain (green), the basic domain (purple) and the predicted processing sites 1, 2 and 3 (black arrowheads) are indicated. Sema3a sequences containing the processing sites are represented within the figure (top). Processing site after signal sequence (open arrowhead) is permanently used. Theoretical molecular weights of cleavage products are shown in kilo Dalton (kDa). Ab: binding region of the used anti-Sema3a antibody. Adapted from Adams *et al.* (1997) and Christensen *et al.* (2005).

After *Sema3a* expression was identified in O9-1 cells by RT-PCR analysis (chapter 3.2, Figure 10), the expression of *Sema3a* was investigated on protein level using cytoplasmic and nuclear O9-1 protein extracts. Secreted *Sema3a* was analyzed using concentrated

cell culture medium of O9-1 cells. The cytoplasmic and nuclear protein extracts were separately isolated and the medium was concentrated after 24 h of usage. In order to check monomeric and dimeric Sema3a protein isoforms, the different proteins were treated with the reducing agent DTT (+DTT) or without reducing agent (-DTT). Medium and protein extracts were analyzed by western blot analysis using an anti-Sema3a antibody and 30 µg of protein per lane.

The representative results are shown in Figure 13. The monomeric isoforms of ~87 kDa (p87), ~85 kDa (p85), ~82 kDa (p82) and ~61 kDa (p61) were observed in concentrated medium with reduction, whereas the dimeric isoforms of ~174 kDa (p87:p87) and ~170 kDa (p85:p85) as well as the monomeric isoforms of ~82 kDa (p82) and ~61 kDa (p61) were detected in concentrated medium without reduction. In cytoplasmic extract with reducing agent, the dimeric isoform of ~170 kDa (p85:p85) and the monomeric isoform of ~85 kDa (p85) were observed. The dimeric isoform p85:p85 possibly indicates an incomplete cleavage of the disulfide bond between the dimer although the reducing agent DTT was added. In cytoplasmic extract without reducing agent, the dimeric isoform of ~170 kDa (p85:p85) was received. The monomeric isoform of ~85 kDa (p85) was observed in nuclear extract with reduction, whereas the dimeric isoform of ~170 kDa (p85:p85) was received without reduction. In nuclear extract, with and without addition of reducing agent, potentially unspecific protein bands due to unspecific binding of the used antibody were detected. To proof this assumption, O9-1 cells with a full-lengths Sema3a plasmid containing a HA-tag between the signal sequence and the semaphorin domain should be performed. By detection the tag using an anti-HA antibody, the same protein band pattern without the potentially unspecific bands should be received.

Detection of  $\alpha$ -Tubulin (~50 kDa protein band) served as loading control for the cytoplasmic extracts. However, the detection of  $\alpha$ -Tubulin in the nuclear extracts revealed the additional existence of cytoplasmic proteins. This fact can be possibly explained by the used protein extraction method. The nuclear protein Baf47 (~47 kDa protein band) was solely received in the nuclear extracts.

Collectively, the investigation of Sema3a in O9-1 cells on protein level revealed that the expressed full-length Sema3a protein undergoes proteolytic processing to shorter isoforms. Moreover, the existence of monomeric and dimeric isoforms as well as the secretion of Sema3a was demonstrated. The obtained results are summarized in Table 1 and Figure 14.

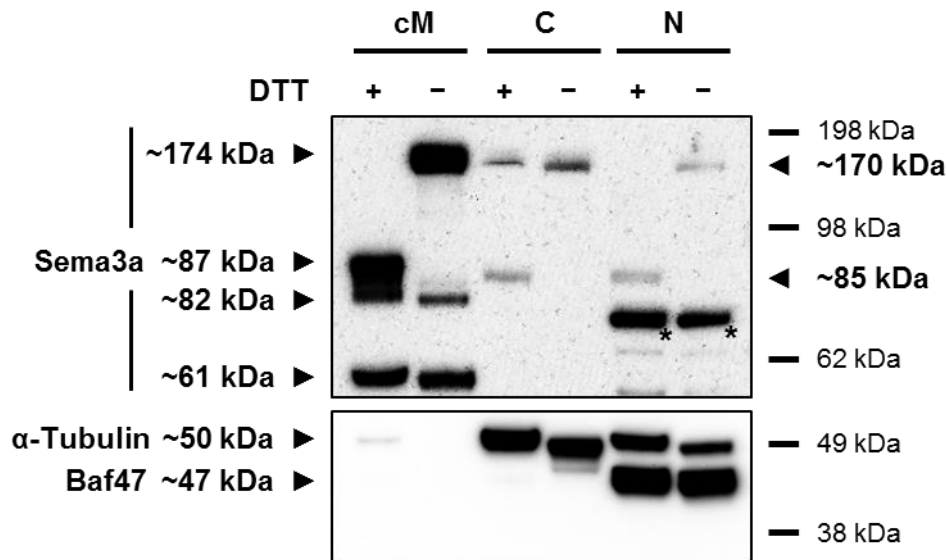


**Figure 13: Isoforms of Sema3a resulting from proteolytic processing and dimerization.**

Cell culture medium was concentrated (cM) after 24 h of usage. Cytoplasmic (C) and nuclear (N) protein extracts of O9-1 cells were separately isolated. 30 µg of protein treated with the reducing agent DTT (+DTT) or without reducing agent (-DTT) was used per lane. The Sema3a isoforms were analyzed by western blot analysis using an anti-Sema3a antibody. In concentrated medium with reducing agent the monomeric isoforms of ~87 kDa (p87), ~85 kDa (p85), ~82 kDa (p82) and ~61 kDa (p61) were detected, whereas in concentrated medium without reducing agent the dimeric isoforms of ~174 kDa (p87:p87) and ~170 kDa (p85:p85) and the monomeric isoforms of ~82 kDa (p82) and ~61 kDa (p61) were observed. In cytoplasmic extract with reduction, the dimeric isoform of ~170 kDa (p85:p85) and the monomeric isoform of ~85 kDa (p85) were received. The dimeric isoform p85:p85 possibly indicates an incomplete cleavage of the disulfide bond between the two p85 monomeric isoforms despite DTT addition. Without reduction, solely the dimeric isoform of ~170 kDa (p85:p85) was observed. In the nuclear extract with reducing agent, the monomeric isoform of ~85 kDa (p85) was received, whereas without reducing agent the dimeric isoform of ~170 kDa (p85:p85) was observed. The detection of α-Tubulin (~50 kDa protein band) served as loading control for the cytoplasmic extracts, revealing the additional existence of cytoplasmic proteins also in the nuclear extracts which can be possible traced back to the used protein extraction method. The nuclear protein Baf47 (~47 kDa protein band) was exclusively detected in the nuclear extracts. Stars (\*) illustrate potentially unspecific protein bands due to unspecific binding of the anti-Sema3a antibody. Molecular weights of proteins and marker bands are indicated in kilo Dalton (kDa).

**Table 1: Sema3a isoforms detected in concentrated medium as well as cytoplasmic and nuclear protein extracts of O9-1 cells.** Medium and protein extracts were treated with the reducing agent DTT (+DTT) and without reducing agent (–DTT) and analyzed by western blot analysis using an anti-Sema3a antibody. Approximate molecular weights of the isoforms are given in kilo Dalton (kDa).

concentrated medium		cytoplasmic extract		nuclear extract	
+DTT	–DTT	+DTT	–DTT	+DTT	–DTT
87 kDa	174 kDa	170 kDa	170 kDa	85 kDa	170 kDa
85 kDa	170 kDa	85 kDa			
82 kDa	82 kDa				
61 kDa	61 kDa				

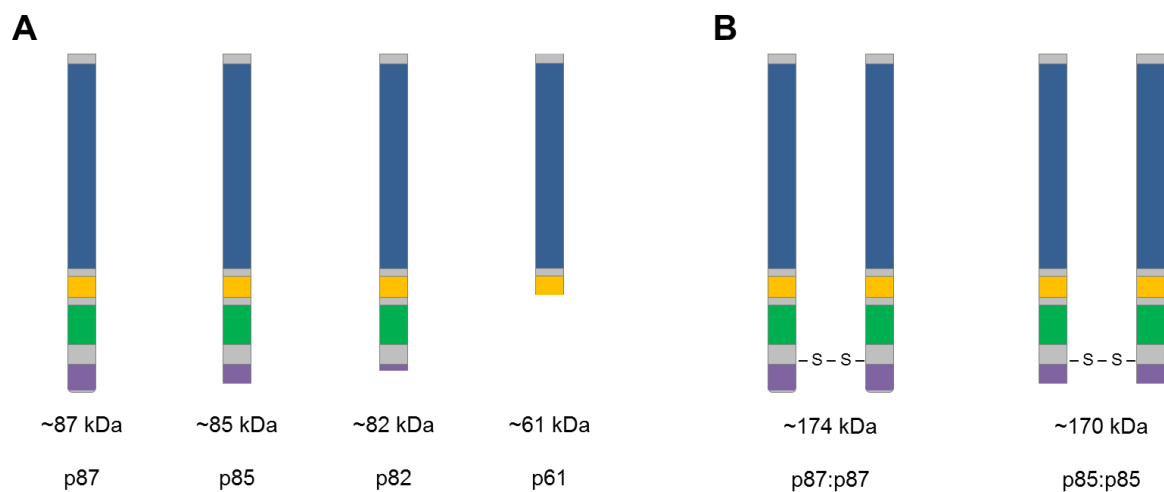


**Figure 14: Schematic representation of proteolytic processed and dimerized Sema3a isoforms identified in concentrated medium as well as cytoplasmic and nuclear protein extracts of O9-1 cells.** Isoforms resulting from combined proteolytic processing and dimerization of Sema3a full length protein are shown, which were detectable with the used anti-Sema3a antibody by western blot analysis. **(A)** Four monomeric isoforms were observed: ~87 kDa (p87), ~85 kDa (p85), ~82 kDa (p82) and ~61 kDa (p61). **(B)** Two dimeric isoforms were detected: the dimeric isoform of ~174 kDa (p87:p87) consist of two ~87 kDa (p87) monomeric isoforms, whereas the dimeric isoform of ~170 kDa (p85:p85) consist of two ~85 kDa (p85) monomeric isoforms. Disulfide bonds between the dimeric isoforms are indicated with –S–S–. Approximate molecular weights of the isoforms are displayed in kilo Dalton (kDa) and in short version (p) (bottom). Adapted from Adams *et al.* (1997) and Christensen *et al.* (2005).

### 3.4 Downregulation of *Chd7* has influence on the expression level of *Sema3a* in O9-1 cells

In order to determine whether the downregulation of *Chd7* has an influence on the expression level of *Sema3a* in NCCs, murine O9-1 cells, which have a high basal *Chd7* expression level (chapter 3.1.3), were transfected with one of three different short interfering RNAs (siRNA 1, 2, 3) against *Chd7*. Total RNA lysates were isolated from O9-1 cells 48 h after siRNA transfection and reverse transcribed into cDNA. Afterwards, the efficiency of the siRNAs was tested by qRT-PCR analysis. All three *Chd7*-specific siRNAs proved to be effective as seen by a reduced *Chd7* expression compared with control siRNA transfected cells (Figure 15). With siRNA 1 or siRNA 3 transfected O9-1 cells had a significantly reduced relative *Chd7* expression between 65–70%.

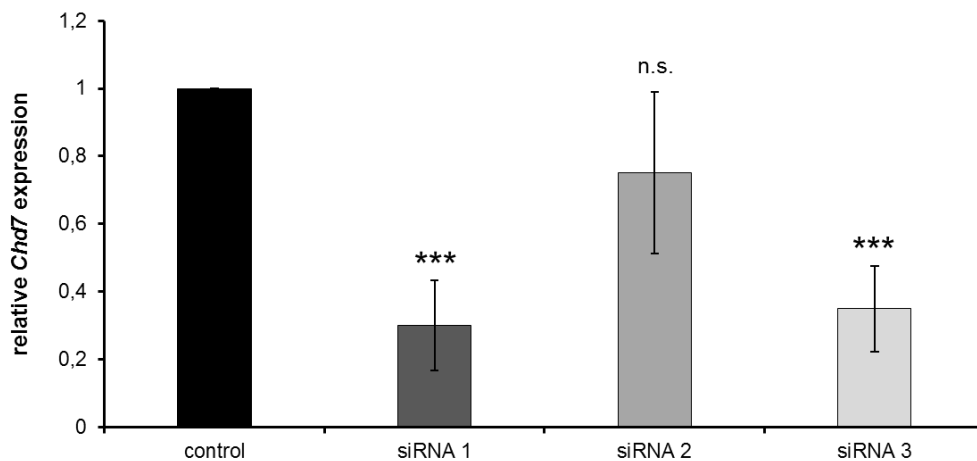


**Figure 15: Analysis of the *Chd7* expression in O9-1 cells after *Chd7* downregulation.**

O9-1 cells were transfected with one of three different *Chd7*-specific siRNAs (siRNA 1, 2, 3). Total RNA lysates of transfected cells were isolated 48 h after siRNA transfection and reverse transcribed into cDNA which was subjected to qRT-PCR analysis. The transfection of *Chd7*-specific siRNAs induced a reduction of the *Chd7* expression compared with control siRNA transfected cells, demonstrating the effectiveness of the siRNAs. With siRNA 1 or siRNA 3 transfected cells had a significantly decreased relative *Chd7* expression between 65–70%. Data are presented as mean  $\pm$  standard of qRT-PCR analysis performed in triplicate. \*\*\*  $p \leq 0.001$ , n.s.: not significant (student's *t* test).

After demonstrating the effectiveness especially of the *Chd7*-specific siRNA 1 and siRNA 3, the influence on the *Sema3a* expression was investigated. Therefore, total RNA lysates of O9-1 cells transfected with siRNA 1 or siRNA 3 were isolated 48 h after transfection. Isolated RNA was reverse transcribed into cDNA and used for qRT-PCR analysis. With *Chd7*-specific siRNA 1 or siRNA 3 transfected cells had a significantly decreased relative *Sema3a* expression of the approximately 30% in comparison with control siRNA transfected cells (Figure 16).

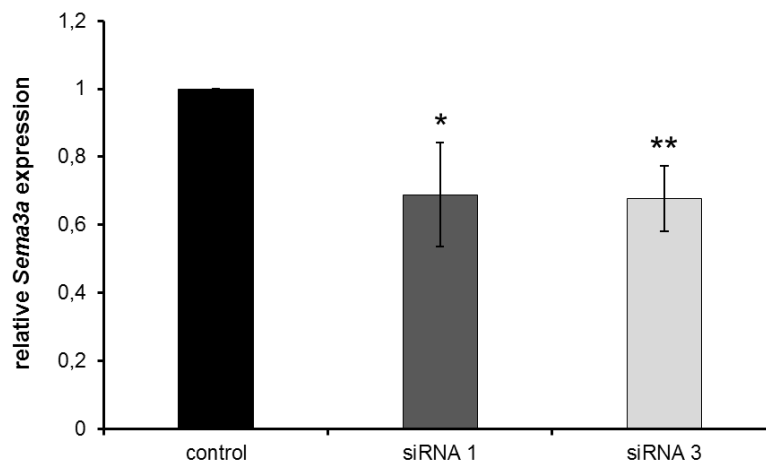


**Figure 16: Analysis of the *Sema3a* expression in O9-1 cells after *Chd7* downregulation.**

Total RNA lysates of O9-1 cells transfected with one of two different *Chd7*-specific siRNAs (siRNA 1, 3) were isolated 48 h after transfection. Into cDNA reverse transcribed RNA was subjected to qRT-PCR analysis to check the *Sema3a* expression after *Chd7* downregulation. Both single transfected *Chd7*-specific siRNAs induced a significant reduction of the relative *Sema3a* expression of approximately 30% compared with control siRNA transfected cells. Data are presented as mean  $\pm$  standard of qRT-PCR analysis performed in triplicate. \*  $p \leq 0.05$ , \*\*  $p \leq 0.01$  (student's *t* test).

### 3.5 Chd7 co-immunoprecipitates with Sema3a in O9-1 cells

In order to analyze the existence of Chd7 and Sema3a in the same nuclear protein complex in NCCs, co-immunoprecipitation (Co-IP) experiments using protein extract of O9-1 cells were performed. Nuclear extract was incubated with an anti-Chd7 antibody to precipitate Chd7. By western blot analysis using an anti-Sema3a antibody, a ~85 kDa protein band corresponding to the estimated size of the monomeric p85-Sema3a isoform was detected (Figure 17 A). This band is probable more intense than in the input control

due to the high amount of applied protein in immunoprecipitation and a strong binding of the anti-Chd7 antibody. To verify the results in a reciprocal experiment, nuclear extract was incubated with an anti-Sema3a antibody to precipitate Sema3a. A ~336 kDa protein band corresponding to the estimated size of Chd7 was detected by western blot analysis using an anti-Chd7 antibody (Figure 17 B). Nuclear extract without antibody incubation served as negative control to prove that Sema3a (Figure 17 A) and Chd7 (Figure 17 B) are not capable to bind unspecific to the magnetic beads used for the Co-IP experiments. 30 µg of nuclear protein per lane was used as input control to demonstrate that Sema3a (Figure 17 A) and Chd7 (Figure 17 B) are expressed in the nucleus of O9-1 cells. In conclusion, the data obtained by the Co-IP experiments demonstrate an interaction of Chd7 with Sema3a in O9-1 cells.

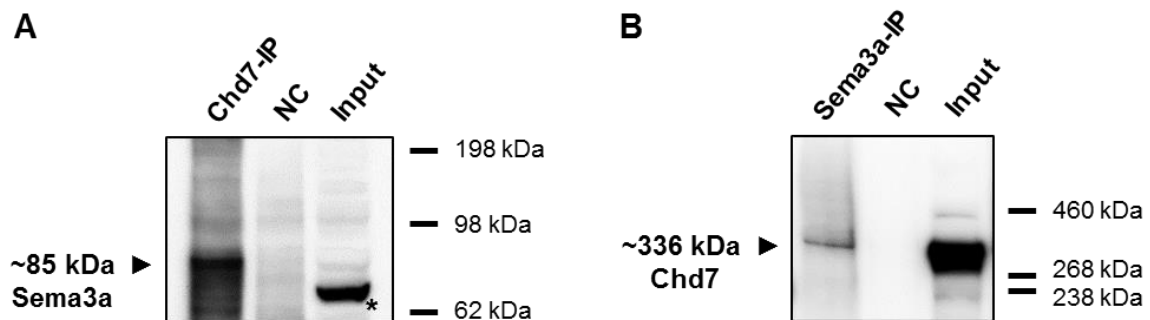


**Figure 17: Co-immunoprecipitation of Chd7 with Sema3a in O9-1 cells.** The Co-IP experiments were performed with nuclear protein extract of O9-1 cells. (A) Chd7 was precipitated with an anti-Chd7 antibody. A ~85 kDa protein band corresponding to the estimated size of the monomeric p85-Sema3a isoform was detected by western blot analysis using an anti-Sema3a antibody. This band is probable more intense than in the input control due to the high amount of applied protein in immunoprecipitation and a strong binding of the anti-Chd7 antibody. (B) The reciprocal experiment was performed to verify the results. Sema3a was precipitated with an anti-Sema3a antibody. By western blot analysis using an anti-Chd7 antibody, a ~336 kDa protein band corresponding to the estimated size of Chd7 was detected. Nuclear extract without antibody incubation was used as negative control (NC) to exclude unspecific binding of Sema3a (A) or Chd7 (B) to the magnetic beads used for the Co-IP experiments. 30 µg of nuclear protein per lane was used as input control to demonstrate the expression of Sema3a (A) and Chd7 (B) in the nucleus of O9-1 cells. Star (\*) illustrate potentially unspecific protein band due to unspecific binding of the used anti-Sema3a antibody. Molecular weights of proteins and marker bands are indicated in kilo Dalton (kDa).



### **3.6 Detection of the non-synonymous *SEMA3A* variant c.2002A>G (p.I668V) in a *CHD7*-positive CHARGE syndrome patient**

CHARGE syndrome is described as a phenotypically heterogeneous disorder. For this reason, it might be possible that there are other genes in addition to *CHD7* which might act as modifiers leading to a mild or a severe phenotype when these genes are mutated. One of these candidate genes could be *SEMA3A*, known to contribute to the phenotype of the CHARGE-related disorder Kallmann syndrome. Therefore, 5 CHARGE patients with a mild phenotype and 10 CHARGE patients with a severe phenotype, but all carrying pathogenic mutations in *CHD7*, were screened for additional mutations in *SEMA3A* (MIM 603961). All 17 coding exons and flanking intronic sequences of *SEMA3A* (NM\_006080.2) were analyzed by amplifying these regions by PCR using genomic DNA and screened for mutations by sequencing analysis. In one patient with a severe phenotype, the non-synonymous variant c.2002A>G (p.I668V) was found (Figure 18) which is located in the Ig-like domain of *SEMA3A* (Figure 19). While the *in silico* programs PolyPhen-2 and SIFT predicted that this new variant is tolerated, the program MutationTaster predicted it as disease causing. Moreover, the alteration is not listed in the database of the Exome Aggregation Consortium (ExAC). Hanchate *et al.* (2012) characterized two other *SEMA3A* mutations: the variant c.196C>T (p.R66W) should lead to an impaired *SEMA3A* secretion, whereas the variant c.2062A>G (p.T688A) should reduce the signal activity of *SEMA3A*. To clarify the new variant p.I668V, functional analysis on human embryonic kidney 293 cells (HEK293 cells) were performed. The wild type *SEMA3A* and the *SEMA3A* variant p.R66W were used as referees.

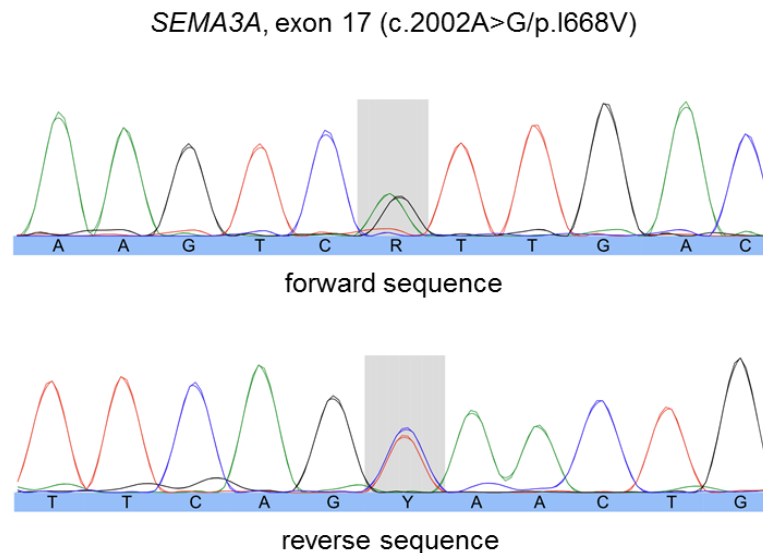


**Figure 18: *SEMA3A* mutation found in a *CHD7*-positive CHARGE syndrome patient.** All 17 coding exons and flanking intronic sequences of the *SEMA3A* gene were sequenced in 5 CHARGE patients with a mild phenotype and 10 CHARGE patients with a severe phenotype, but all carrying pathogenic mutations in the *CHD7* gene. One non-synonymous variant was identified in a patient with a severe phenotype: c.2002A>G (p.I668V). The mutation is indicated by gray background in the forward and the reverse sequence, respectively.



**Figure 19: Schematic representation of full length *SEMA3A* protein with identified mutation.** The non-synonymous variant c.2002A>G (p.I668V), which was identified in a *CHD7*-positive CHARGE syndrome patient, is located in the Ig-like domain (green) of *SEMA3A*.

### 3.7 Generation of *SEMA3A* plasmids

The plasmid *SEMA3A*-WT-pcDNA3.1/*myc*-His B (NP\_006071.1, kindly provided by my research group), which contains the human *SEMA3A* wild type (WT) sequence, was used to generate pcDNA3.1/*myc*-His B plasmids carrying the c.196C>T (p.R66W) and the c.2002A>G (p.I668V) mutation, respectively. The plasmid with the variant c.196C>T (p.R66W) was used as referee, because this mutation was characterized by Hanchate

*et al.* (2012) leading to an impaired SEMA3A secretion. The mutations were generated using the QuikChange II XL Site-Directed Mutagenesis Kit (Agilent Technologies) (chapter 2.2.1.4.4). The generated plasmids SEMA3A-R66W-pcDNA3.1/*myc*-His B and SEMA3A-I668V-pcDNA3.1/*myc*-His B were validated for the correct nucleotide sequence and reading frame by sequencing analysis.

Afterwards, the *SEMA3A* WT sequence and the two *SEMA3A* mutation sequences were separately cloned into the pCMV-HA vector (Invitrogen), containing a hemagglutinin (HA) epitope tag, as well as into the pGADT7 vector (Clontech) using the In-Fusion<sup>®</sup> HD Cloning Kit (Clontech) (chapter 2.2.1.4.2). Sequencing analysis was used to validate the correct nucleotide sequence and reading frame of the generated plasmids. The analysis revealed the existence of the HA-tag in front of the SEMA3A signal sequence in the generated plasmids.

### **3.8 SEMA3A variants have no effect on the expression, processing and secretion as well as dimerization of SEMA3A**

The effect of the SEMA3A variant p.I668V, which was detected in a *CHD7*-positive CHARGE syndrome patient (chapter 3.6), was analyzed concerning expression, processing and dimerization as well as secretion of SEMA3A. As referees, SEMA3A WT and the SEMA3A variant p.R66W were used.

Therefore, transient overexpression of SEMA3A WT and SEMA3A variants was performed with the generated SEMA3A-pCMV-HA plasmids (chapter 3.7) using HEK293 cells. This cell line was chosen to test the plasmids in a human cell system by western blot analysis.

HEK293 cells were single transfected with SEMA3A-pCMV-HA plasmids containing the human sequence of *SEMA3A* WT or of the *SEMA3A* variants c.196C>T (p.R66W) and c.2002A>G (p.I668V) to initially analyze the expression of the overexpressed plasmids and if the overexpressed SEMA3A undergoes proteolytic processing. HEK293 cells without plasmid treatment (untransfected) were used to investigate the SEMA3A expression level. Cytoplasmic and nuclear protein extracts were separately isolated 24 h after transfection. Western blot analysis was performed using 30 µg of protein per lane. Endogenous and overexpressed SEMA3A was detected with an anti-SEMA3A antibody

(Figure 20 A), while an anti-HA antibody was used for the detection of the plasmid containing HA-tag (Figure 20 B). In cytoplasmic and nuclear protein extracts of untransfected HEK293 cells only two potentially unspecific protein bands due to unspecific binding of the used anti-SEMA3A antibody were detected, demonstrating that HEK293 cells express almost undetectable levels of SEMA3A (Figure 20 A). In cytoplasmic and nuclear protein extracts of transfected HEK293 cells the monomeric SEMA3A isoforms of ~87 kDa (p87) and ~85 kDa (p85) were detected (Figure 20 A), suggesting proteolytic processing of the overexpressed SEMA3A. Moreover, the results demonstrate that the overexpressed SEMA3A WT plasmid in comparison with the overexpressed SEMA3A variant plasmids show the same expression pattern in the nucleus and cytoplasm of HEK293 cells.

Using an anti-HA antibody, no protein bands were detected neither in the cytoplasmic nor in the nuclear protein extracts except from the positive control, indicating the HA-tag gets lost in HEK293 cells after transfection of the SEMA3A plasmids due to proteolytic cleavage (Figure 20 B). For this reason the HA-tag could not be detected with the anti-HA antibody. Nevertheless, due to an almost undetectable SEMA3A expression level in HEK293 cells, the overexpressed SEMA3A was detected in further experiments using an anti-SEMA3A antibody. To proof the assumption concerning the unspecific protein bands, HEK293 cells should be transfected with SEMA3A WT and SEMA3A variant plasmids containing a HA-tag between the signal sequence and the semaphorin domain. Consequently, the potentially unspecific protein bands should not be detected using an anti-HA antibody.

Detection of  $\alpha$ -Tubulin (~50 kDa protein band) served as loading control (Figure 20 B). Although  $\alpha$ -Tubulin is expressed in the cytoplasm it was also detected in the nuclear protein extracts which can possibly be traced back on the used protein extraction method.

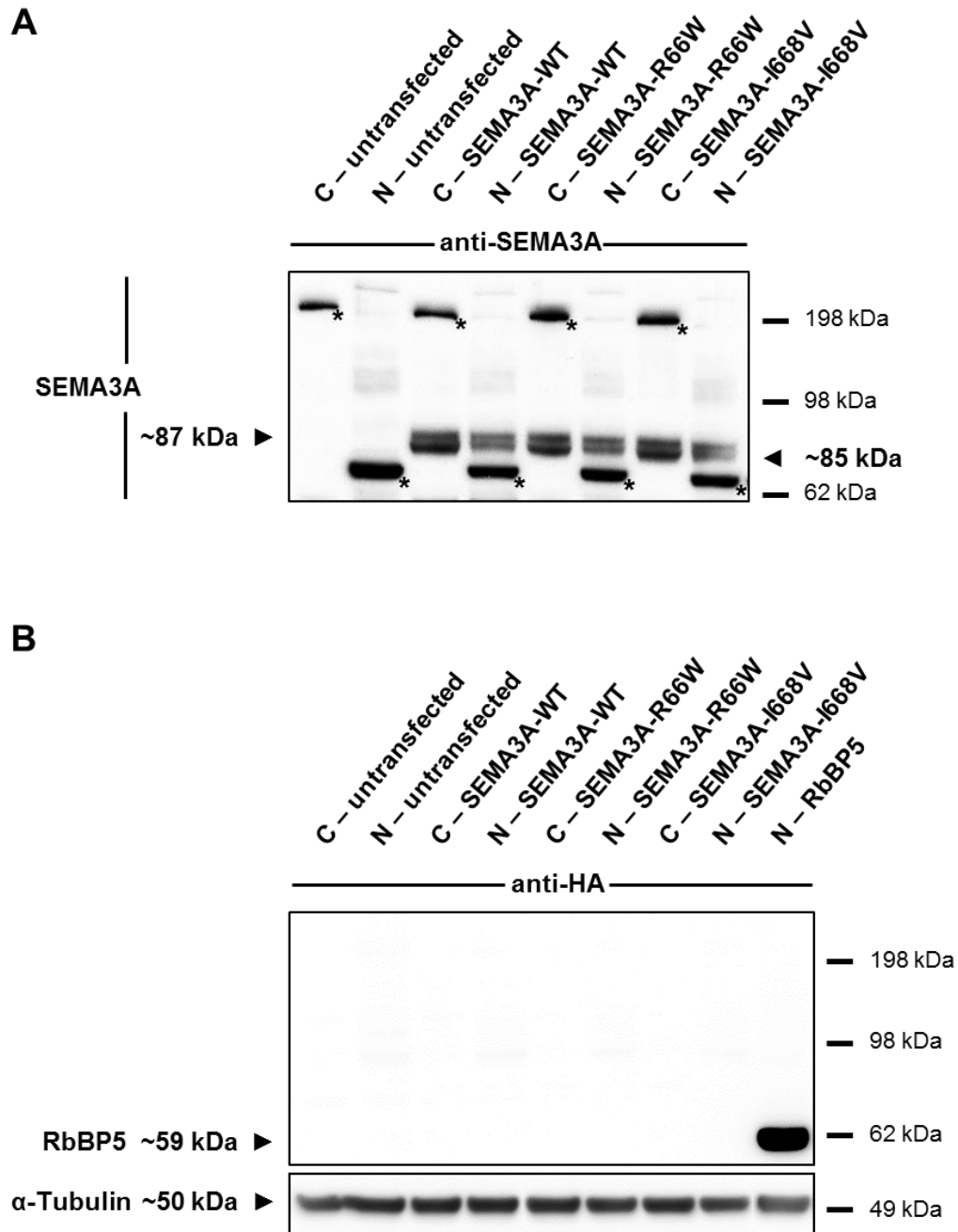


**Figure 20: Expression and proteolytic processing of transient overexpressed SEMA3A WT and SEMA3A variants in HEK293 cells.** HEK293 cells were single transfected with SEMA3A-pCMV-HA plasmids containing the human sequence of SEMA3A WT or of the SEMA3A variants c.196C>T (p.R66W) and c.2002A>G (p.I668V). Cytoplasmic (C) and nuclear (N) protein extracts were separately isolated 24 h after transfection. 30 µg of protein was used per lane. (A) Endogenous and overexpressed SEMA3A was detected by western blot analysis using an anti-SEMA3A antibody. In untransfected cytoplasmic and nuclear extracts no specific SEMA3A protein bands were detected, demonstrating that HEK293 cells express almost undetectable levels of SEMA3A. In transfected cytoplasmic and nuclear extracts the monomeric SEMA3A isoforms of ~87 kDa (p87) and ~85 kDa (p85) were observed, suggesting proteolytic processing of the

overexpressed SEMA3A. Nevertheless, no differences in the cytoplasmic and nuclear expression pattern of the overexpressed SEMA3A WT plasmid in comparison with the overexpressed SEMA3A variant plasmids were observed. Stars (\*) illustrate potentially unspecific protein bands due to unspecific binding of the used anti-SEMA3A antibody. **(B)** In the transfected cytoplasmic and nuclear extracts no SEMA3A protein bands were detected with an anti-HA antibody, suggesting the HA-tag loss of the generated SEMA3A plasmids due to proteolytic cleavage. Nuclear protein extract of HEK293 cells transfected with RbBP5-pCMV-HA plasmid (~59 kDa protein band) was used as positive control. The detection of  $\alpha$ -Tubulin (~50 kDa protein band) served as loading control. Due to the protein extraction method,  $\alpha$ -Tubulin was detected in the cytoplasmic and the nuclear protein extracts. Molecular weights of proteins and marker bands are indicated in kilo Dalton (kDa).

In addition, the dimerization and secretion of overexpressed SEMA3A were analyzed. Unspecific binding of the used anti-SEMA3A antibody in unused, concentrated cell culture medium and concentrated cell culture medium of untransfected HEK293 cells was excluded by western blot analysis (data not shown). Single transfections of HEK293 cells with SEMA3A-pCMV-HA plasmids containing the human sequence of SEMA3A WT or of the SEMA3A variants c.196C>T (p.R66W) and c.2002A>G (p.I668V) were performed. 24 h after transfection, the cell culture medium was concentrated and the cytoplasmic and nuclear protein extracts were separately isolated. Western blot analysis was performed using 30  $\mu$ g of protein per lane treated with the reducing agent DTT (+DTT) or without reducing agent (-DTT). The overexpressed SEMA3A was detected with an anti-SEMA3A antibody. The representative results are shown in Figure 21. In concentrated medium with reducing agent, the secreted monomeric isoforms of ~87 kDa (p87) and ~61 kDa (p61) were detected. In concentrated medium without reducing agent, the secreted dimeric isoforms of ~174 kDa (p87:p87) and ~112 kDa (p87:p25) as well as the secreted monomeric isoforms of ~87 kDa (p87) and ~61 kDa (p61) were received. The secreted monomeric p87-SEMA3A isoform without reducing agent is displayed by a lower protein band possibly due to the missing of DTT. In cytoplasmic and nuclear extracts with reduction, the monomeric isoforms of ~87 kDa (p87) and ~85 kDa (p85) were observed, whereas without reduction a ~170 kDa protein band was identified, potentially representing the dimeric p85:p85-SEMA3A isoform.

Based on these findings, no consequences on the secretion and dimerization of SEMA3A could be identified by comparing HEK293 cells transfected with the SEMA3A WT plasmid and HEK293 cells transfected with the two SEMA3A plasmids with mutation. Thus, the

impaired SEMA3A secretion due to the p.R66W mutation described by Hanchate *et al.* (2012) could not be validated.

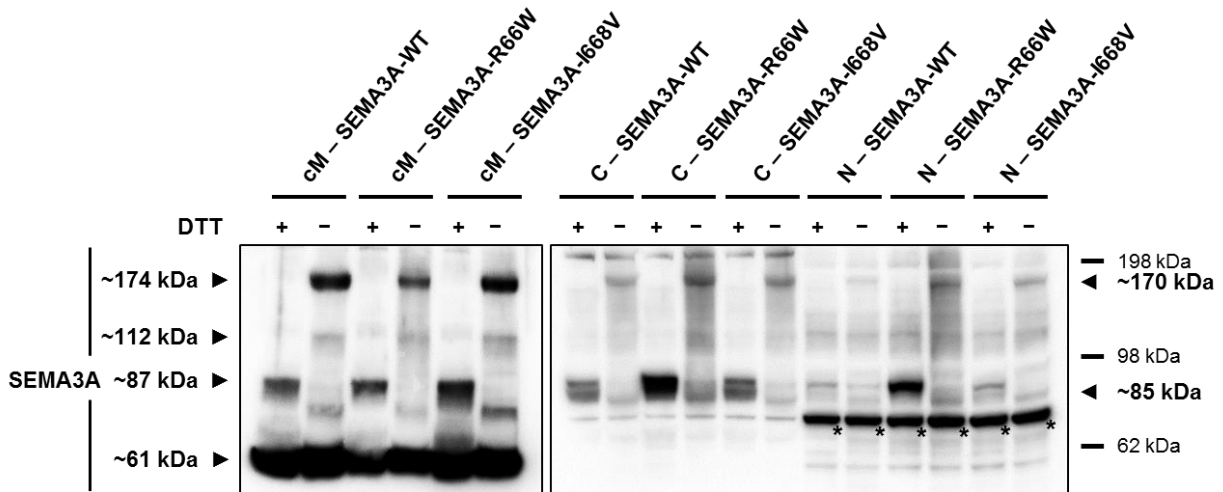


**Figure 21: Secretion and dimerization of transient overexpressed SEMA3A WT and SEMA3A variants in HEK293 cells.** HEK293 cells were single transfected with SEMA3A-pCMV-HA plasmids containing the human sequence of *SEMA3A* WT or of the *SEMA3A* variants c.196C>T (p.R66W) and c.2002A>G (p.I668V). 24 h after transfection, the cell culture medium was concentrated (cM) and the cytoplasmic (C) and nuclear (N) protein extracts were separately isolated. Western blot analysis was performed with an anti-SEMA3A antibody for the detection of overexpressed SEMA3A proteins. 30 µg of protein treated with the reducing agent DTT (+DTT) or without reducing agent (-DTT) was used per lane. In concentrated medium with reduction, the secreted monomeric isoforms of ~87 kDa (p87) and ~61 kDa (p61) were detected. In concentrated medium without reduction, the secreted dimeric isoforms of ~174 kDa (p87:p87) and ~112 kDa (p87:p25) as well as the secreted monomeric isoforms of ~87 kDa (p87) and ~61 kDa (p61) were received. The secreted monomeric p87-SEMA3A isoform without reducing agent is displayed by a lower protein band possibly due to the missing of DTT. In cytoplasmic and nuclear extracts with reducing agent, the monomeric isoforms of ~87 kDa (p87) and ~85 kDa (p85) were detected, whereas without reducing agent a ~170 kDa protein band was identified, potentially representing the dimeric p85:p85-SEMA3A isoform. Consequently, the SEMA3A variants had no effect on the secretion and dimerization of SEMA3A by comparing HEK293 cells transfected with the SEMA3A WT plasmid and HEK293 cells transfected with the two SEMA3A plasmids with mutation. Stars (\*) illustrate potentially unspecific protein bands due to unspecific binding of the used antibody. Molecular weights of proteins and marker bands are indicated in kilo Dalton (kDa).

### **3.9 CHD7 co-immunoprecipitates with SEMA3A WT and SEMA3A variants**

Chd7 and Sema3a interact in the nucleus of the murine NCC line O9-1 (chapter 3.5). To investigate this interaction in HEK293 cells and in order to check whether the interaction holds up in presence of SEMA3A mutations, Co-IP experiments were performed. Therefore, HEK293 cells were single transfected with SEMA3A-pCMV-HA plasmids containing the human sequence of SEMA3A WT or of the SEMA3A variants c.196C>T (p.R66W) and c.2002A>G (p.I668V). Nuclear extracts were isolated 24 h after transfection. The immunoprecipitation of endogenous CHD7 was performed using an anti-CHD7 antibody. Endogenous and overexpressed SEMA3A was detected by western blot analysis using an anti-SEMA3A antibody (Figure 22). A ~87 kDa protein band corresponding to the estimated size of the monomeric p87-SEMA3A isoform was detected. Because of the high amount of applied protein in the immunoprecipitation, an interaction of endogenous CHD7 and endogenous SEMA3A was also identified in untransfected HEK293 cells. Nuclear extract of HEK293 cells transfected with SEMA3A WT plasmid without incubation of an anti-CHD7 antibody served as negative control to prove that SEMA3A is not capable to bind unspecific to the magnetic beads used for the Co-IP experiments. 30 µg nuclear protein of untransfected and transfected HEK293 cells per lane was used as input and transfection control, validating the SEMA3A overexpression due to the detection of the monomeric isoforms of ~87 kDa (p87) and ~85 kDa (p85) in nuclear extracts of transfected HEK293 cells.

In summary, the data obtained by the Co-IP experiments reveal an interaction of CHD7 with the overexpressed SEMA3A WT and the overexpressed SEMA3A variants in HEK293 cells.



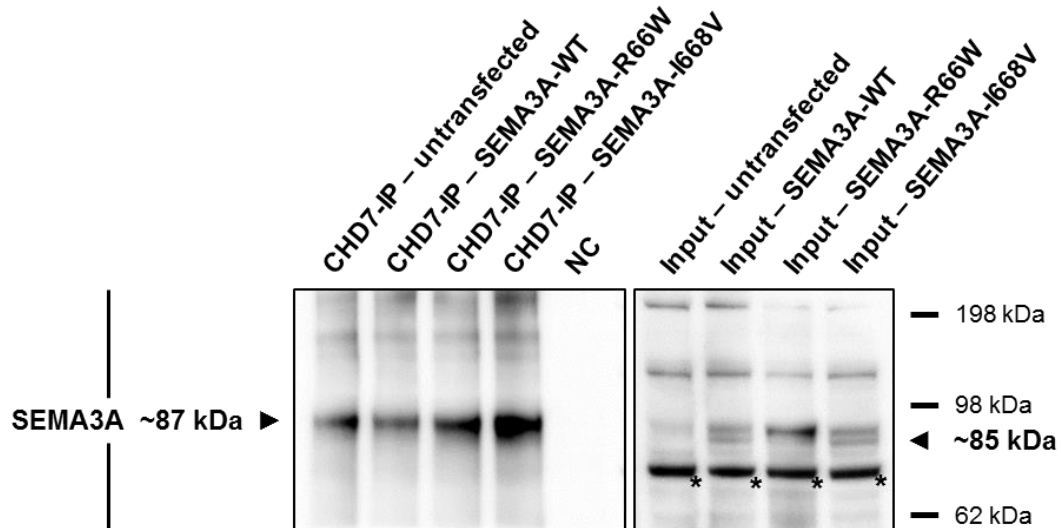


**Figure 22: Co-immunoprecipitation of CHD7 with SEMA3A WT and SEMA3A variants in HEK293 cells.** HEK 293 cells were single transfected with SEMA3A-pCMV-HA plasmids containing the human sequence of SEMA3A WT or of the SEMA3A variants c.196C>T (p.R66W) and c.2002A>G (p.I668V). 24 h after transfection, nuclear protein extracts were isolated. The immunoprecipitation of endogenous CHD7 was performed using an anti-CHD7 antibody. By western blot analysis using an anti-SEMA3A antibody, endogenous and overexpressed SEMA3A was detected. A ~87 kDa (p87) protein band corresponding to the estimated size of the monomeric p87-SEMA3A isoform was observed. An interaction of endogenous CHD7 and endogenous SEMA3A was also identified in untransfected HEK293 cells, because of the high amount of applied protein in the immunoprecipitation. To verify that SEMA3A does not bind unspecific to the magnetic beads used for the Co-IP experiments, nuclear extract of HEK293 cells transfected with SEMA3A WT plasmid without incubation of an anti-CHD7 antibody was used as negative control (NC). 30 µg nuclear protein of untransfected and transfected HEK293 cells per lane served as input and transfection control, validating the SEMA3A overexpression due to the detection of the monomeric isoforms of ~87 kDa (p87) and ~85 kDa (p85) in nuclear extracts of transfected HEK293 cells. The Co-IP experiments demonstrate an interaction of CHD7 with the overexpressed SEMA3A WT and the overexpressed SEMA3A variants in HEK293 cells. Stars (\*) illustrate potentially unspecific protein bands due to unspecific binding of the used anti-SEMA3A antibody. Molecular weights of proteins and marker bands are indicated in kilo Dalton (kDa).

### **3.10 CHD7 shows no direct interaction with SEMA3A WT or SEMA3A variants**

To demonstrate the correct expression of the generated full-length SEMA3A plasmids (chapter 3.7) for yeast two-hybrid assay, yeast cells were single transformed with the HA-tag containing plasmids SEMA3A-WT-pGADT7, SEMA3A-R66W-pGADT7 and SEMA3A-I668V-pGADT7. Whole yeast cell protein lysates were isolated and analyzed with antibodies against the HA-tag and SEMA3A by western blot analysis. The representative results are shown in Figure 23. The detection of a ~97 kDa protein band corresponding to the estimated size of the generated SEMA3A plasmids indicated no proteolytic cleavage and thus the usability of the plasmids for yeast two-hybrid assay. Whole protein lysate of yeast cells double transformed with CHD7-Cr1-3-pGBKT7 (NP\_060250.2) and CHD8-pGADT7-Rec (NP\_065971.2) were used as positive control for HA-tag expression (~70 kDa protein band) as well as negative control for SEMA3A expression (no detectable protein band). The detection of  $\alpha$ -Tubulin (~50 kDa protein band) ensured equal protein loading.

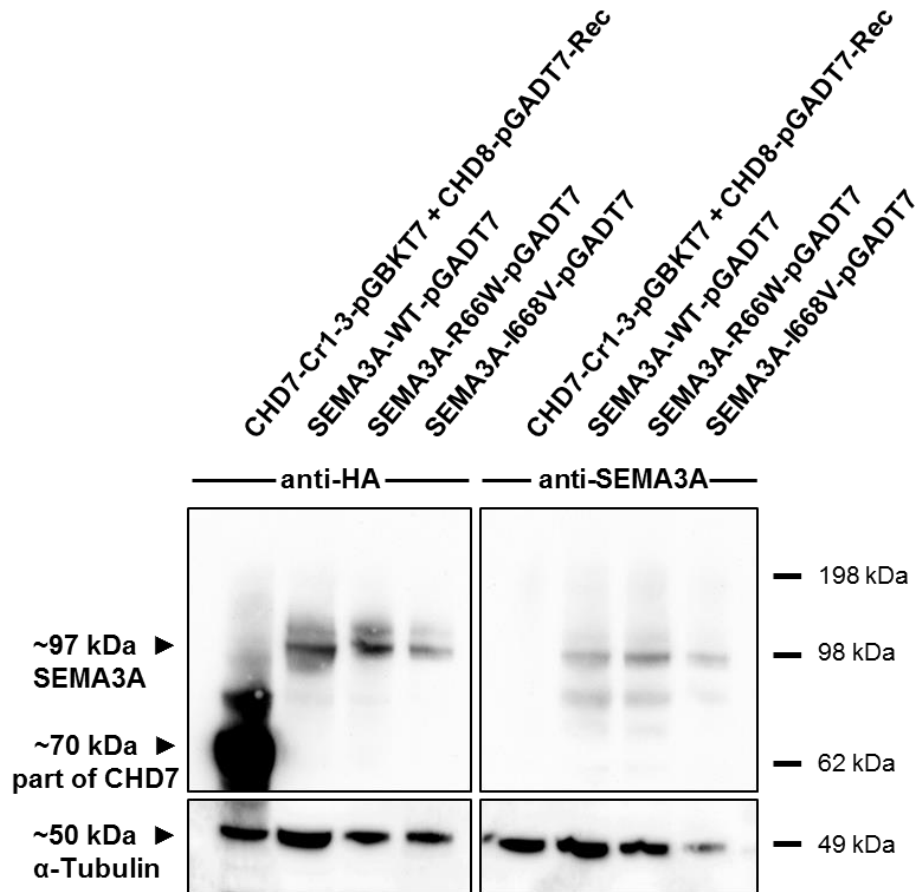


**Figure 23: Expression of the full-length SEMA3A isoform in yeast cells.** To validate that the SEMA3A yeast-two hybrid plasmids do not undergo proteolytic cleavage, yeast cells were single transformed with the HA-tag containing plasmids SEMA3A-WT-pGADT7, SEMA3A-R66W-pGADT7 and SEMA3A-I668V-pGADT7. Whole yeast cell protein lysates were incubated with an anti-HA antibody (upper, left panel) or an anti-SEMA3A antibody (upper, right panel). By western blot analysis, a ~97 kDa protein band corresponding to the estimated size of the generated SEMA3A plasmids was detected, indicating no proteolytic cleavage and thus the usability of the plasmids for yeast two-hybrid assay. Whole protein lysate of yeast cells double transformed with CHD7-Cr1-3-pGBKT7 (NP\_060250.2) and CHD8-pGADT7-Rec (NP\_065971.2) were used as positive control for HA-tag expression (~70 kDa protein band) as well as negative control for SEMA3A expression (no detectable protein band). Lower panel: Detection of α-Tubulin (~50 kDa protein band) ensured equal protein loading. Molecular weights of proteins and marker bands are indicated in kilo Dalton (kDa).

To determine a direct interaction of CHD7 with SEMA3A, yeast two-hybrid assay was performed. Four CHD7 plasmids were available as bait plasmids namely CHD7-1-pGBKT7 (amino acids 1–799), CHD7-2-pGBKT7 (amino acids 732–1567), CHD7-3-pGBKT7 (amino acids 1533–2380) and CHD7-4-pGBKT7 (amino acids

2325–2997) (Schulz *et al.*, 2014a). These plasmids divide the human full length CHD7 protein into four overlapping fragments without disruption of a known functional domain (Figure 24). Owing to autoactivation of the CHD7-1-pGBKT7 plasmid in the yeast system, no yeast two-hybrid assay could be performed with this plasmid (Schulz *et al.*, 2014a). In addition, the CHD7-Cr1-3-pGBKT7 plasmid was used as bait, spanning the amino acids 1591-2181 (Figure 24) (Batsukh *et al.*, 2010). All appropriate bait plasmids were used with the prey plasmids SEMA3A-WT-pGADT7, SEMA3A-R66W-pGADT7 and SEMA3A-I668V-pGADT7 for yeast two-hybrid assay, respectively. The plasmid SEMA3A-R66W-pGADT7 contain the already known SEMA3A missense mutation p.R66W (Hanchate *et al.*, 2012), whereas the plasmid SEMA3A-I668V-pGADT7 include the missense mutation identified in a CHD7-positive CHARGE syndrome patient (chapter 3.6). Yeast colonies on –LT agar plates indicated a successful transformation (Figure 25 A, C and E). No autoactivation of the yeast reporter gens could be observed on –LTHA agar plates using an empty pGBKT7 bait vector together with the prey plasmids in an autoactivation test, respectively (Figure 25 B, D and F). As positive control, the bait plasmid CHD7-Cr1-3-pGBKT7 and the prey plasmid CHD8-pGADT7-Rec (amino acids 1789–2091) were used (Batsukh *et al.*, 2010) (Figure 25 B, D and F). The yeast two-hybrid assay with the SEMA3A plasmids SEMA3A-WT-pGADT7, SEMA3A-R66W-pGADT7 and SEMA3A-I668V-pGADT7 revealed no direct interactions with the plasmids CHD7-2-pGBKT7, CHD7-3-pGBKT7, CHD7-4-pGBKT7 and CHD7-Cr1-3-pGBKT7 (Figure 25 B, D and F), demonstrating that these parts of CHD7 do not directly bind to SEMA3A WT or SEMA3A variants.

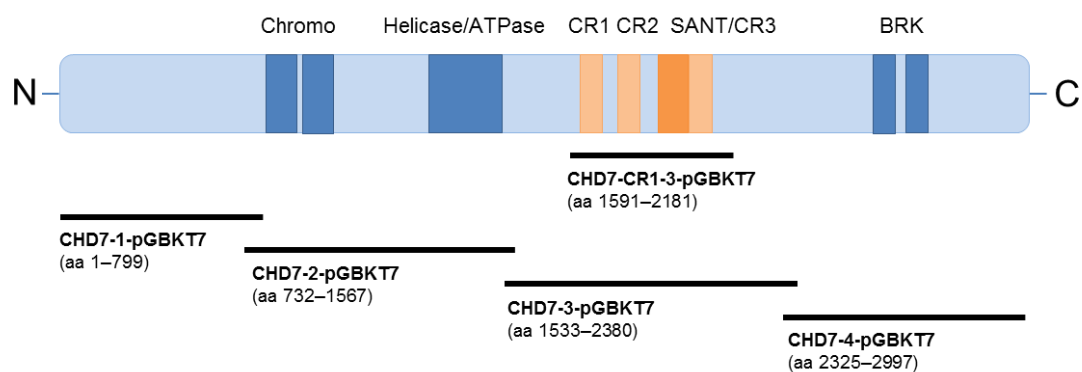


**Figure 24: Schematic overview of the used CHD7 yeast two-hybrid assay plasmids.** The plasmids CHD7-1-pGBKT7 to CHD7-4-pGBKT7 divide the full-length CHD7 protein into four overlapping parts. A known functional domain is thereby not disrupted. The plasmid CHD7-Cr1-3-pGBKT7 achieves this requirement as well. Schulz *et al.* (2014a).

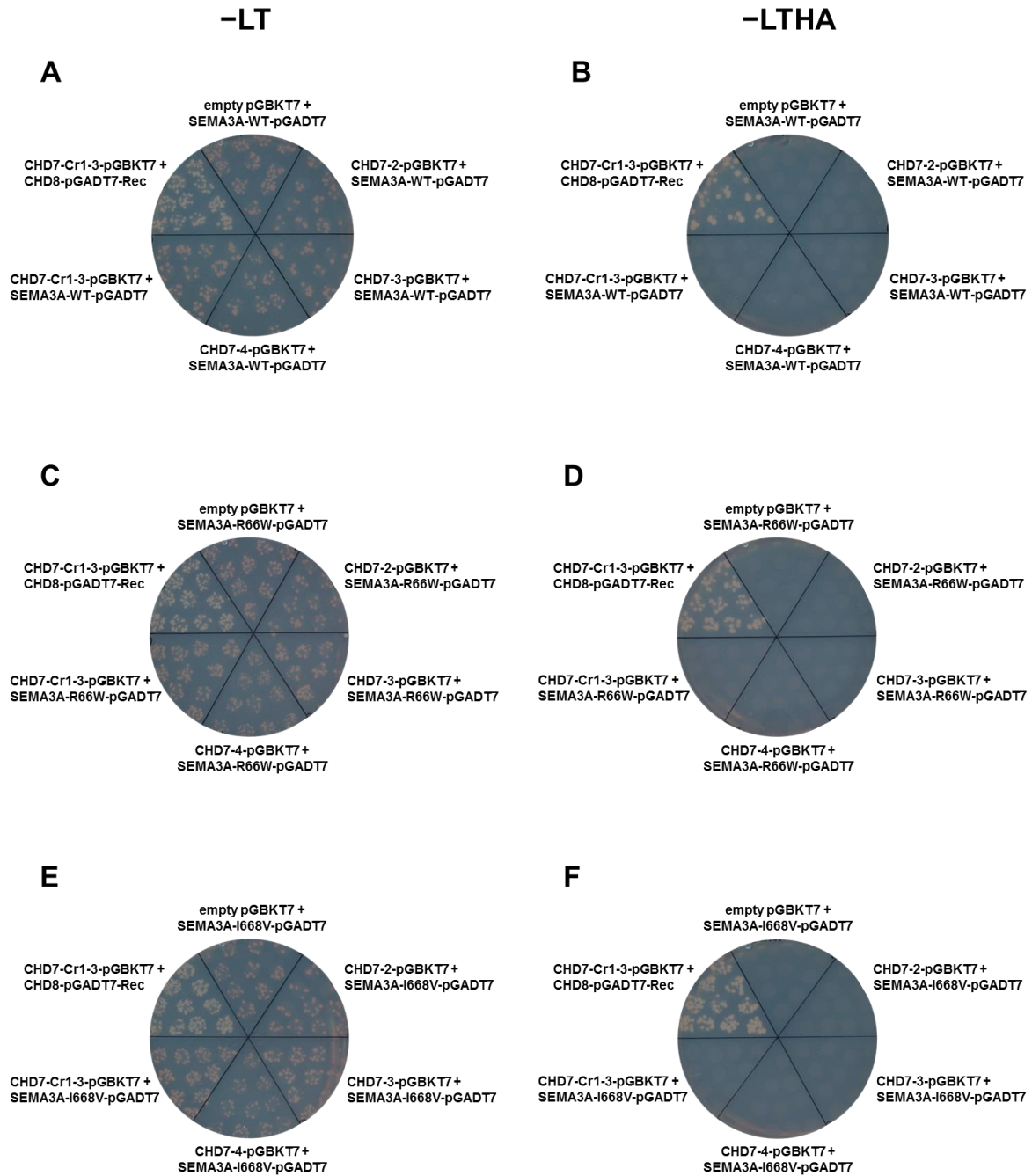


**Figure 25: Yeast two-hybrid assay.** Yeast two-hybrid assay was performed with the plasmids CHD7-2-pGBKT7, CHD7-3-pGBKT7, CHD7-4-pGBKT7 and CHD7-Cr 1-3-pGBKT7 as baits, which are parts of the human full-length CHD7 protein. The plasmids SEMA3A-WT-pGADT7, SEMA3A-R66W-pGADT7 and SEMA3A-I668V-pGADT7 were used as preys. Yeast colonies on -LT agar plates indicated a successful transformation (**A**, **C** and **E**). All prey plasmids were tested on -LTHA agar plates for autoactivation of the Y2HGold yeast strain reporter gens with the empty pGBKT7 bait vector (**B**, **D** and **F**). As positive control, the bait plasmid CHD7-Cr1-3-pGBKT7 and the prey plasmid CHD8-pGADT7-Rec were used (**B**, **D** and **F**). The yeast two-hybrid assay revealed no direct interaction of the CHD7 parts with the SEMA3A WT or the SEMA3A variants (**B**, **D** and **F**).

## 4 Discussion

### 4.1 Summary of the results

Using RT-PCR analysis, the two different murine NCC lines JoMa and O9-1 were characterized for the expression of different marker genes and *Chd7*. The nuclear expression of *Chd7* was validated in both NCC lines by western blot analysis and in the O9-1 cells also with immunocytochemical staining. The results of the western blot analysis revealed a strong *Chd7* expression in O9-1 cells in comparison with JoMa cells. Based on these findings, further experiments were performed with O9-1 cells. With RT-PCR analysis it was further shown that O9-1 cells express beside the receptors of class 3 semaphorins also class 3 semaphorins itself. The nuclear and cytoplasmic *Sema3a* expression was confirmed by immunocytochemical staining and western blot analysis. Moreover, proteolytic processing, dimerization and secretion of *Sema3a* were identified using western blot analysis. A downregulation of *Chd7* with specific siRNAs revealed a reduced *Sema3a* expression in O9-1 cells. Using Co-IP experiments, the nuclear interaction of *Chd7* with *Sema3a* was shown in two ways: by precipitation of *Chd7* and detection of *Sema3a* as well as by precipitation of *Sema3a* and detection of *Chd7*.

A mutational screen of the coding sequence of *SEMA3A* in 5 CHARGE patients with a mild phenotype and 10 CHARGE patients with a severe phenotype, but all carrying pathogenic mutations in the *CHD7* gene, was performed. In one patient, the non-synonymous variant c.2002A>G (p.I668V) was identified in a heterozygous state. This new identified variant, as well as the already published variant p.R66W, were characterized in the human HEK293 cell line using overexpressing *SEMA3A* plasmids containing one of the mutations, respectively. Western blot analyses demonstrated that expression, proteolytic processing and dimerization as well as secretion of *SEMA3A* were not affected by both mutations. The performed Co-IP experiments revealed that *CHD7* interacts with *SEMA3A* WT and the two *SEMA3A* variants, p.R66W and p.I668V. However, yeast two-hybrid assay identified no direct interaction of the used *CHD7* fragments with full-length constructs of wildtype or mutated *SEMA3A*.

## 4.2 NCCs – which *in vitro* model to choose?

The symptoms seen in CHARGE syndrome patients likely predominantly result from defects of the cranial NCCs and their subpopulation, the cardiac NCCs, cell populations largely responsible for forming the vertebrate head, heart and the peripheral nervous system (Kulesa *et al.*, 2010). The assumption that the malformations and defects seen in CHARGE syndrome patients result from abnormalities during NCC development were already published in 1985 (Siebert *et al.*, 1985). Furthermore, defects in the interaction between mesoderm and NCCs (Van Meter and Weaver, 1996) or disturbances in mesenchymal-epithelial interactions (Williams, 2005) were also supposed as pathogenic mechanisms causing CHARGE. In 2004, Vissers *et al.* identified mutations in the *CHD7* gene as the underlying cause leading to the complex developmental disorder CHARGE syndrome (Vissers *et al.*, 2004). In several other studies, further heterozygous mutations or deletions of *CHD7* were described in CHARGE syndrome patients (Aramaki *et al.*, 2006; Jongmans *et al.*, 2006; Lalani *et al.*, 2006; Sanlaville *et al.*, 2006; Wincent *et al.*, 2008). *CHD7* was also identified as a member of complexes which regulate time and tissue specific gene expression (Layman *et al.*, 2010). The initial presumption that CHARGE belongs to the neurocristopathies was confirmed by Bajpai *et al.* (2010) for the first time. Performing *Chd7* knockdown experiments in *Xenopus laevis* embryos, Bajpai *et al.* (2010) demonstrated that *Chd7* is essential for the formation of NCCs by activating transcriptions factors such as *Snai2* (previously named *Slug*), *Sox9* and *Twist* and observed abnormal NCC migration into the pharyngeal arches. Bajpai *et al.* (2010) also identified the association of *Chd7* with the PBAF complex and supposed that this cooperation regulates the gene expression during NCC formation in *Xenopus laevis*.

A suitable NCC model for *in vitro* studies was essential to investigate the functions of *Chd7* in NCC. To examine that these cell line truly represents NCC and express *Chd7*, the two murine NCC lines, the trunk JoMa cells and the cranial O9-1 cells, were characterized by RT-PCR and western blot analysis as well as immunocytochemical staining. Both cell lines grow as monolayers and display a stellate like morphology, typical for NCCs (Rao and Anderson, 1997). Furthermore, they can be cultured in a suitable culture medium without loss of their self-renewal capacity and multipotency. Maurer *et al.* (2007) generated the immortalized cell line JoMa1 and a clonally derived cell line termed JoMa1.3 using transgenic mice (Jager *et al.*, 2004) at E8.75, expressing a conditional 4-Hydroxytamoxifen (4-OHT) inducible allele of c-Myc (c-MycER<sup>T</sup>; Pelengaris *et al.*, 1999; Rudolph *et al.*, 2000). JoMa cells proliferate robustly as long as c-MycER<sup>T</sup> is active in a

4-OHT dependent manner (Maurer *et al.*, 2007). They were described to express amongst others the two NCC markers *Sox10* and *Ngfr* (previously named *P75*), indicating that these cells have the potential to differentiate into various cell types *in vivo* (Maurer *et al.*, 2007). A detailed look at the RT-PCR primers used by Maurer *et al.* (2007) for the expression analysis of marker genes in JoMa cells revealed that several primers were not useful for RT-PCR analysis due to recognition sites in intronic sequences. For this reason, the *Sox10* expression in JoMa cells described by Maurer *et al.* (2007) is questionable. Maurer *et al.* (2007) successfully differentiated both JoMa cell lines into neurons, glia, melanocytes, smooth muscle cells and chondrocytes *in vitro*. The second murine NCC line, the O9-1 cells, was generated by Ishii *et al.* (2012). This cell line was obtained from mass culture of *Wnt1-Cre;R26R-GFP* reporter-expressing NCCs from mouse embryos at E8.5 (Ishii *et al.*, 2012). Whole-genome expression profiling suggested that this cell line stably expresses both NCC and stem cell markers and was successfully differentiated into osteoblasts, chondrocytes, smooth muscle cells and glia (Ishii *et al.*, 2012).

By RT-PCR analysis on cDNA obtained from total RNA of JoMa and O9-1 cells the initial situation of both NCC lines was monitored concerning the expression of different marker genes and *Chd7*. In contrast to the tested NCC markers *Ngfr*, *Snai2*, *Pax3*, *Snai1* and *Twist1*, the NCC marker *Sox10* was not detected in both cell lines, indicating JoMa and O9-1 cells are no pre-migratory cell lines. The further tested marker genes for neurons, glial cells, smooth muscle cells, melanocytes and chondrocytes displayed in both NCC lines a similar expression pattern. The additionally analyzed *Chd7* gene was found to be expressed in both NCC lines. To verify the results of the *Chd7* expression on protein level, nuclear protein extracts of JoMa cells and O9-1 cells were tested by western blot analysis. The expression of *Chd7* could be confirmed in O9-1 cells, but not in JoMa cells because no clear protein band of *Chd7* was detected. By immunocytochemical staining it was shown that *Chd7* is specifically and intensely expressed in the nucleus of O9-1 cells. The strong *Chd7* expression strengthens the hypothesis that the symptoms seen in CHARGE syndrome can be explained by a dysfunction of the cranial NCCs and not of the trunk NCCs. For this reason, further experiments were performed with the cranial O9-1 cell line, representing multipotent mesenchymal cranial NCCs.



### 4.3 NCCs express class 3 semaphorins and secrete Sema3a

Randall *et al.* (2009) demonstrated that the phenotype of pharyngeal arch artery defects in *Chd7* heterozygous mice could not be rescued by expression of *Chd7* in the murine NCCs alone, whereas *Chd7* expression in both NCCs and the pharyngeal ectoderm led to a full rescue of the pharyngeal arch artery alterations. As candidate genes for the interaction between the ectoderm and the NCCs, semaphorins, ephrins, slits, Pdgfs and Vegfs were suggested (Randall *et al.*, 2009). To identify *Chd7* target genes in different tissues with functions in NCC development and possible other pathways which might also contribute to the phenotype of CHARGE syndrome, Schulz *et al.* (2014b) performed a genome-wide microarray expression analysis on whole wild type and *Chd7* deficient (*Chd7*<sup>Whi/+</sup> and *Chd7*<sup>Whi/Whi</sup>) embryos of the *Whirligig* mouse line at E9.5 and identified 98 differentially expressed genes. Many of the misregulated genes are known to play a role in NCC migration and axon guidance like class 3 semaphorins and ephrins as well as transcription factors, overall genes belonging to the candidate molecules for the interaction between the ectoderm and the NCCs assumed by Randall *et al.* (2009).

During development, NCCs are guided to their appropriate target regions through the embryo by many attractive and repulsive cues. A group of guidance cues that is well investigated are the semaphorins which exert their effects through the binding to multimeric receptor complexes at the cell membrane and initiating of unique intracellular signal transduction cascades (Jongbloets and Pasterkamp, 2014).

To test whether the NCC line O9-1 expresses semaphorin receptors, RT-PCR analysis on cDNA obtained from total RNA of O9-1 cells was performed, representing expression of neuropilin and plexin receptors. Plein *et al.* (2015) performed *Sema3c in situ* hybridization (ISH) on outflow tracts of mouse embryos and identified *Sema3c* expression in myocardial cuff cells and in the area where cardiac NCCs were located. In contrast to prior studies, who interpreted this result as an indication that *Sema3c* guide cardiac NCCs into this area, Plein *et al.* (2015) suggested that cardiac NCCs express *Sema3c* itself. By performing a *Sema3c* ISH on *Wnt1-Cre Rosa*<sup>Yfp</sup> outflow tracts, they found that *Sema3c* was expressed in a subpopulation of cardiac NCCs. Therefore, they supposed that semaphorins might act not only as guidance cues, but also have additional functions (Plein *et al.*, 2015). After the validation of the semaphorin receptor expression in O9-1 cells, which are essential for the guidance of the semaphorins, a possible semaphorin expression in NCC itself was investigated. RT-PCR analysis on cDNA of

O9-1 cells identified the expression of class 3 semaphorins, in particular *Sema3a*, *Sema3c*, *Sema3d* and *Sema3e*, in NCCs for the first time.

These results raised several questions:

1. In which cell compartments of NCCs are class 3 semaphorins localized?
2. Exist class 3 semaphorins as monomeric and dimeric isoforms in NCCs?
3. Undergo class 3 semaphorins proteolytic processing in NCCs?
4. Are class 3 semaphorins secreted by NCCs?

For SEMA3A, a secreted class 3 semaphorin with repulsive effects on primary olfactory axons, a contribution to the phenotype of Kallmann syndrome was demonstrated (Hanchate *et al.*, 2012; Young *et al.*, 2012). Phenotypic features of the heterogeneous congenital disorder Kallmann syndrome, like a hypogonadotropic hypogonadism and an absent or impaired sense of smell (anosmia) (Dodé and Hardelin, 2009), are also frequently observed in patients with CHARGE syndrome (Chalouhi *et al.*, 2005; Pinto *et al.*, 2005; Ogata *et al.*, 2006). In addition, mutations in the *CHD7* gene can be found in patients with CHARGE and in a minority of patients with Kallmann syndrome (Kim *et al.*, 2008; Bergman *et al.*, 2011). For this reason, the Kallmann syndrome was suggested to represent the mild end of the phenotypic spectrum of CHARGE syndrome (Jongmans *et al.*, 2009). Consequently, if *CHD7* and *SEMA3A* play a role in the pathogenesis of Kallmann syndrome, it might be possible that beside *CHD7* additional *SEMA3A* contributes to the pathogenesis of CHARGE syndrome. Therefore, Sema3a was further investigated in the NCC line O9-1 by immunocytochemical staining and western blot analysis. Sema3a localization was not only identified in concentrated culture medium, exposing secretion of Sema3a by O9-1 cells, but also in the cytoplasm and nucleus of O9-1 cells. The localization of Sema3a in the nucleus is not due to a nuclear localization signal which is not present in Sema3a. It could be explained by glycosylation of the Sema3a isoforms (Rondanino *et al.*, 2003). The isoforms detectable with the used anti-Sema3a antibody displayed full-size and partially processed monomers and dimers, indicating proteolytic cleavage of the full-length Sema3a by furin and furin-like endoproteases or matrix metalloproteases and dimerization as described for related class 3 semaphorins (Adams *et al.*, 1997; Klostermann *et al.*, 1998; Koppel and Raper, 1998; Christensen *et al.*, 2005; Esselens *et al.*, 2010). Processing of the inactive full-length Sema3a isoform is described to result in activation of its repulsive properties and

generation of functionally different isoforms (Adams *et al.*, 1997). Adams *et al.* (1997) further assumed that specific proteases and protease inhibitors might locally activate or modulate repulsive signals and consequently contribute to class 3 semaphorin specificity. Nevertheless, further experiments are needed to clarify these aspects.

In conclusion, the experiments demonstrate that NCCs express, process and secrete *Sema3a*, providing *Sema3a* itself. These results lead to the suggestion that *Sema3a* has in addition to its NCC guidance aspect other diverse functions.

#### **4.4 *Chd7* regulates *Sema3a* expression and is associated with *Sema3a* in NCCs**

*Chd7* is highly conserved across species and orthologs have been identified in mouse, chicken, zebrafish, *Xenopus laevis* and others (Bosman *et al.*, 2005; Aramaki *et al.*, 2007; Bajpai *et al.*, 2010). A downregulation of *Chd7* in *Xenopus laevis* embryos displayed major features seen in CHARGE syndrome patients (Bajpai *et al.*, 2010) and led to induction and migration defects of NCCs (Bajpai *et al.*, 2010; Schulz *et al.*, 2014b), while downregulation of *Sema3a* in *Xenopus laevis* embryos only affected NCC migration (Schulz *et al.*, 2014b). *Sema3a* expression analysis in heterozygous (*Chd7*<sup>Whi/+</sup>) as well as homozygous (*Chd7*<sup>Whi/Whi</sup>) *Whirligig* mice and after downregulation of *Chd7* in *Xenopus laevis* embryos revealed a decreased or complete depletion of *Sema3a* expression exposing the evolutionary conservation of the *Chd7*-*Sema3a* regulatory loop (Schulz *et al.*, 2014b).

To analyze whether this regulatory mechanism is also found in NCCs, knockdown experiments were performed by transfecting O9-1 cells with *Chd7*-specific siRNAs. Analysis of *Sema3a* expression after downregulation of *Chd7* revealed a decreased expression of *Sema3a*, demonstrating that the regulatory loop is also present in NCCs.

Co-IP experiments performed with O9-1 cells further demonstrated an interaction of *Chd7* with *Sema3a* in nuclear extract of NCCs suggesting an association of *Chd7* and *Sema3a* in the same protein complex. *Chd7* rescue experiment performed by co-injection of a *Chd7* morpholino and *Sema3a* RNA demonstrated a partially rescue of the *Chd7* knockdown phenotype seen in *Xenopus laevis* embryos (Borchers, unpublished data), indicating a possible role of *Sema3a* in the pathogenesis of CHARGE syndrome.

## 4.5 **SEMA3A might act as modifier in CHARGE syndrome**

High clinical inter- and intra-familial variability is observed in the malformation disorder CHARGE syndrome (Aramaki *et al.*, 2006; Jongmans *et al.*, 2006; Lalani *et al.*, 2006). Genetic modifiers make an important contribution to different kinds of disease like neurological (Kearney, 2011) or arrhythmogenic disorders (Crotti *et al.*, 2005). Modifier can enhance or suppress the phenotype of a disorder. To analyze whether *SEMA3A* mutations contribute to the pathogenesis of CHARGE syndrome and maybe negatively modulate the phenotypic outcome of the affected patients, 5 patients with a mild and 10 patients with a severe phenotype, but all carrying a pathogenic mutation in the *CHD7* gene, were sequenced for the presence of additional mutations in the coding sequence of the *SEMA3A* gene.

One non-synonymous mutation in a heterozygous state, namely c.2002A>G (p.I668V) was identified in a patient with a severe phenotype. This variant is not listed in the database of the Exome Aggregation Consortium (ExAC). While two *in silico* programs predicted this variant to be tolerated (PolyPhen-2 and SIFT), the *in silico* program MutationTaster predicted the variant as disease causing. Interestingly, Schulz *et al.* (2014b) screened 45 patients diagnosed with CHARGE, but lacking a mutation in the *CHD7* gene for mutations in *SEMA3A* and identified also the non-synonymous variant c.2002A>G (p.I668V) in one patient and two other non-synonymous variations namely c.196C>T (p.R66W) and c.2062A>G (p.T688A) in a heterozygous state in two other patients. Two of the later found mutations were already described in patients with Kallmann syndrome leading to an impaired *SEMA3A* secretion (p.R66W) or a reduced signal activity of *SEMA3A* (p.T688A) (Hanchate *et al.*, 2012). Based on these findings, a pathogenic effect of *SEMA3A* in Kallmann syndrome was assumed (Hanchate *et al.*, 2012). Nevertheless, Hanchate *et al.* (2012) supposed that heterozygous *SEMA3A* mutations are not sufficient to induce the phenotype of Kallmann syndrome alone, but might contribute to it by a combination with other mutated Kallmann syndrome causing gene mutations due to digenic inheritance. This hypothesis was fleshed out by identification that the non-synonymous mutation p.R66W was inherited from the healthy father of a CHARGE syndrome patient (Schulz *et al.*, 2014b) and can be further strengthen because of two independently described patients with bi-allelic mutations in *SEMA3A* causing an autosomal recessive type of syndromic short stature (Hofmann *et al.*, 2013; Baumann *et al.*, 2017).

Functional analyses on transfected HEK293 cells were performed to analyze the effect of the new identified *SEMA3A* mutation p.I668V in a *CHD7*-positive CHARGE syndrome patient. Therefore, the mutation was induced by site-directed mutagenesis into a plasmid containing the human *SEMA3A* WT sequence to generate an overexpression plasmid with the defect and to study the effect of the new *SEMA3A* mutation. As referees, overexpression plasmids containing either the already described *SEMA3A* mutation p.R66W or the *SEMA3A* WT sequence were used. With the performed western blot analyses, no alterations concerning the expression, processing or dimerization as well as secretion of *SEMA3A* were detected by the mutations p.R66W and p.I668V. These results indicate that the p.R66W mutation might have no effect on the secretion of *SEMA3A* as assumed by Hanchate *et al.* (2012). However, the results obtained by Hanchate *et al.* (2012) were limited by the analysis of only conditioned medium without transfection control. During writing this thesis, my research group studied the effect of tunicamycin, a glycosylation inhibitor, on the glycosylation of overexpressed *SEMA3A* in HEK293 cells using overexpressing plasmids containing either the *SEMA3A* WT or the *SEMA3A* mutations p.R66W and p.I668V. The results of the western blot analysis revealed that after tunicamycin treatment of transfected HEK293 cells, in nuclear and cytoplasmic extracts, which contained the overexpressed *SEMA3A* WT and the overexpressed *SEMA3A* with the mutation p.I668V, only unglycosylated *SEMA3A* was detected. Indeed, in nuclear and cytoplasmic extracts containing the overexpressed *SEMA3A* with the mutation p.R66W, unglycosylated as well as glycosylated *SEMA3A* was received. These results might be explained due to structural modifications of *SEMA3A* caused by the p.R66W mutation. *Sema3a* rescue experiments in *Xenopus laevis* embryos performed by co-injection of a *Chd7* morpholino with *Sema3a-WT*, *Sema3a-p.R66W* or *Sema3a-p.I668V* RNA supposed that only the *Sema3a-p.R66W* RNA cannot compensate the defects produced by the *Chd7* morpholino (Borchers, unpublished data). These data strengthen the hypothesis that the p.R66W mutation is pathogenic, whereas the pathogenicity of the p.I668V mutation could not be clarified. Nevertheless, as presumed in previous studies, heterozygous *SEMA3A* mutations alone are not sufficient to cause a pathogenic phenotype, but might act as modifier or contribute to it through their interactions with other mutated genes due to digenic inheritance. In addition, *Sema3a* was identified in this thesis to be expressed and secreted by the NCC line O9-1 suggesting a new function of *SEMA3A*. Although Co-IP experiments on transfected HEK293 cells indicated a co-existence of *CHD7* and *SEMA3A* in the same protein

complex, yeast two-hybrid assay revealed no direct interaction for CHD7 and SEMA3A. The association of CHD7 and SEMA3A in a nuclear protein complex might indicate a function for SEMA3A as transcription factor beside the guidance function as described by Kuriyama and Mayor (2008). Moreover, another effectiveness of Sema3a might be possible, because it is secreted by NCCs itself and not only by the surrounding tissue.

## 4.6 Future perspectives

The Sema3a expression analysis in the NCC line O9-1 revealed the existence of Sema3a not only in the secreted medium, but also in the cytoplasm and in the nucleus of the cells although Sema3a is predicted not to have a nuclear localization signal. To test the accuracy of the detected endogenous Sema3a in O9-1 cells and furthermore of the overexpressed SEMA3A in HEK293 cells, plasmids containing a detectable HA-tag with and without mutation should be used for transfection and western blot analysis. My research group already started with these experiments during writing my thesis.

In order to identify the precise localization of Sema3a in the cytoplasm as well as in the nucleus, a co-immunostaining using different cell organelle markers could be performed.

To elucidate Sema3a target genes in NCCs, the expression profiles of O9-1 cells treated with and without siRNA against *Sema3a* should be compared by whole-genome microarray analysis. The identified genes could be validated by qRT-PCR analysis and chromatin immunoprecipitation (ChIP) assay.

To confirm the identified association of Chd7 and Sema3a in the same nuclear protein complex in O9-1 cells, Duolink proximity ligation assay (PLA) should be performed. Further, the composition of the whole protein complex should be analyzed. Therefore, a chemical crosslinking in combination with mass spectrometry could be used to examine the structure and composition of the likely heterogenic complex.

To identify *Sema3a* target genes in NCCs, the expression profiles of O9-1 cells treated with and without siRNA against *Sema3a* should be compared by whole-genome microarray analysis.

NCCs are guided by semaphorins, but also express semaphorins themselves as demonstrated in the present thesis. Using a migration assay, the influence of downregulated or mutated *Sema3a* as well as *Chd7* on the migration of NCCs could be examined.

In this thesis it is supposed that mutated *SEMA3A* might act as modifier in the phenotypic variable malformation syndrome CHARGE contributing to a more severe phenotype of the affected patients. To strengthen this hypothesis further mild and severe affected CHARGE syndrome patients carrying a pathogenic *CHD7* mutation should be screened for additional mutations in the *SEMA3A* gene. Possible identified new *SEMA3A* mutations as well as already known *SEMA3A* mutations either assumed to contribute to the phenotype of Kallmann syndrome (Hanchate *et al.*, 2012; Young *et al.*, 2012) or causing an autosomal recessive type of syndromic short stature (Hofmann *et al.*, 2013; Baumann *et al.*, 2017) should be investigated by functional analysis as performed in this thesis. Moreover, the *Xenopus laevis* model could be used for further functional analyses regarding selected mutations. After a *Sema3a* knockdown using *Sema3a* morpholinos, other selected mutations could be used for rescue experiments to analyze the effect of the mutations.

## 5 Summary

CHARGE syndrome is a complex congenital malformation disorder, caused in more about two-thirds of the cases by heterozygous loss of function mutations in the chromodomain helicase DNA-binding protein 7 (*CHD7*). The acronym CHARGE reflects the main clinical features seen in the most CHARGE syndrome patients namely coloboma, heart defects, atresia of the choanae, retarded growth and development, genital hypoplasia and ear anomalies/deafness. Because of the phenotypic spectrum, it was supposed that the CHARGE syndrome belongs to the neurocristopathies. In addition, the essential role of *CHD7* for the formation and migration of neural crest cells (NCCs), which give rise to many tissues of the embryo including craniofacial and heart structures, was recently demonstrated.

Two murine NCC lines, the trunk JoMa cells and the cranial O9-1 cells, were characterized for the expression of NCC and other molecular marker genes as well as *Chd7* by RT-PCR analysis. The results revealed that the two cell lines do not differ much in the expression of the tested marker genes for NCCs, neurons, glial cells, smooth muscle cells, melanocytes and chondrocytes as well as *Chd7*. The nuclear expression of *Chd7* was validated by western blot analysis and for O9-1 cells also by immunocytochemical staining. The results of the western blot analysis demonstrated a strong *Chd7* expression in O9-1 cells in comparison with JoMa cells. This strengthens the assumption that the symptoms seen in CHARGE syndrome are caused by a dysfunction of the cranial NCCs and not of the trunk NCCs.

Proper NCC guidance through the embryo depends on guidance cues and the large family of the semaphorins thereby plays an important role. Subsequent experiments were performed with the NCC line O9-1. Using RT-PCR analysis, the expression of semaphorin receptors and for the first time of class 3 semaphorins was identified in NCCs. *Sema3a* expression was proven by immunocytochemical staining and western blot analysis. Further experiments were carried out to check the localization of *Sema3a* in the different cell compartments and a possible *Sema3a* secretion into the cell culture medium. Western blot analysis revealed both the expression in the nucleus and the cytoplasm and the secretion into the medium. Moreover, the proteolytic cleavage and dimerization of *Sema3a* could be identified as described for class 3 semaphorins. Recently, the described regulatory effect of *Chd7* on *Sema3a* in *Xenopus laevis* embryos and mouse embryos could be confirmed in O9-1 cells through the *Sema3a* downregulation by siRNA-mediated



depletion of *Chd7*. Further experiments revealed a co-immunoprecipitation of Chd7 with Sema3a, indicating the association of these two proteins in the same protein complex.

A further part of the present thesis focused on the identification of possible mutations in the *SEMA3A* gene of *CHD7*-positive CHARGE syndrome patients. *SEMA3A* mutations are hypothesized to negatively modulate the phenotype of CHARGE patients and are known to be involved in the pathogenesis of the allelic disorder Kallmann syndrome, which is suggested to represent the mild end of the phenotypic abnormalities seen in CHARGE syndrome. The non-synonymous *SEMA3A* mutation c.2002A>G (p.I668V) was identified in a severe affected CHARGE syndrome patient. This finding might strengthen the hypothesis that *SEMA3A* act as modifier in CHARGE patients with a pathogenic mutation in the *CHD7* gene contributing to a more severe phenotype in these patients due to digenic inheritance. It would also explain the high clinical inter- and intra-familial variability of CHARGE syndrome. The new identified mutation and the already published variant p.R66W were characterized with overexpressing plasmids in the human HEK293 cell line on protein level. The obtained results showed no effect of the mutations on expression, proteolytic processing, dimerization or secretion of SEMA3A. By co-immunoprecipitation experiments it was demonstrated that CHD7 interacts with SEMA3A WT and the two SEMA3A variants, p.R66W and p.I668V. Yeast-two hybrid assay indeed revealed no direct interaction between CHD7 and SEMA3A with or without mutation.

In summary, the results of the present thesis are another step towards understanding the pathomechanism behind the neurocristopathy CHARGE syndrome.

## 6 References

- Acloque** H, Adams MS, Fishwick K, Bronner-Fraser M, Nieto MA (2009). Epithelial-mesenchymal transitions: the importance of changing cell state in development and disease. *The Journal of clinical investigation* 119(6): 1438–1449.
- Adams** RH, Lohrum M, Klostermann A, Betz H, Puschel AW (1997). The chemorepulsive activity of secreted semaphorins is regulated by furin-dependent proteolytic processing. *The EMBO journal* 16(20): 6077–6086.
- Aramaki** M, Kimura T, Udaka T, Kosaki R, Mitsunashi T, Okada Y, Takahashi T, Kosaki K (2007). Embryonic expression profile of chicken CHD7, the ortholog of the causative gene for CHARGE syndrome. *Birth defects research. Part A, Clinical and molecular teratology* 79(1): 50–57.
- Aramaki** M, Udaka T, Kosaki R, Makita Y, Okamoto N, Yoshihashi H, Oki H, Nanao K, Moriyama N, Oku S, Hasegawa T, Takahashi T, Fukushima Y, Kawame H, Kosaki K (2006). Phenotypic spectrum of CHARGE syndrome with CHD7 mutations. *The Journal of pediatrics* 148(3): 410–414.
- Bajpai** R, Chen DA, Rada-Iglesias A, Zhang J, Xiong Y, Helms J, Chang C-P, Zhao Y, Swigut T, Wysocka J (2010). CHD7 cooperates with PBAF to control multipotent neural crest formation. *Nature* 463(7283): 958–962.
- Batsukh** T, Pieper L, Koszucka AM, Velsen N von, Hoyer-Fender S, Elbracht M, Bergman JEH, Hoefsloot LH, Pauli S (2010). CHD8 interacts with CHD7, a protein which is mutated in CHARGE syndrome. *Human molecular genetics* 19(14): 2858–2866.
- Baumann** M, Steichen-Gersdorf E, Krabichler B, Muller T, Janecke AR (2017). A recognizable type of syndromic short stature with arthrogryposis caused by bi-allelic SEMA3A loss-of-function variants. *Clinical Genetics*.
- Bergman** JE, Janssen N, Hoefsloot LH, Jongmans MC, Hofstra RM, van Ravenswaaij-Arts CM (2011). CHD7 mutations and CHARGE syndrome: the clinical implications of an expanding phenotype. *Journal of Medical Genetics* 48(5): 334–342.

- Blake** KD, Davenport SL, Hall BD, Hefner MA, Pagon RA, Williams MS, Lin AE, Graham JM JR (1998). CHARGE association: an update and review for the primary pediatrician. *Clinical pediatrics* 37(3): 159–173.
- Bosman** EA, Penn AC, Ambrose JC, Kettleborough R, Stemple DL, Steel KP (2005). Multiple mutations in mouse Chd7 provide models for CHARGE syndrome. *Human molecular genetics* 14(22): 3463–3476.
- Bradford** MM (1976). A rapid and sensitive method for the quantitation of microgram quantities of protein utilizing the principle of protein-dye binding. *Analytical biochemistry* 72: 248–254.
- Bronner** ME and LeDouarin NM (2012). Development and evolution of the neural crest: an overview. *Developmental biology* 366(1): 2–9.
- Carmona-Fontaine** C, Thevenneau E, Tzekou A, Tada M, Woods M, Page KM, Parsons M, Lambris JD, Mayor R (2011). Complement fragment C3a controls mutual cell attraction during collective cell migration. *Developmental cell* 21(6): 1026–1037.
- Chalouhi** C, Faulcon P, Le Bihan C, Hertz-Pannier L, Bonfils P, Abadie V (2005). Olfactory Evaluation in Children: Application to the CHARGE Syndrome. *Pediatrics* 116(1): e81-e88.
- Christensen** C, Ambartsumian N, Gilestro G, Thomsen B, Comoglio P, Tamagnone L, Guldberg P, Lukanidin E (2005). Proteolytic processing converts the repelling signal Sema3E into an inducer of invasive growth and lung metastasis. *Cancer research* 65(14): 6167–6177.
- Crotti** L, Lundquist AL, Insolia R, Pedrazzini M, Ferrandi C, Ferrari GM de, Vicentini A, Yang P, Roden DM, George AL JR, Schwartz PJ (2005). KCNH2-K897T is a genetic modifier of latent congenital long-QT syndrome. *Circulation* 112(9): 1251–1258.
- Delahaye** A, Sznajer Y, Lyonnet S, Elmaleh-Berges M, Delpierre I, Audollent S, Wiener-Vacher S, Mansbach AL, Amiel J, Baumann C, Bremond-Gignac D, Attie-Bitach T, Verloes A, Sanlaville D (2007). Familial CHARGE syndrome because of CHD7 mutation: clinical intra- and interfamilial variability. *Clinical Genetics* 72(2): 112–121.

- Dodé C** and Hardelin J-P (2009). Kallmann syndrome. *European Journal of Human Genetics* 17(2): 139–146.
- Dupin E** and Sommer L (2012). Neural crest progenitors and stem cells: from early development to adulthood. *Developmental biology* 366(1): 83–95.
- Eickholt BJ**, Mackenzie SL, Graham A, Walsh FS, Doherty P (1999). Evidence for collapsin-1 functioning in the control of neural crest migration in both trunk and hindbrain regions. *Development (Cambridge, England)* 126(10): 2181–2189.
- Esselens C**, Malapeira J, Colome N, Casal C, Rodriguez-Manzaneque JC, Canals F, Arribas J (2010). The cleavage of semaphorin 3C induced by ADAMTS1 promotes cell migration. *The Journal of biological chemistry* 285(4): 2463–2473.
- Etchevers HC**, Amiel J, Lyonnet S (2006). Molecular bases of human neurocristopathies. *Advances in experimental medicine and biology* 589: 213–234.
- Etchevers HC**, Amiel J, Lyonnet S (2007). Genetic and molecular bases of neurocristopathies. *Archives de pediatrie organe officiel de la Societe francaise de pediatrie* 14(6): 668–672.
- Flanagan JF**, Blus BJ, Kim D, Clines KL, Rastinejad F, Khorasanizadeh S (2007). Molecular implications of evolutionary differences in CHD double chromodomains. *Journal of molecular biology* 369(2): 334–342.
- Flaus A**, Martin DM, Barton GJ, Owen-Hughes T (2006). Identification of multiple distinct Snf2 subfamilies with conserved structural motifs. *Nucleic acids research* 34(10): 2887–2905.
- Gammill LS** and Bronner-Fraser M (2003). Neural crest specification: migrating into genomics. *Nature reviews. Neuroscience* 4(10): 795–805.
- Gershoni JM** and Palade GE (1983). Protein blotting: principles and applications. *Analytical biochemistry* 131(1): 1–15.
- Gong S-G** (2014). Cranial neural crest: migratory cell behavior and regulatory networks. *Experimental cell research* 325(2): 90–95.

- Gu C**, Yoshida Y, Livet J, Reimert DV, Mann F, Merte J, Henderson CE, Jessell TM, Kolodkin AL, Ginty DD (2005). Semaphorin 3E and plexin-D1 control vascular pattern independently of neuropilins. *Science (New York, N.Y.)* 307(5707): 265–268.
- Hall BD (1979)**. Choanal atresia and associated multiple anomalies. *The Journal of Pediatrics* 95(3): 395–398.
- Hall BK (2000)**. The neural crest as a fourth germ layer and vertebrates as quadroblastic not triploblastic. *Evolution and Development* 2(1): 3–5.
- Hall JA and Georgel PT (2007)**. CHD proteins: a diverse family with strong ties. *Biochemistry and cell biology = Biochimie et biologie cellulaire* 85(4): 463–476.
- Hanchate NK**, Giacobini P, Lhuillier P, Parkash J, Espy C, Fouveaut C, Leroy C, Baron S, Campagne C, Vanacker C, Collier F, Cruaud C, Meyer V, Garcia-Pinero A, Dewailly D, Cortet-Rudelli C, Gersak K, Metz C, Chabrier G, Pugeat M, Young J, Hardelin J-P, Prevot V, Dode C (2012). SEMA3A, a gene involved in axonal pathfinding, is mutated in patients with Kallmann syndrome. *PLoS genetics* 8(8): e1002896.
- Hittner HM**, Hirsch NJ, Kreh GM, Rudolph AJ (1979). Colobomatous microphthalmia, heart disease, hearing loss, and mental retardation. A syndrome. *Journal of Pediatric Ophthalmology and Strabismus* 16(2): 122–128.
- Hofmann K**, Zweier M, Sticht H, Zweier C, Wittmann W, Hoyer J, Uebe S, van Haeringen A, Thiel CT, Ekici AB, Reis A, Rauch A (2013). Biallelic SEMA3A defects cause a novel type of syndromic short stature. *American journal of medical genetics. Part A* 161A(11): 2880–2889.
- Ishii M**, Arias AC, Liu L, Chen Y-B, Bronner ME, Maxson RE (2012). A stable cranial neural crest cell line from mouse. *Stem cells and development* 21(17): 3069–3080.
- Issekutz KA**, Graham JM JR, Prasad C, Smith IM, Blake KD (2005). An epidemiological analysis of CHARGE syndrome: preliminary results from a Canadian study. *American journal of medical genetics. Part A* 133A(3): 309–317.
- Jager R**, Maurer J, Jacob A, Schorle H (2004). Cell type-specific conditional regulation of the c-myc proto-oncogene by combining Cre/loxP recombination and tamoxifen-mediated activation. *Genesis (New York, N.Y. 2000)* 38(3): 145–150.

- Janssen** BJ, Robinson RA, Perez-Branguli F, Bell CH, Mitchell KJ, Siebold C, Jones EY (2010). Structural basis of semaphorin-plexin signalling. *Nature* 467(7319): 1118–1122.
- Janssen** N, Bergman JEH, Swertz MA, Tranebjaerg L, Lodahl M, Schoots J, Hofstra RMW, van Ravenswaaij-Arts CMA, Hoefsloot LH (2012). Mutation update on the CHD7 gene involved in CHARGE syndrome. *Human mutation* 33(8): 1149–1160.
- Jones** NC, Lynn ML, Gaudenz K, Sakai D, Aoto K, Rey J-P, Glynn EF, Ellington L, Du C, Dixon J, Dixon MJ, Trainor PA (2008). Prevention of the neurocristopathy Treacher Collins syndrome through inhibition of p53 function. *Nature medicine* 14(2): 125–133.
- Jongbloets** BC and Pasterkamp RJ (2014). Semaphorin signalling during development. *Development (Cambridge, England)* 141(17): 3292–3297.
- Jongmans** MC, Admiraal RJ, van der Donk KP, Vissers LE, Baas AF, Kapusta L, van Hagen JM, Donnai D, Ravel TJ de, Veltman JA, van Geurts KA, Vries BB de, Brunner HG, Hoefsloot LH, van Ravenswaaij CM (2006). CHARGE syndrome: the phenotypic spectrum of mutations in the CHD7 gene. *Journal of Medical Genetics* 43(4): 306–314.
- Jongmans** MC, Hoefsloot LH, van der Donk KP, Admiraal RJ, Magee A, van de Laar I, Hendriks Y, Verheij JB, Walpole I, Brunner HG, van Ravenswaaij CM (2008). Familial CHARGE syndrome and the CHD7 gene: a recurrent missense mutation, intrafamilial recurrence and variability. *American journal of medical genetics. Part A* 146A(1): 43–50.
- Jongmans** MC, van Ravenswaaij-Arts CM, Pitteloud N, Ogata T, Sato N, Claahsen-van der Grinten, H L, van der Donk K, Seminara S, Bergman JE, Brunner HG, Crowley WF JR, Hoefsloot LH (2009). CHD7 mutations in patients initially diagnosed with Kallmann syndrome--the clinical overlap with CHARGE syndrome. *Clinical Genetics* 75(1): 65–71.
- Kearney** JA (2011). Genetic modifiers of neurological disease. *Current opinion in genetics & development* 21(3): 349–353.
- Kerosuo** L and Bronner-Fraser M (2012). What is bad in cancer is good in the embryo: importance of EMT in neural crest development. *Seminars in cell & developmental biology* 23(3): 320–332.

- Keyte** A and Hutson MR (2012). The neural crest in cardiac congenital anomalies. *Differentiation; research in biological diversity* 84(1): 25–40.
- Kim** H-G, Kurth I, Lan F, Meliciani I, Wenzel W, Eom SH, Kang GB, Rosenberger G, Tekin M, Ozata M, Bick DP, Sherins RJ, Walker SL, Shi Y, Gusella JF, Layman LC (2008). Mutations in CHD7, encoding a chromatin-remodeling protein, cause idiopathic hypogonadotropic hypogonadism and Kallmann syndrome. *American journal of human genetics* 83(4): 511–519.
- Kirby** ML and Hutson MR (2014). Factors controlling cardiac neural crest cell migration. *Cell adhesion & migration* 4(4): 609–621.
- Klostermann** A, Lohrum M, Adams RH, Puschel AW (1998). The chemorepulsive activity of the axonal guidance signal semaphorin D requires dimerization. *The Journal of biological chemistry* 273(13): 7326–7331.
- Knecht** AK and Bronner-Fraser M (2002). Induction of the neural crest: a multigene process. *Nature reviews. Genetics* 3(6): 453–461.
- Kolodkin** AL, Matthes DJ, Goodman CS (1993). The semaphorin genes encode a family of transmembrane and secreted growth cone guidance molecules. *Cell* 75(7): 1389–1399.
- Koppel** AM and Raper JA (1998). Collapsin-1 covalently dimerizes, and dimerization is necessary for collapsing activity. *The Journal of biological chemistry* 273(25): 15708–15713.
- Kulesa** PM, Bailey CM, Kasemeier-Kulesa JC, McLennan R (2010). Cranial neural crest migration: new rules for an old road. *Developmental biology* 344(2): 543–554.
- Kuriyama** S and Mayor R (2008). Molecular analysis of neural crest migration. *Philosophical transactions of the Royal Society of London. Series B, Biological sciences* 363(1495): 1349–1362.
- Laemmli** UK (1970). Cleavage of structural proteins during the assembly of the head of bacteriophage T4. *Nature* 227(5259): 680–685.

- Lalani S**, Safiullah AM, Fernbach SD, Harutyunyan KG, Thaller C, Peterson LE, McPherson JD, Gibbs RA, White LD, Hefner M, Davenport SL, Graham JM, Bacino CA, Glass NL, Towbin JA, Craigen WJ, Neish SR, Lin AE, Belmont JW (2006). Spectrum of CHD7 mutations in 110 individuals with CHARGE syndrome and genotype-phenotype correlation. *American journal of human genetics* 78(2): 303–314.
- Layman WS**, Hurd EA, Martin DM (2010). Chromodomain proteins in development: lessons from CHARGE syndrome. *Clinical Genetics* 78(1): 11–20.
- Liu H**, Juo ZS, Shim AH, Focia PJ, Chen X, Garcia KC, He X (2010). Structural basis of semaphorin-plexin recognition and viral mimicry from Sema7A and A39R complexes with PlexinC1. *Cell* 142(5): 749–761.
- Marfella CG** and Imbalzano AN (2007). The Chd Family of Chromatin Remodelers. *Mutation research* 618(1-2): 30–40.
- Martin DM** (2015). Epigenetic Developmental Disorders: CHARGE syndrome, a case study. *Current genetic medicine reports* 3(1): 1–7.
- Maurer J**, Fuchs S, Jager R, Kurz B, Sommer L, Schorle H (2007). Establishment and controlled differentiation of neural crest stem cell lines using conditional transgenesis. *Differentiation; research in biological diversity* 75(7): 580–591.
- Mayanil CS** (2013). Transcriptional and epigenetic regulation of neural crest induction during neurulation. *Developmental neuroscience* 35(5): 361–372.
- Mayor R** and Carmona-Fontaine C (2010). Keeping in touch with contact inhibition of locomotion. *Trends in cell biology* 20(6): 319–328.
- Mayor R** and Theveneau E (2013). The neural crest. *Development (Cambridge, England)* 140(11): 2247–2251.
- Messina A** and Giacobini P (2013). Semaphorin signaling in the development and function of the gonadotropin hormone-releasing hormone system. *Frontiers in endocrinology* 4: 133.
- Milet C** and Monsoro-Burq AH (2012). Neural crest induction at the neural plate border in vertebrates. *Developmental biology* 366(1): 22–33.



- Mullis K**, Faloona F, Scharf S, Saiki R, Horn G, Erlich H (1986). Specific enzymatic amplification of DNA in vitro: the polymerase chain reaction. *Cold Spring Harb Symp Quant Biol* 51: 263–273.
- Neufeld G**, Sabag AD, Rabinovicz N, Kessler O (2012). Semaphorins in angiogenesis and tumor progression. *Cold Spring Harbor perspectives in medicine* 2(1): a006718.
- Nogi T**, Yasui N, Mihara E, Matsunaga Y, Noda M, Yamashita N, Toyofuku T, Uchiyama S, Goshima Y, Kumanogoh A, Takagi J (2010). Structural basis for semaphorin signalling through the plexin receptor. *Nature* 467(7319): 1123–1127.
- Ogata T**, Fujiwara I, Ogawa E, Sato N, Udaka T, Kosaki K (2006). Kallmann syndrome phenotype in a female patient with CHARGE syndrome and CHD7 mutation. *Endocrine journal* 53(6): 741–743.
- Pagon RA**, Graham JM JR, Zonana J, Yong SL (1981). Coloboma, congenital heart disease, and choanal atresia with multiple anomalies: CHARGE association. *The Journal of pediatrics* 99(2): 223–227.
- Passos-Bueno MR**, Ornelas CC, Fanganiello RD (2009). Syndromes of the first and second pharyngeal arches: A review. *American journal of medical genetics. Part A* 149A(8): 1853–1859.
- Pauli S**, Pieper L, Häberle J, Grzmil P, Burfeind P, Steckel M, Lenz U, Michelmann HW (2009). Proven germline mosaicism in a father of two children with CHARGE syndrome. *Clinical Genetics* 75(5): 473–479.
- Pelengaris S**, Littlewood T, Khan M, Elia G, Evan G (1999). Reversible activation of c-Myc in skin: induction of a complex neoplastic phenotype by a single oncogenic lesion. *Molecular cell* 3(5): 565–577.
- Pinto G**, Abadie V, Mesnage R, Blustajn J, Cabrol S, Amiel J, Hertz-Pannier L, Bertrand AM, Lyonnet S, Rappaport R, Netchine I (2005). CHARGE Syndrome Includes Hypogonadotropic Hypogonadism and Abnormal Olfactory Bulb Development. *The Journal of Clinical Endocrinology & Metabolism* 90(10): 5621–5626.

- Plein A**, Calmont A, Fantin A, Denti L, Anderson NA, Scambler PJ, Ruhrberg C (2015). Neural crest-derived SEMA3C activates endothelial NRP1 for cardiac outflow tract septation. *The Journal of clinical investigation* 125(7): 2661–2676.
- Prasad MS**, Sauka-Spengler T, LaBonne C (2012). Induction of the neural crest state: control of stem cell attributes by gene regulatory, post-transcriptional and epigenetic interactions. *Developmental biology* 366(1): 10–21.
- Randall V**, McCue K, Roberts C, Kyriakopoulou V, Beddow S, Barrett AN, Vitelli F, Prescott K, Shaw-Smith C, Devriendt K, Bosman E, Steffes G, Steel KP, Simrick S, Basson MA, Illingworth E, Scambler PJ (2009). Great vessel development requires biallelic expression of Chd7 and Tbx1 in pharyngeal ectoderm in mice. *The Journal of clinical investigation* 119(11): 3301–3310.
- Rao MS** and Anderson DJ (1997). Immortalization and controlled in vitro differentiation of murine multipotent neural crest stem cells. *Journal of neurobiology* 32(7): 722–746.
- Rondanino C**, Bousser M-T, Monsigny M, Roche A-C (2003). Sugar-dependent nuclear import of glycosylated proteins in living cells. *Glycobiology* 13(7): 509–519.
- Rudolph B**, Hueber A-O, Evan GI (2000). Reversible activation of c-Myc in thymocytes enhances positive selection and induces proliferation and apoptosis in vitro. *Oncogene* 19(15): 1891–1900.
- Sanger F**, Nicklen S, Coulson AR (1977). DNA sequencing with chain-terminating inhibitors. *Proceedings of the National Academy of Sciences of the United States of America* 74(12): 5463–5467.
- Sanlaville D**, Etchevers HC, Gonzales M, Martinovic J, Clement-Ziza M, Delezoide AL, Aubry MC, Pelet A, Chemouny S, Cruaud C, Audollent S, Esculpavit C, Goudefroye G, Ozilou C, Fredouille C, Joye N, Morichon-Delvallez N, Dumez Y, Weissenbach J, Munnich A, Amiel J, Encha-Razavi F, Lyonnet S, Vekemans M, Attie-Bitach T (2006). Phenotypic spectrum of CHARGE syndrome in fetuses with CHD7 truncating mutations correlates with expression during human development. *Journal of Medical Genetics* 43(3): 211–217.
- Sanlaville D** and Verloes A (2007). CHARGE syndrome: an update. *European journal of human genetics EJHG* 15(4): 389–399.

- Schulz Y, Freese L, Manz J, Zoll B, Volter C, Brockmann K, Bogershausen N, Becker J, Wollnik B, Pauli S (2014a).** CHARGE and Kabuki syndromes: a phenotypic and molecular link. *Human molecular genetics* 23(16): 4396–4405.
- Schulz Y, Wehner P, Opitz L, Salinas-Riester G, Bongers EM, van Ravenswaaij-Arts CM, Wincent J, Schoumans J, Kohlhasse J, Borchers A, Pauli S (2014b).** CHD7, the gene mutated in CHARGE syndrome, regulates genes involved in neural crest cell guidance. *Human genetics* 133(8): 997–1009.
- Sekido Y, Bader S, Latif F, Chen JY, Duh FM, Wei MH, Albanesi JP, Lee CC, Lerman MI, Minna JD (1996).** Human semaphorins A(V) and IV reside in the 3p21.3 small cell lung cancer deletion region and demonstrate distinct expression patterns. *Proceedings of the National Academy of Sciences of the United States of America* 93(9): 4120–4125.
- Serini G, Valdembri D, Zanivan S, Morterra G, Burkhardt C, Caccavari F, Zammataro L, Primo L, Tamagnone L, Logan M, Tessier-Lavigne M, Taniguchi M, Puschel AW, Bussolino F (2003).** Class 3 semaphorins control vascular morphogenesis by inhibiting integrin function. *Nature* 424(6947): 391–397.
- Shellard A and Mayor R (2016).** Chemotaxis during neural crest migration. *Seminars in cell & developmental biology* 55: 111–118.
- Siebert JR, Graham JM JR, MacDonald C (1985).** Pathologic features of the CHARGE association: support for involvement of the neural crest. *Teratology* 31(3): 331–336.
- Suzuki K, Kumanogoh A, Kikutani H (2008).** Semaphorins and their receptors in immune cell interactions. *Nature immunology* 9(1): 17–23.
- Takahashi T, Fournier A, Nakamura F, Wang LH, Murakami Y, Kalb RG, Fujisawa H, Strittmatter SM (1999).** Plexin-neuropilin-1 complexes form functional semaphorin-3A receptors. *Cell* 99(1): 59–69.
- Takamatsu H and Kumanogoh A (2012).** Diverse roles for semaphorin-plexin signaling in the immune system. *Trends in immunology* 33(3): 127–135.

- Tamagnone L**, Artigiani S, Chen H, He Z, Ming GI, Song H, Chedotal A, Winberg ML, Goodman CS, Poo M, Tessier-Lavigne M, Comoglio PM (1999). Plexins are a large family of receptors for transmembrane, secreted, and GPI-anchored semaphorins in vertebrates. *Cell* 99(1): 71–80.
- Tamagnone L** and Comoglio PM (2004). To move or not to move? Semaphorin signalling in cell migration. *EMBO reports* 5(4): 356–361.
- Theveneau E** and Mayor R (2012). Neural crest migration: interplay between chemorepellents, chemoattractants, contact inhibition, epithelial-mesenchymal transition, and collective cell migration. *Wiley interdisciplinary reviews. Developmental biology* 1(3): 435–445.
- Toyofuku T**, Yabuki M, Kamei J, Kamei M, Makino N, Kumanogoh A, Hori M (2007). Semaphorin-4A, an activator for T-cell-mediated immunity, suppresses angiogenesis via Plexin-D1. *The EMBO journal* 26(5): 1373–1384.
- Toyofuku T**, Yoshida J, Sugimoto T, Yamamoto M, Makino N, Takamatsu H, Takegahara N, Suto F, Hori M, Fujisawa H, Kumanogoh A, Kikutani H (2008). Repulsive and attractive semaphorins cooperate to direct the navigation of cardiac neural crest cells. *Developmental biology* 321(1): 251–262.
- van Meter TD** and Weaver DD (1996). Oculo-auriculo-vertebral spectrum and the CHARGE association: clinical evidence for a common pathogenetic mechanism. *Clinical dysmorphology* 5(3): 187–196.
- Verloes A** (2005). Updated diagnostic criteria for CHARGE syndrome: a proposal. *American journal of medical genetics. Part A* 133A(3): 306–308.
- Vissers LE**, van Ravenswaaij CM, Admiraal R, Hurst JA, Vries BB de, Janssen IM, van der Vliet WA, Huys EH, Jong PJ de, Hamel BC, Schoenmakers EF, Brunner HG, Veltman JA, van Kessel AG (2004). Mutations in a new member of the chromodomain gene family cause CHARGE syndrome. *Nature genetics* 36(9): 955–957.

- Vuorela P**, Ala-Mello S, Saloranta C, Penttinen M, Poyhonen M, Huoponen K, Borozdin W, Bausch B, Botzenhart EM, Wilhelm C, Kaariainen H, Kohlhase J (**2007**). Molecular analysis of the CHD7 gene in CHARGE syndrome: identification of 22 novel mutations and evidence for a low contribution of large CHD7 deletions. *Genetics in medicine official journal of the American College of Medical Genetics* 9(10): 690–694.
- Williams MS** (**2005**). Speculations on the pathogenesis of CHARGE syndrome. *American journal of medical genetics. Part A* 133A(3): 318–325.
- Winberg ML**, Noordermeer JN, Tamagnone L, Comoglio PM, Spriggs MK, Tessier-Lavigne M, Goodman CS (**1998**). Plexin A is a neuronal semaphorin receptor that controls axon guidance. *Cell* 95(7): 903–916.
- Wincent J**, Holmberg E, Stromland K, Soller M, Mirzaei L, Djureinovic T, Robinson K, Anderlid B, Schoumans J (**2008**). CHD7 mutation spectrum in 28 Swedish patients diagnosed with CHARGE syndrome. *Clinical Genetics* 74(1): 31–38.
- Woodage T**, Basrai MA, Baxevanis AD, Hieter P, Collins FS (**1997**). Characterization of the CHD family of proteins. *Proceedings of the National Academy of Sciences* 94(21): 11472–11477.
- Young J**, Metay C, Bouligand J, Tou B, Francou B, Maione L, Tosca L, Sarfati J, Brioude F, Esteva B, Briand-Suleau A, Brisset S, Goossens M, Tachdjian G, Guiochon-Mantel A (**2012**). SEMA3A deletion in a family with Kallmann syndrome validates the role of semaphorin 3A in human puberty and olfactory system development. *Human reproduction (Oxford, England)* 27(5): 1460–1465.
- Zhang D**, Ighaniyan S, Stathopoulos L, Rollo B, Landman K, Hutson J, Newgreen D (**2014**). The neural crest: a versatile organ system. *Birth defects research. Part C, Embryo today reviews* 102(3): 275–298.

## 7 Acknowledgements

I would like to express my gratitude to PD Dr. Silke Pauli for being my referee and supervisor, for given me the opportunity to work on this interesting project and for her guidance and support during the entire process of my PhD study.

I sincerely thank Prof. Steven A. Johnsen, PhD and Prof. Dr. Ahmed Mansouri for being my thesis committee members.

Moreover, I am very thankful to Prof. Dr. Ralf Dressel, Prof. Dr. Thomas Meyer and Prof. Dr. Lutz Walter, who kindly agreed to evaluate my dissertation and participate in the examination.

I thank the Deutsche Forschungsgemeinschaft (DFG) for financing my PhD study.

I would like to thank Dr. Roser Ufartes Mas for her support and helpful suggestions during the last year of my PhD study.

A special thank goes to my lab colleague Johanna Mänz for her patient help and advice and for the cheerful and friendly atmosphere in the lab.

I would like to thank all other current and former colleagues of the Institute of Human Genetics, especially Dr. Nadine Mellies, Dr. Jessica Nolte-Kaitschick and Dr. Yvonne Schulz, for their advice and support as well as the friendly working atmosphere.

I express my heartfelt gratitude to my parents, who always believe in me. You supported me unconditionally with your encouragement and patience throughout my PhD time. Thanks for your trust and love! Therefore, I dedicate this thesis to you!

Thank you André for always backing me up, putting faith in me, encouraging me and cheering me up, especially during the hard times of my study!

## 8 Curriculum vitae

### Personal details

---

<b>Name</b>	Luisa Freese
<b>Date of birth</b>	03/17/1986
<b>Place of birth</b>	Halberstadt, Germany
<b>Nationality</b>	german
<b>Address</b>	Haeckelstr. 4, 30173 Hanover

### Education

---

<b>Since November 2013</b>	PhD study of Molecular Medicine at the Institute of Human Genetics Georg-August University Göttingen <u>Doctoral Thesis:</u> Elucidating the pathomechanism behind the neurocristopathy CHARGE syndrome
<b>2011–2013</b>	Master of Science study of Biomedicine Hannover Medical School <u>Master Thesis:</u> Untersuchungen zur Funktion des humanen Testis-spezifischen Proteins, Y-kodiert (TSPY) bei <i>TSPY</i> -transgenen KIT-defizienten Mäusen
<b>2008–2011</b>	Bachelor of Science study of Plant Biotechnology Gottfried Wilhelm Leibniz University Hannover <u>Bachelor Thesis:</u> Optimierung der Anwendung von Mikrosatelliten für <i>Diaeretiella rapae</i> und erstes Screening einer Feldpopulation

---

<b>2005–2008</b>	Training for Biology Laboratory Technician Research Center Borstel – Leibniz-Center for Medicine and Biosciences
<b>1996–2005</b>	Secondary School: Käthe-Kollwitz-Gymnasium, Halberstadt
<b>1992–1996</b>	Primary School: Grundschule Anne Frank, Halberstadt